Czech University of Life Sciences Prague

Faculty of Engineering

ANALYSIS OF AGRICULTURAL CROP STRESS FACTORS

USING SPECTRAL IMAGING

Dissertation Thesis

Author: Ing. Kateřina Křížová

Supervisor: doc. Mgr. Jitka Kumhálová, Ph.D.   Prague, 2022

Declaration

I hereby declare that this Dissertation is my own original work and has not been submitted before to any institution for assessment purposes.

Further, I have acknowledged all sources used and have cited these in the Reference section.

In Prague on the 1st of February 2022   Kateřina Křížová

Acknowledgements

In Prague on the 1ˢᵗ of February 2022   Kateřina Křížová

„The highest function of ecology is understanding consequences.”

Frank Herbert, Dune

Abstract

The concept of Precision Agriculture (PA) has developed rapidly in recent decades. As the population grows and specialised technologies are enhanced, the methods of site-specific farming are gaining still more attention. Many studies have been conducted with the aim to describe relations between various soil and vegetation characteristics and information acquired by remotely sensed (RS) data. Such knowledge is essential to obtain a complex overview of how the natural processes may be explained by spectral imagery. The major advantage of such an approach is the possibility to conduct the measurements in a completely non-destructive mode. Related analyses may be thus undertaken repeatedly during a growing season. It was determined that spectral characteristics of vegetation are related to various vegetation properties such as biochemical composition, physical structure, or plant status. Based on this knowledge there is not only the possibility to evaluate the crop status at the canopy scale, but it is also possible to detect some within-field heterogeneity.

This Dissertation presents findings published on the topic of utilisation of spectral imaging for describing the soil-plant environment characteristics. The ability of selected sensors to predict crop yield was evaluated, since their spectral bandwidths often differ. Variability of crop status within investigated canopies was caused either by varying soil conditions, nutrient level, or fertilisation management was investigated. Eventually, based on the gathered knowledge, a novel low-cost handheld sensor was developed as a tool for direct practical crop stress estimation.

Keywords: abiotic stressors, precision agriculture, spectral index.

List of Acronyms

EC	Soil Electrical Conductivity
EMR	Electromagnetic Radiation
ESA	European Space Agency
GIS	Geographical Information Systems
GLM	Generalized Linear Model
GNDVI	Green Normalized Difference Vegetation Index
GPS	Global Positioning System
GS	GreenSeeker
MSAVI	Modified Soil-Adjusted Vegetation Index
MSI	Moisture Stress Index
NASA	National Aeronautics and Space Administration
NDRE	Normalized Difference Red Edge Vegetation Index
NDVI	Normalized Difference Vegetation Index
NDWI	Normalized Difference Water Index
NIR	Near Infra-red
LAI	Leaf Area Index
LCC	Leaf Chlorophyll Content
LED	Light-emitting Diode
PA	Precision Agriculture
RS	Remote Sensing
SLM	Simple Linear Model
SOM	Soil Organic Matter
SWIR	Short-wave Infra-red
Tc	Canopy Temperature
UAV	Unmanned Aerial Vehicle
USGS	United States Geological Survey
VARI	Visible Atmospherically Resistant Index
VI	Vegetation Index
WI	Water Index

Table of Contents

1 Introduction

Agriculture, as one of the staple humankind activities, may be described as a process of transformation of the natural ecosystem to food production (Poonia et al., 2018). Nowadays, it embraces various branches of crop cultivation and animal husbandry science, both of which are connected as well. This connection follows one of the basic ecological models that describe the energy flow through the ecosystem – a food pyramid. This simple model emphasises the irreplaceable role of autotrophic organisms in the basis of the pyramid, as they can receive the energy emitted by the Sun and incorporate it into biomass through the process of photosynthesis (Tomera, 2001). Thus, crop cultivation is nothing else than guided primary production managed by a human to provide the source of energy for itself – the top of the food pyramid.

Crop production is a complex activity that includes knowledge of plant physiology and ecology and requires precise timing of agro-operations using convenient agro-technologies. Until recently, agricultural management was based mostly on common practices inherited from previous generations of farmers. Socially political changes in recent decades, however, created substantial pressure on the quantity and quality of primary production. Various other challenges are also connected with Climate change as well as Population Growth.

Strategies for meeting human needs and mitigating the negative impacts of agriculture involve rapid development in the field of technology together with the application of scientific research and its results. This concept is today known as *Precision Agriculture* (PA) and its wider adoption is crucial for introducing and maintaining sustainable crop production.

2 Literature Review

2.1 Current Agriculture and its Ecological Aspects

The nature of agricultural practice and its impact on the environment are strongly bonded with specific time periods since the Neolithic Revolution (Bairoch, 1991). Contemporary history describes a breakthrough known as the *Green Revolution*. Since the 1950s a set of research-based technologies has been implemented to heighten crop yields (wheat and rice mostly) to satisfy the needs of a growing world population (Jain, 2010). Besides others, the most significant means of this agricultural transition were high-yielding varieties, as a result of intensive plant breeding, and massive utilisation of newly invented fertilisers and pesticides. Along with indisputable achievements, farming itself was becoming more and more intensive, supporting larger holdings, and suppressing smallholders (Conway & Barbier, 2013). Before long, negative aspects of such an intensive approach became observable. In connection with the Green Revolution, new issues occurred, such as biodiversity reduction due to monocropping, fragmentation of the natural ecosystem, freshwater pollution, alteration in nutrient balance (Poonia et al., 2018).

Today's agriculture is strongly influenced by several *Global Issues.* First, there has been rapid *Population Growth* in recent decades. While there were 7.7 billion people in 2019, the latest estimates predict to be 8.5 billion in 2030, 9.7 billion in 2050, and up to 10.9 billion in 2100 (United Nations, 2019). Demands for quality resources are, therefore, increasing, while the space for production remains limited (Zhang, 2016). Up to the 1960s, increasing crop production was enabled by the expansion of agricultural areas, nevertheless, this trend significantly slowed down when the percentage of arable land reached 9% of the total area worldwide (Moldan, 2015). And there is *Climate Change* as the second major issue, that forces common practice to be adjusted. As the average global temperature tends to increase, significant changes in the spatial and temporal distribution of atmospheric precipitation are observable, having severe consequences on the Earth's surface (Davoudi et al., 2009).

2.2 Plant Status and Stress Conditions

Based on plant physiological principles, the crop yield and yield quality are highest in the optimum ecological conditions. These are, however, barely ever optimal

for a long period. In terms of (not only) plant ecology, the Gaussian curve describes the tolerance of an organism to adapt to the varying range of a particular factor. The efficiency of a specific physiological process on the y-axis refers mainly to a) plant growth, b) its development and c) the ability to reproduce (Hnilička & Středa, 2016). Suitable conditions in the so-called *physiological optimum* are bordered from both sides by critical limits. Behind those limits, zones of physiological stress occur. Stressors, in general, disturb the homeostatic equilibrium of an individual due to morphological and physiological alterations and may result in biomass and yield losses (Venkateswarlu et al., 2012). Finally, lower and upper lethal limits indicate the border where the organism is no more capable to tolerate the stressors pressure which leads to the organism's death (Putman & Wratten, 2012).

The effect of a stress factor depends on several properties, such as i) its power, ii) duration and iii) a number of expositions. In natural conditions, stressors rarely impact the organism separately. Most of the time, stress factors occur concurrently, and their interactions may be potentially positive (e.g., ultraviolet radiation and pathogens), potentially negative (e.g., high temperature and drought) or there may not be any co-dependent impact at all (Mittler, 2006). A complete understanding of stressors mechanisms impacting crop growth requires information from several biological levels. *The molecular and cellular* level helps to study plant internal adaptations, while the level of *plant and its community* to understand the effect of alterations in cultivars, varieties, or management (Hall, 2000).

The overall result of the crop production effort is based on these factors (Perkins, 1997):

- selection of the appropriate crop variety
- planting seeds in properly prepared soil
- providing enough water and nutrients
- protection of plants against pests
- right timing of agrotechnical operations

These steps, adapted to a specific crop and climatic and geographical conditions, help to effectively utilise the basic natural resources, i.e., *solar radiation*, *water,* and *soil* (Perkins, 1997). However, any of these steps can initiate a crop stress status when not adjusted or chosen properly.

2.3 Crop Stress Factors

Regarding the source, stress factors are commonly divided into *abiotic* and *biotic*, while the effect of climate change has been recently involved as well since it describes the phenomena in a wider context (Figure 1).
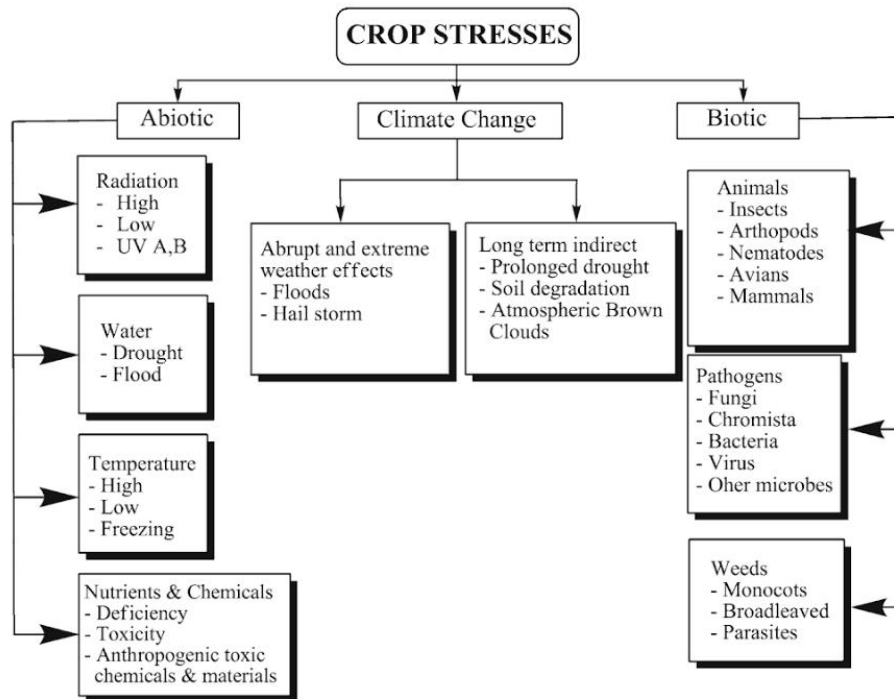
Figure 1. Crop stress factors according to their origin and further specified (Maheswari et al., 2012).

Abiotic stress factors have their origin in atmospheric phenomena, such as *temperature*, *precipitation*, or *solar radiation*. The character of abiotic stressors is very variable and reflects several site characteristics. Physical soil properties (texture, structure, bulk density, or porosity) are significant factors influencing the soil moisture and other hydro-physical properties, such as water capacity, or permeability (Loganathan, 1987). Important influence also has the site's topography. Within-field elevation variability affects the distribution of both water and nutrients (Kumhálová & Moudrý, 2014).

According to Minhas et al. (2017), more than 50 % of agricultural losses are a result of serious damage to a plant function or development caused by abiotic stressors. The damage rate is strongly dependent on specific plant responses (Maheswari et al., 2012).

2.3.1 Drought

Drought is one of the two extremes in terms of water availability. It depends not only on the spatial and temporal distribution of precipitation but also on the plot's geomorphological properties and its infiltration capacity. Drought is considered one of the most dangerous natural disasters endangering crop production in recent decades and it is expected to intensify in the future (Aroca, 2012). It also amplifies other stresses, such as soil salinity, pathogens attacks, or heat stress (Ahluwalia et al., 2021). Wilhite & Glantz (1985) determined the drought categories, all of which are connected causing significant economic, social, and environmental impacts (Figure 2). The urgency to mitigate the effects of drought is therefore indisputable.

Natural plant mechanisms, by which they can adapt to the dry season, includes i) drought escape (drought-sensitive stages, like flowering or seed and fruit development, are postponed to the season with a higher water supply), or ii) drought resistance (assimilation to the lack of water) (Hall, 2000).

In terms of agricultural management, strategies are based on i) land readjustment, ii) selecting more resilient varieties, iii) balanced crop rotation, iv) introducing of intermediate crops, v) soil management innovations, vi) fertilisation together with different soil management, and potentially vii) irrigation systems (Žalud et al., 2020).
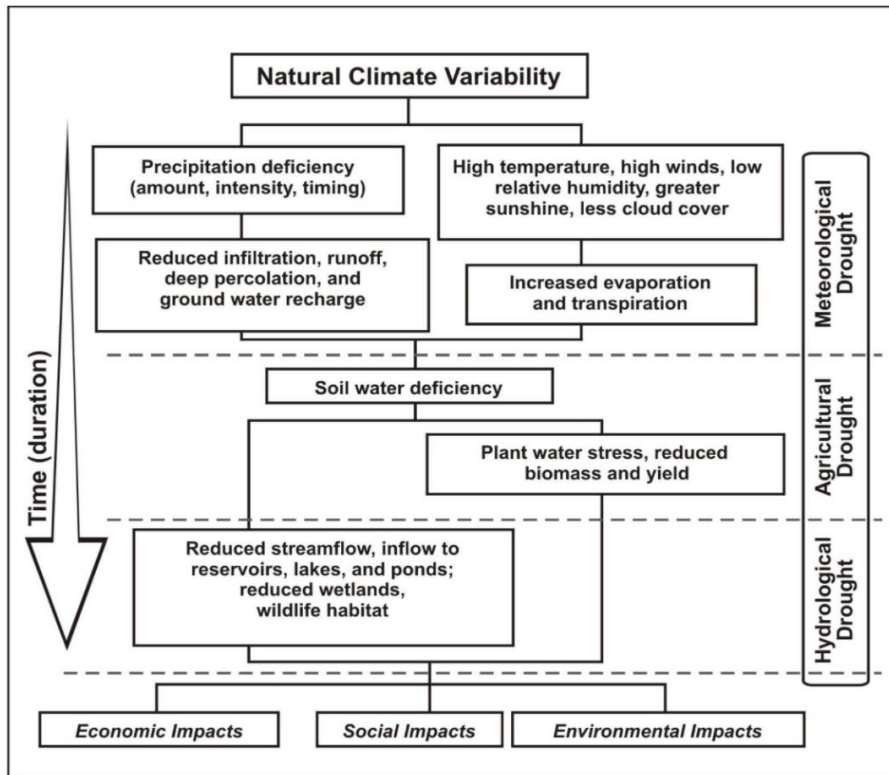
Figure 2. Climate variability-induced drought, its categories and impacts (National Drought Mitigation Center, 2022).

2.3.2 Temperature Extremes

The *low* temperature might cause severe damage especially in sensitive growth stages, such as germination and reproduction (Liu et al., 2019). On the other hand, *high* temperatures cause heat stress, which induces a higher evaporation rate and might therefore result in severe water deficit. At this point, heat stress is strongly connected to drought conditions. High temperatures also increase the rate of reproductive development and therefore, the whole life cycle of a plant is considerably shortened (Wani & Kumar, 2020). Current strategies in terms of mitigation of temperature extremes are similar as by drought. More resilient crop varieties or varieties with shorter growing periods are provided by crop-breeding research and introduced into warmer regions.

2.3.3 Soil Fertility and Nutrient Supply

Crop growth and development depend largely on the fertility of soil profile (Mäder et al., 2002). This soil feature is determined by a complex set of i) physical soil properties (texture, structure, susceptibility to erosion), ii) agrochemical factors (pH,

micro- and macronutrients content), iii) organic and biological factors (organic matter content, soil edaphon), and iv) water regime.

Lower soil fertility is often connected with soil degradation, a decrease of the organic matter, and reduction of soil biota (Gregory & Nortcliff, 2012) while all these negative aspects are amplified by intensive agricultural management.

The efforts to restore and maintain the sustainable level of soil fertility today encompass managemental adjustments, preferable utilisation of the organic fertilisers over mineral ones, and an optimal crop rotation system (Anderson et al., 2020). Since the amount of organic fertilisers produced has decreased significantly over the last few decades, new approaches are taken (Sulewska et al., 2012). To maximise the effect of organic matter, several soil amendments such as biochar, NeOsol, or Z'Fix are tested. Recently, their positive impact on soil compaction and moisture of the top layer (Krzywy-Gawrońska, 2012), the enzymatic activity of sand and clay soils (Bielińska et al., 2013), higher nutrient content (Šařec et al., 2017a), water and nutrient uptake (Porro & Pedò, 2016), or photosynthesis and plant growth of cereal crops (Borowiak et al., 2016) was described.

2.4 Agricultural Management and Decision Making

A general aim of agriculture has always been to achieve the maximum output (crop yield) while minimising inputs (resources). This simple equation is a bottom line of every agricultural management, which is supposed to schedule all agro-technical operations to the right time and order so that the most optimal conditions for crop growth are ensured.

Agro-technical operation schedules are often crop-specific. However, applying mineral fertilisers is typical and necessary for all crops under conventional agriculture today. Considerable proportions of nitrogen, phosphorus, and potassium are lost due to non-optimal management (Duhan et al., 2017). This has both economic and environmental negative consequences, which are the major two drivers of the current transition towards sustainability. Environmental aspects of crop production have become a subject of discussion on an international level.

Hence, optimal agricultural management must:

- ensure the optimal conditions for the highest yield
- mitigate the negative environmental effects as much as possible
- work with a reasonable economics

Quality in-field data gives valuable insights to both spatial and temporal variability of weather and soil conditions or crop status. Such knowledge is essential for any decision-making process. Especially nowadays, when the field of technology and shared knowledge has evolved rapidly, using such data is beneficial for adjusting agricultural management precisely to specific crop and site conditions.

2.5 Precision Agriculture

The above-mentioned trend of applying modern technologies and latest knowledge in agriculture formed into the concept of *Precision Agriculture* (but also *Precision Farming*, *Site-Specific Agriculture*, or *Smart Farming*). PA is considered a complex ecosystem that provides a wide range of activities from data acquisition to its transformation into direct action (Pham & Stack, 2018). One of its major contributions is the possibility to omit the large area management based on a hypothetical average condition. Instead, spatially explicit data is leveraged to apply site-specific management (Paxton et al., 2011). This transition results in water, fertilisers, herbicides, and pesticides use reduction as well as in the reduction of the associated workforce (Cisternas et al., 2020).

2.5.1 PA Adoption

Adoption of PA techniques into common management brings farmers several major benefits, such as crop yield increase, stabilising the yield variability, and reducing the input costs (Yost et al., 2017). Barnes et al. (2019) have conducted a study to assess the most important motivation for adopting those techniques. They were working with a number of 971 respondents from five European countries (Belgium, Germany, Greece, the Netherlands, and the UK). Their results are obviously in line with the proclaimed objective of the PA concept; hence, the farmers expect mostly cost reduction and more accurate agricultural operations. Nevertheless, there are still some constraints that hold the adoption back. According to the study, the reason for

non-adopters to maintain their usual management is a belief in their own knowledge as well as scepticism towards the economic returns. The associated costs of technologies and further management make this practice affordable rather for large- than smallholders (Cisternas et al., 2020).

2.5.2 *Major PA Technologies*

An extensive systematic literature review of Cisternas et al. (2020) was published on the topic of implementations of PA. The authors focused on the question of mostly used technologies and their appropriate selection in different contexts of agricultural management. By reviewing 257 publications, they divided results into two major sections: i) technologies and ii) software, systems, and techniques. In the technologies section, substantial attention was given to Global Positioning System (GPS), Multimedia, Nanosensors, Remote Sensing (RS), Sensors in General, Unmanned Aerial Vehicles (UAV), Unmanned Ground Vehicles (UGV), Variable Rate Technology (VRT), and Wireless Sensor Networks (WSN). Nevertheless, GPS and RS were cited the most. Regarding the software systems and techniques, Geographic Information Systems (GIS), Multispectral images, Soil Mapping, Yield maps, and Yield monitors were listed, while GIS and yield maps came out as the most used.

Each of the above-mentioned technologies provides valuable information or performs necessary steps in data analysis or interpretation. To provide a solid background for decision making, however, they are usually utilised in combinations.

2.6 Spectral Analysis and Vegetation Indices

Spectral analysis is nowadays an indispensable tool that helps to effectively and non-destructively detect crops under stress conditions and their growth dynamics.

Plant response to an incident electromagnetic radiation (EMR) and its potential to provide data on biophysical properties of vegetation has been determined already decades ago. The character of the reflected EMR wave in specific bands defined by the chemical and morphological characteristics of the canopy initiated establishing the first so-called *Vegetation Indices* (VIs) (Richards, 2013; Rouse et al., 1974). Before long, the advantages of such algorithms became leveraged in terms of agronomic perspective for crop identification and condition assessment (Bauer, 1985). To date,

hundreds of VIs are described in scientific literature. Their development and applicability are summarised for example by the study of Xue & Su (2017). This study also describes advantages and disadvantages of the most used VIs while emphasising the necessity of proper selection of instrumentation and platform regarding specific applications of VI.

2.6.1 Spectral Response to Drought

Plants experience significant morphological and physiological changes to minimise the impact of the drought stress factor. In general, the stomatal oscillations and plant water and nutrients status are disturbed on a physiological level. Concurrently, a reduced rate of cell division results in limitations of leaf size, stem elongation, and root proliferation (Aroca, 2012). Although the character of these alterations is highly crop-specific, there were mechanisms developed to detect even early stages of drought through the spectral analysis leveraging the absorption in *near infra-red* (NIR) and *short-wave infra-red* (SWIR) regions of EMR (Bauer, 1985). It was determined that leaf water content can be best indicated by bands centred at wavelengths of 1450 and 1940 nm (Wang et al., 2009). Several VIs are based on these facts and are already well-established nowadays, namely *Moisture Stress Index* (MSI) by Hunt Jr & Rock (1989), *Normalized Difference Water Index* (NDWI) by Gao (1996), or *Water index* (WI) by Penuelas et al. (1993).

2.6.2 Spectral Response to Heat Stress

Affected by high temperatures, plants begin to produce so-called Heat Shock Proteins that are supposed to mitigate the effects of heat stress. However, longer periods of heat induce higher evapotranspiration which might eventually result in a severe water deficit (Wani & Kumar, 2020). Thus, the effects of drought and heat stress might be both described by above-mentioned water-related VIs.

Several methods were also established for the estimation of evaporation rate based on the surface temperature using RS techniques. A recent study by Wagner et al. (2022) introduces an enhanced method for evapotranspiration retrieval based on data acquired by *Operational Land Imager* (OLI) and *Thermal Infrared Sensor* (TIRS) carried by the Landsat 8 satellite.

2.6.3 Spectral Response to Nitrogen Supply

Nitrogen is one of the staple nutrients for crop growth and development. It is strongly linked to the amount of chlorophyll in plant tissue, which in fact defines the quality of photosynthetic potential (Filella et al., 1995). The green pigment content also determines the intensity of leaf colour. While healthy and well-nourished vegetation is characterised by dark green shades, plants with poorer nutrition status are often recognized by pale green to yellow colour (Evans, 1983). A variety of broadband and narrowband chlorophyll-related VIs are described nowadays. The most common *Normalized Difference Vegetation Index* (NDVI) developed by Rouse et al. (1974) reflects the general essence of multispectral VIs that always work with a ratio of reflectances in chlorophyll absorption and reflection peaks. The modifications of other VIs rely on utilisation of different spectral bands to emphasise or reduce the impact of specific features. *Green Normalized Difference Vegetation Index* (GNDVI) is trusted to reflect the photosynthetic material more accurately than simple NDVI in maturity stages (Gitelson et al., 1996). *Modified Soil-Adjusted Vegetation Index* (MSAVI) is designed to mitigate the influence of soil pixels in scarce canopies (Qi et al., 1994). *Normalized Difference Red Edge Vegetation Index* (NDRE) uses the narrowband called *Red Edge* (approx. 740 nm) to provide even more precise estimates over dense canopies (Barnes et al., 2000). However, there are also some VIs based solely on the visible part of the EMR bringing valuable information, such as the *Visible Atmospherically Resistant Index* (VARI) that is designed to have low sensitivity to atmospheric effects (Gitelson et al., 2002).

2.7   Sensors and Image Resolution

The spectral response of vegetation is recorded during the sensing process using any of the available sensors. Generally, the information is provided either as a spatial point value in the case of contact imaging or as a spatial distribution when RS imagery is used.

Generally, i) spectral, ii) radiometric, iii) spatial, or iv) temporal resolution describes the character and detail of information provided by spectral imaging.

The *spectral resolution* defines the wavelengths of EMR to which the sensor is sensitive. It is usually given by spectral bands specified by their location and width. Satellite systems and some of the UAV sensors are divided into three major categories

based on the spectral resolution. There are *multispectral* data that are sensitive to the visible region of EMR and to the NIR band. Depending on the number of bands included, there are either four-bands or eight-bands imagery, while eight-bands imagery usually also covers the thermal radiation. *Hyperspectral* imagery contains dozens to hundreds of very narrow spectral bands across visible and NIR regions. Recently, *radar* imagery based on actively emitted pulses in microwave wavelengths has become a subject of research in terms of their utilisation for soil and crop status properties assessment (Lillesand et al., 2014).

The *radiometric resolution* gives a hint of the sensor sensitivity to approaching reflected EMR and thus its capability to distinguish slight energy variations (Thenkabail, 2015).

The *spatial resolution* defines the detail of the information described as pixel size. Generally, the spatial resolution ranges from kilometres to centimetres (Lillesand, 2014). It is challenging to select a sensor with an appropriate spatial resolution since the agricultural fields are usually highly variable in terms of size, elevation, and land fragmentation (Psomiadis et al., 2016).

Eventually, the *temporal resolution* in fact determines the revisit time, thus the operational capability of a sensor to obtain imagery of a particular spot on the Earth's surface in a repetitive mode (Lippitt et al., 2015). The temporal resolution of a satellite platform mostly depends on its orbit and viewing angle (Borra et al., 2019).

2.7.1 Remote Sensors and Platforms

Remote sensors are carried either by airborne or satellite platforms. Given the fact that these sensors basically capture the image over an area of interest, the spatial distribution of investigated canopy features is produced by the following spectral analysis. Hence, spatial-temporal variations of crop status can be eventually geographically displayed.

Regarding the satellite platforms, two major open-source imagery providers are the National Aeronautics and Space Administration[1] (NASA) in cooperation with the United States Geological Survey[2] (USGS), and the European Space Agency[3] (ESA).

---

[1] https://www.nasa.gov/
[2] https://www.usgs.gov/
[3] https://www.esa.int/

NASA provides free imagery of the Landsat[4] mission already since 1972 with the spatial resolution of 30 m concerning the most used spectral bands in terms of vegetation monitoring (USGS, 2022). As stated in the study of Kumhálová et al. (2014), such resolution is sufficient for predicting crop yield and related parameters within approx. 11 ha filed. ESA's Sentinel-2[5] mission provides a shorter time series than Landsat, however, the spatial resolution of 10 m ensures more detailed information given by multispectral imagery (ESA, 2022). Concurrently, several commercial imagery providers offer products with a finer spatial resolution (e.g., SPOT-7[6] with 6 m, WorldView-2[7] with 2 m, or QuickBird[7] with only 0.6 m).

2.7.2 Handheld Sensors

Besides the GreenSeeker[8] sensor that in fact combines the approach of remote (i.e., contactless) imaging with the major features of handheld sensors, the vast majority of handheld sensors are designed for contact imaging. Direct in-field sampling provides the information related to a specific point and therefore, to acquire spatial information, the data must be interpolated.

The methodology of sampling with contact handheld sensors is based on pulses of EMR in specific wavelengths actively emitted through the plant tissue. Either fluorescence (CCM-300[9]) or transmittance (CCM-200 plus[10], SPAD-502Plus[11]) is recorded and such data serves as an input for specific index calculation. Regarding the sensor design, this index is claimed to be related to some of the vegetation properties, such as plant vigour, leaf chlorophyll content (LCC), or nitrogen content (Richardson et al., 2002).

Handheld sensors are currently considered tools providing prompt information about actual crop status and therefore crucial for decision making. The affordability of such instruments became an issue though. As a reaction to the high prices of commercial sensors, several studies were published on the topic of inventing new low-

---

[4] https://www.usgs.gov/landsat-missions/landsat-satellite-missions

[5] https://sentinel.esa.int/web/sentinel/missions/sentinel-2

[6] https://www.intelligence-airbusds.com/en/8693-spot-67

[7] https://www.digitalglobe.com/company/about-us/

[8] https://agriculture.trimble.com/product/greenseeker-handheld-crop-sensor/

[9] https://www.optisci.com/ccm-300.html

[10] https://www.optisci.com/ccm-200.html

[11] https://www5.konicaminolta.eu/en/measuring-instruments/products/colour-measurement/chlorophyll-meter/spad-502plus/introduction.html

cost alternatives to those sensors. These efforts were based either on i) digital cameras utilisation (Tavakoli & Gebbers, 2019; Meyer & Neto, 2008), ii) smartphones (Vesali et al., 2015), iii) novel techniques using existing devices (Cortazar et al., 2015; Ali et al., 2012), and iv) new prototypes invention (Pérez-Patricio et al., 2018). Most of these studies were conducted to demonstrate the feasibility of the proposed approach in terms of vegetation monitoring (Misra et al., 2018). However, their findings and conclusion may serve as a valuable input for future specifically oriented solutions development.

3 Hypotheses

By integrating modern technologies in agricultural research and practice, many new questions have arisen along with significant achievements. Questions that concern both methodologies of data acquisition and interpreting the results. In the context of spectral analysis and crop stress factors assessment, the research is mostly focused on describing:

- sensors properties in terms of spatial and spectral resolution
- spectral response of crops under specific growth conditions
- utilisation of different bands of EMR to describe crop status using existing or newly developed VIs

Hence, describing complex relationships between specific crops, sensors, and imagery based on results of various research experiments is indispensable for introducing new more precise technologies.

Studies included in this Dissertation were conducted to verify the following hypotheses:

H1: Different spectral settings of selected commercial and free-available sensors have no impact on their capability to predict crop yield

H2: Remotely sensed thermal data reflect the within-field variability of soil conditions represented by soil electrical conductivity (EC)

H3: Analysis of multispectral satellite data can help to evaluate the effect of specific soil treatments via crop status-related spectral indices

In terms of the adoption and application of new technologies, Maat (2011) summarised that the nature of agricultural experiments is now characterised by a growing distance between farmers and actual scientific results. That was highlighted also in the study of Pathak et al. (2019). The adoption of new PA-oriented technologies always requires a certain degree of skills and knowledge, which could be problematic. Future research should focus on inventing such technologies that are more suitable for end-users emphasising low costs and simple operation (Cisternas et al., 2020). Therefore, the following hypothesis has been formulated:

H4: Advanced knowledge of major spectral analysis principles can be leveraged for the development of new affordable technological solutions for vegetation monitoring.

4 Objectives

The Dissertation Thesis aimed to verify or disprove the above-arisen hypotheses concerning the utilisation of spectral analysis in agricultural research. To do so, several studies were conducted specifically oriented on particular questions.

O1: Spectral resolution and bandwidth of selected sensors were compared and evaluated in terms of the capability of crop yield prediction.

O2: The relation between RS data and soil conditions was examined since the plant-soil environment is a complex interacting ecosystem. Spatial variability of the thermal response of vegetation was compared with soil conductivity data to evaluate the relationship between these two variables.

O3: Studies were conducted to describe the crop status response on fertilisation management utilising soil amendments NeOsol and Z'Fix.

O4: The acquired knowledge of spectral analysis principles was leveraged for developing a new affordable handheld sensor that met the requirements of low financial cost and simple operation scheme while still providing data with a significant level of accuracy.

5 Materials and Methods

In this chapter, methodologies of the below-presented studies are summarised. A detailed description of specific experimental material and research methods used is provided in particular sections of Appendices 1-5.

5.1 Experimental Sites and Crops

For particular purposes of the studies related to this Dissertation, experimental agricultural fields with various sizes were utilised (with one exception: Appendix 5). Thus, both RS and terrestrial sampling were undertaken on vegetation in real field conditions. All examined plots were located in the Czech Republic, Central and Eastern Bohemia respectively.

Comparison of selected sensors in terms of yield prediction was based on data acquired within two plots. An experimental field of the Crop Research Institute in Prague-Ruzyně with an area of 11.5 ha and a 26.4 ha field in Vendolí were utilised. Both plots were managed according to local common practice and during the examined seasons of 2007 and 2015, spring barley and winter barley were cropped.

The study on soil EC was undertaken in 2017 within a field in Sojovice on winter wheat. This particular experimental plot is subdivided into three smaller fields with the areas 5.8 ha, 8.4 ha, and 10 ha and is considerably variable in terms of soil conditions. This fact is yearly depicted also by a specific vegetation pattern.

For the crop status assessment influenced by soil amendments NeOsol and Z'Fix, experimental plots divided into specific fertilisation variants were used. Such small-plots had variable areas, from 0.63 ha to 5 ha. These studies were undertaken over several cropping seasons; thus, various crops were investigated, namely winter wheat, corn, sugar beet, and poppy seed.

Only in the case of the last study dealing with the novel handheld sensor development experimental plant material from controlled conditions was used. Winter rapeseed was planted in the phytotron of the Crop Research Institute in Prague under controlled temperature and light conditions. Variable doses of nitrogen were supplied to a set of 50 plants to produce a sampling material with different nutrition status. The nutrition variability was essential for the sensor calibration and validation process in terms of demonstrating the ability to sufficiently describe LCC variation. Winter

rapeseed was selected for such purposes for several reasons. Besides it is one of the most common crops in the Czech Republic, rapeseed leaves size was found more convenient for initial measurement than for example winter wheat with relatively narrow leaves. Finally, the experimental material of winter rapeseed was prepared in a relatively short time-period, since only two true leaves were required by the methodology of the following measurement.

5.2   Data Sources and VIs

Both commercial and freely available sources of RS data were used. Commercial data often provide finer spatial and spectral resolution, their utilisation is, however, limited by the costs of a single image. Besides purchased imagery sensed by the QuickBird, SPOT-7, and WorldView satellites, freely available images of Landsat-5, Landsat-7, Landsat-8, and Sentinel-2 were analysed. However, mostly the data from the Sentinel satellite constellation were used, since both spatial and temporal resolution is convenient for agricultural studies of such kind. Actual, but also historical data acquired by any of the Landsat satellites are free to be downloaded from the USGS Global Visualization Viewer[12]. Sentinel imagery is freely available on the Copernicus Open Access Hub[13]. The commercial imagery was ordered and purchased from the ARCDATA PRAHA[14], a company that provides not only satellite imagery, but also different kinds of software for its processing.

Spatial data was acquired also using UAV. A lightweight fixed-wing drone eBee (SenseFly, Cheseaux-sur-Lausanne Switzerland) first carried a thermal sensor thermoMap (SenseFly, Cheseaux-sur-Lausanne Switzerland) that provided the data on canopy temperature. During the second flight, eBee was equipped with a multispectral sensor multiSPEC 4C (SenseFly, Cheseaux-sur-Lausanne Switzerland) to record the vegetation reflectance in multispectral bands.

All acquired multispectral RS data was processed to derive VIs (Table 1) to describe a crop status over the investigated area of interest.

---

[12] https://glovis.usgs.gov/

[13] https://scihub.copernicus.eu/dhus/#/home

[14] https://www.arcdata.cz/

Properties	Index	Formula	Reference
biomass, crop yield	NDVI (Normalized Difference Vegetation Index)	(NIR-Red)/(NIR+Red)	Rouse et al., 1974
leaf area	LAI (Leaf Area Index)	3.618*EVI-0.118	Boegh et al., 2002
water content, water stress	NDWI (Normalized Difference Water Index)	(NIR-SWIR)/ (NIR+SWIR)	Gao, 1996

Table 1. Vegetation Indices and their application potential (edited according to Index DataBase[15]).

Note: EVI = Enhanced Vegetation Index (Huete et al., 2002).

Handheld sensors also played a crucial role in data acquisition. The GreenSeeker (GS) (Trimble, Sunnyvale, California, USA) was used to determine an NDVI value within selected sampling points across the investigated agricultural fields. SPAD-502Plus (Konica Minolta, Tokyo, Japan) has been used over many studies and its SPAD value has been proven to significantly reflect the LCC (Uddling et al., 2007). Therefore, it has been chosen as a reference for calibration and validation of the newly developed handheld sensor.

5.3 Software for Data Processing

Calculation of VI involves a simple mathematical operation with the image bands. These operations could be conducted either in specialised software with a user interface, or the image could be processed directly using any of several programming languages. In the beginning, imagery pre-processing, and indices calculations were undertaken in specialised commercial software ENVI 5.4 (Exelis Visual Information Solutions, Boulder, Colorado, USA) and ArcGIS 10.5 (ESRI, Redlands, California, USA) was used for the following indices and other raster or vector data processing and presentation. Later, primarily open-source tools, such as ESA SNAP (ESA) and QGIS

---

[15] https://www.indexdatabase.de/

(QGIS Development Team) as the two alternatives to commercial software were utilised. However, the most convenient solution became the API of Google Earth Engine[16] (GEE) since it enables to conduct of the full process image analysis based on a custom script written in JavaScript (alternatively in Python). This process involves all steps from i) selecting cloud-free images in the desired time range, to ii) their analysis, and ii) final extraction of the results. The major advantage of this approach is the possibility of processing the data in batches without the necessity to download it and process it one by one.

Statistics were conducted in all cases in the actual version of R in the R Studio (R Core Team), using specific available packages.

5.4   Statistical Analysis

Results of the spectral analysis, whether it was canopy temperature or one of derived VIs, were statistically tested i) on their relation to reference in-field measurements, or ii) to determine potential significant differences among the variants.

In the first case, a test of association between two variables, using Pearson's correlation coefficient was determined. In the second case, the analysis of variance was undertaken. Based on the distribution of the dependent variable either non-parametric Kruskal-Wallis's test or parametric ANOVA was applied.

Statistical analysis regarding the prototype of the new handheld sensor is given separately below (chapter 5.5).

5.5   Rasp2SPAD Prototype Development

The development of the prototype was preceded by a literature review focusing on the determination of the most common disadvantages of current low-cost handheld solutions. A device named *Rasp2SPAD* was developed in order to estimate the SPAD value while reflecting the most cited issues. The essential part of the prototype was a single board computer (Raspberry Pi 3B+) supplemented by other components, such as Raspberry Pi Camera, LED, textile diffuser, and micro-SD card. Eventually, a piece of hardware of convenient size was finalised by encapsulating it in a 3D print case.

Simplified, the methodology behind the SPAD value estimate is based on capturing and analysis of a simple colour image. Based on the literature review, mostly

---

[16] https://earthengine.google.com/

used VIs were determined and automatically calculated by Rasp2SPAD, to further help to assess a calibration equation for the SPAD value estimate. The process of measurement itself was controlled by a Python-based source code and it is therefore highly modifiable for future adjustments.

The Rasp2SPAD testing run on winter rapeseed experimental plant material involved 100 leaves measurement performed by both the Rasp2SPAD prototype and commercial sensor SPAD-502Plus, which was established as a reference. Following statistical analysis was conducted first to describe correlations between VIs (Pearson's correlation coefficient). The dataset eventually contained 89 valid records that were further divided into i) training dataset (containing 60 randomly selected values), and ii) testing dataset (remaining 29 values). Three different approaches were taken to estimate the SPAD value based on acquired parameters. The fitting of a simple linear model (SLM) and a generalised linear model (GLM) was done as a stepwise optimization by removing non-significant parameters. Eventually, two calibration equations were produced and evaluated. The artificial neural network (ANN) approach was also applied to estimate the SPAD value based on 100 successful runs.

6 Results and Discussion

By comparing selected RS and handheld sensors their capability to predict crop yield via NDVI was determined (Appendix 1). Results of the correlation analysis between NDVI and crop yield data are given by Table 4 (Appendix 1). Praha-Ruzyně plot indicated the strongest correlation for both Landsat-5 and QuickBird data (r=0.861, r=0.861) in 2007. Winter barley was at growth stage BBCH 59 indicating a fully emerged plant. On the same plot (Praha-Ruzyně) the relationship was weaker in 2015 using the Landsat-8 and WorldView-2 (r=0.264, r=0.133). Here, the growth stage was BBCH 21-22 meaning early tillering. Eventually, a plot with spring barley (2015) in Vendolí sensed by Landsat-8 and the SPOT-7 satellite gave correlation with the yield data (r=0.341, r=0.565). The crop was at BBCH 75 that describes medium milk in the kernel. As presented, the performance of a particular sensor differs, nevertheless, the differences were found rather across investigated plots and seasons. Overall information about specific sensor performance is valuable, although not well comparable since the sensors evaluated various plots in different crop growth stages. According to the study of Fetch et al. (2004), the coefficient of determination for yield prediction using NDVI is highest between BBCH 47 and BBCH 73. Results of Appendix 1 concur with this statement since the correlation was strongest in BBCH 59 with no regard to the sensor used.

When evaluating summary statistics of NDVI (Appendix 1: Table 6), several results are observable. First, Landsat images provide higher maximum, mean, and standard deviation values compared to other commercial sensors. It can be explained by the differences in Red and NIR bandwidth among the sensors (Appendix 1: Table 3). All commercial sensors have a wider band range than any Landsat sensor. Narrower bandwidth, therefore, seems to produce higher NDVI values. The second fact obtained from summary statistics is that resampling of commercial imagery to a coarser spatial resolution (30 m), which meant a significant reduction of the number of pixels, almost did not change the summary statistic values. In the case of WV-2, however, it reduced correlation coefficient significance.

GS data was available only in the 2015 cropping season, its results were therefore evaluated separately while compared to results of Landsat imagery only (Appendix 1: Table 5). Here, very ambiguous results were gained. On the Ruzyně plot, GS values were not able to correlate with yield. Some correlation was found with Landsat-8, more significant later in the season. On the contrary, GS data was very well correlated with both the yield and Landsat-8 in Vendolí. Landsat-7 was correlated neither with yield nor with GS.

This study (Appendix 1) demonstrated that different bandwidth of selected sensors does not significantly impact the NDVI index performance (Appendix 1: Table 6), however, it was indicated that Landsat imagery tends to produce higher NDVI statistics. The growth stage seemed to strongly influence the crop yield prediction of winter barley, spring barley respectively. Therefore, the sensing should be scheduled accordingly.

The NDVI index is utilised not only as a tool for yield prediction. It also helps to determine the overall crop health status and biomass. In the case of the study presented in Appendix 2, it was used to depict the within-field variability of vegetation. Highly variable spatial pattern in the winter wheat canopy (Appendix 2: Figure 2) was evaluated also by thermal imaging. The relationship of these two crop variables with soil conditions represented by soil EC was evaluated.

Strong correlations were found between all three parameters (Appendix 2: Figure 3). Canopy temperature (Tc) was negatively correlated with both EC (r=-0.82) and NDVI (r=-0.86). Conversely, NDVI and EC were found to be positively correlated (r=0.86). Hence, the higher temperature of the plant cover indicates lower biomass and conductivity inhibition. Regression analysis then determined the trend of EC relationship with Tc (R^2=0.671) and NDVI (R^2=0.742) (Appendix 2: Figure 4 a,b). Eventually, it was concluded that EC spatial distribution is closely related to canopy characteristics derived from RS data, such as Tc and healthy biomass indicator NDVI. This finding might help to explain spatial variability in crop status when the impact of topography and topography-related soil features (water and nutrient irregular distribution) are excluded.

Soil-plant relation is a complex environment. Crop status depends heavily on soil conditions since soil properties define the water and nutrient uptake potential. Z'Fix is a farmyard manure agent that should enhance several soil characteristics.

Therefore, its secondary impact on crop status was evaluated (Appendix 3). ANOVA with the random effect of the term was performed for each of the three investigated seasons, crops respectively (Appendix 3: Table 4). In all cases, significant differences were found among variants (control – C, pure manure – FYM, manure enriched by Z'Fix – FYM_ZF). By a poppy seed in 2019, where the best performing variant changes during the cropping period, the effect was uncertain. However, sugar beet in 2018 and winter wheat in 2020 both indicated the highest NDVI values within FYM_ZF. Enhanced crop conditions also resulted in the highest crop yield in all seasons, although significantly different was only the FYM_ZF variant and the C. FYM_ZF and FYM variants were non-significant. Nevertheless, the positive trend is obvious, concerning both the crop status and yield. This beneficial effect of soil organic matter (SOM) enriched by the Z'Fix agent was also observable during very dry periods, especially in July and August 2018 (Appendix 3: Figure 1). This result only confirms the statement of Šařec et al. (2017b) that Z'Fix addition can mitigate the vegetation stress in conditions of drought.

Similarly, the potential effect of the soil agent NeOsol on soil properties and crop status was investigated (Appendix 4) via three spectral indices: NDVI, NDWI, and LAI (Appendix 4: Figure 4). Analysis of variance with the random effect of term followed by multiple comparisons gave a complex overview about differences between variants. Concurrently, it provided a timeline that described the trend of selected indices through the period of four years (Appendix 4: Table 4). Although no significant difference was indicated between any specific manure type in pure and NeOsol enriched form, the trend of increasing differences across all variants is observable. An interesting result for example was the significant difference of LAI within cattle and poultry manure treatment in 2020. Other combinations of pure manure variants were not found significantly different. In 2020, significant differences of NPK variant, NPK with NeOsol respectively, with all the other treatments were indicated by all three spectral indices. These differences were negative in all cases, meaning that the major factor influencing the favourable crop condition is very likely any kind of SOM and not the addition of the soil agent NeOsol.

The process of development, calibration, and validation of a novel handheld sensor for vegetation monitoring is given in Appendix 5. Major issues of available low-cost sensors determined based on a literature review are i) intrusion of the natural

light, and ii) the necessity of post-processing the data using external software. The prototype called Rasp2SPAD (Appendix 5: Figure 1) eliminated both issues. Based on 22 parameters derived from the colour image SPAD value was estimated. The calibration equations for winter rapeseed were determined as given in Equation 1 and Equation 2 (Appendix 5). SLM and GLM estimates were both tested against the actual SPAD value given by the SPAD-502Plus handheld sensor. Both have proven relatively high accuracy of the estimate, R^2=0.81 (Appendix 5: Figure 7), nevertheless, GLM estimated the SPAD value with a slightly lower mean absolute difference (Appendix 5: Tables 4 and 5). Surprisingly, both models evaluated two parameters from the YUV colour model as the most useful: Cb (blue chroma component) and Cr (red chroma component). Since the chroma components represent solely the colour because the brightness fraction is described by Y (luma component), it was concluded that chroma components might be more sensitive to colour variations while assessing the nutrition saturation level of a plant.

Naturally, crop-specific calibration equations need to be determined and incorporated. However, by now, the prototype has proven to deliver valuable data describing the crop status of winter rapeseed.

7 Conclusion

Results of the studies presented by this Dissertation have proven that spectral imaging is a powerful tool in current agricultural research and practice. It provides valuable information about crop status acquired in a non-destructive manner, which is one of the major advantages of using such methods. Moreover, by utilising any of the remote sensing platforms to carry the sensor rather than the handheld sensor, spatially related information is obtained. That helps to understand the spatial variability of crop and soil characteristics within the investigated agricultural plot.

The amount of relationships that need to be described in order to precise the methodology and prove it for standard practical use is considerable. These relationships involve crops, soil types, agricultural management, meteorological conditions, and also sensor settings, and image resolution (spatial, spectral, temporal). Some of these relationships were investigated by presented studies.

By comparing selected sensors, Hypothesis 1 was confirmed, hence, that bandwidth of utilised spectral bands does not impact the crop yield prediction potential via NDVI. However, more detailed research on this topic was suggested. It is always important to select the appropriate sensor regarding the actual research question, nevertheless, it is also crucial to focus the sensing in the most sensitive growth stage. That might, however, differ among crops and VIs.

Hypothesis 2 was confirmed by the study describing the association of soil EC and canopy characteristics (NDVI, Tc). The thermal response of the vegetation to some extent reflects the soil conditions, namely soil EC that is claimed to be further related to the soil moisture and pH. This finding is beneficial since soil sampling is often expensive (equipment) and time-consuming (sampling).

Hypothesis 3 was both verified and disproved. Spectral imaging and analysis were able to reflect the crop status variability in the case of Z'Fix manure agent. However, results were not significant when soil amendment NeOsol was used. These ambiguous results are very likely associated with the soil amendment used itself. The utilisation of RS methods to describe crop status caused by enhanced soil conditions is a complex task and is affected by many factors. Nevertheless, RS methods can be used not only for spatial variability of investigated VI, canopy features respectively. The temporal variability is also a crucial indicator. Since there is open-source imagery

available in longer time-periods, VI timelines help to reveal the time effect of investigated soil treatments. These timelines might be further compared with the trend of meteorological conditions (temperature and precipitation mostly). Such analysis might elucidate the crop performance within investigated variants of the experiment for example under drought conditions.

In order to verify Hypothesis 4, a prototype of a low-cost handheld sensor named Rasp2SPAD was developed and calibrated for winter rapeseed chlorophyll status monitoring. It was demonstrated that such custom-made handheld sensors can produce reliable data for the 5% price of the commercial sensor. Since only low-cost components were utilised and a source code is available under an open-source licence, Rasp2SPAD might now be constructed and used by anybody with the basic knowledge of electronics. The prototype was constructed to be modifiable regarding both hardware and software, which assures its high potential to be adjusted to other plant species in future studies.

References

Ahluwalia, O., Singh, P. C., & Bhatia, R. (2021). A review on drought stress in plants: Implications, mitigation and the role of plant growth promoting rhizobacteria. *Resources, Environment and Sustainability*, *5*, 100032. https://doi.org/10.1016/j.resenv.2021.100032

Ali, M. M., Al-Ani, A., Eamus, D., & Tan, D. K. Y. (2012). A New Image Processing Based Technique to Determine Chlorophyll in Plants. *American-Eurasian Journal of Agricultural and Environmental Sciences*, *12*(10), 1323–1328. https://doi.org/10.5829/idosi.aejaes.2012.12.10.1917

Anderson, R., Bayer, P. E., & Edwards, D. (2020). Climate change and the need for agricultural adaptation. *Current Opinion in Plant Biology*, *56*, 197–202. https://doi.org/10.1016/j.pbi.2019.12.006

Aroca, R. (2012). *Plant responses to drought stress : from morphological to molecular features*. Springer.

Bairoch, P. (1991). *Cities and economic development : from the dawn of history to the present*. University of Chicago Press. https://books.google.de/books?id=Cg7JYZO_nEMC&dq=neolithic+revolution &hl=cs&source=gbs_navlinks_s

Barnes, A. P., Soto, I., Eory, V., Beck, B., Balafoutis, A., Sanchez, B., Vangeyte, J., Fountas, S., van der Wal, T., & Gómez-Barbero, M. (2019). Influencing incentives for precision agricultural technologies within European arable farming systems. *Environmental Science & Policy*, *93*, 66–74. https://doi.org/10.1016/j.envsci.2018.12.014

Barnes, E. M., Clarke, T. R., Richards, S. E., Colaizzi, P. D., Haberland, J., Kostrzewski, M., Waller, P., Choi C., R. E., Thompson, T., Lascano, R. J., Li, H., & Moran, M. S. (2000). Coincident detection of crop water stress, nitrogen status and canopy density using ground based multispectral data. *Proc. 5th Int. Conf. Precis Agric*, *January*.

Bauer, M. E. (1985). Spectral inputs to crop identification and condition assessment. *Proceedings of the IEEE*, *73*(6), 1071–1085.

https://doi.org/10.1109/PROC.1985.13238

Bielińska, E. J., Futa, B., Bik-Mołodzińska, M., Szewczuk, C., Sugier, D., Bielińska, E. J., Futa, B., Bik-Mołodzińska, M., Szewczuk, C., & Sugier, D. (2013). The Impact of Fertilizing Agents on the Enzymatic Activity of Soils. *Journal of Research and Applications in Agricultural Engineering*, *58*(3).

Boegh, E., Soegaard, H., Broge, N., Schelde, K., Thomsen, A., Hasager, C. B., & Jensen, N. O. (2002). Airborne multispectral data for quantifying leaf area index, nitrogen concentration, and photosynthetic efficiency in agriculture. *Remote Sensing of Environment*, *81*(2–3), 179–193. https://doi.org/10.1016/S0034-4257(01)00342-X

Borowiak, K., Niewiadomska, A., Sulewska, H., Szymanska, G., Gluchowska, K., & Wolna-Maruwka, A. (2016). Effect of PRP SOL and PRP EBN Nutrition on Yield, Photosynthesis Activity and Soil Microbial Activity of Three Cereal Species. *Fresenius Environmental Bulletin*, *25*(6), 2026–2035.

Borra, S., Thanki, R., & Dey, N. (2019). *Satellite image analysis : clustering and classification.* Springer. https://books.google.cz/books?id=akWHDwAAQBAJ&dq=image+spatial+resolution&hl=cs&source=gbs_navlinks_s

Cisternas, I., Velásquez, I., Caro, A., & Rodríguez, A. (2020). Systematic literature review of implementations of precision agriculture. *Computers and Electronics in Agriculture*, *176*, 105626. https://doi.org/10.1016/j.compag.2020.105626

Conway, G., & Barbier, E. (2013). *After the Green Revolution: Sustainable agriculture for development.* Routledge. https://books.google.cz/books?id=mSr_AQAAQBAJ&dq=green+revolution&hl=cs&source=gbs_navlinks_s

Cortazar, B., Koydemir, H. C., Tseng, D., Feng, S., & Ozcan, A. (2015). Quantification of plant chlorophyll content using Google Glass. *Lab on a Chip*, *15*(7), 1708–1716. https://doi.org/10.1039/C4LC01279H

Davoudi, S., Crawford, J., & Mehmood, A. (2009). *Planning for climate change : strategies for mitigation and adaptation for spatial planners.* Earthscan. https://books.google.de/books?id=rnEfm7tok4cC&dq=climate+change&hl=cs&source=gbs_navlinks_s

Duhan, J. S., Kumar, R., Kumar, N., Kaur, P., Nehra, K., & Duhan, S. (2017).

Nanotechnology: The new perspective in precision agriculture. *Biotechnology Reports*, *15*, 11–23. https://doi.org/10.1016/J.BTRE.2017.03.002

ESA (2022). Sentinel-2 - Missions. Retrieved January 18, 2022, from https://sentinel.esa.int/web/sentinel/missions/sentinel-2

Evans, J. R. (1983). Nitrogen and Photosynthesis in the Flag Leaf of Wheat (Triticum aestivum L.). *Plant Physiology*, *72*(2), 297–302. https://doi.org/10.1104/pp.72.2.297

Fetch, T. G., Steffenson, Jr., B. J., & Pederson, V. D. (2004). Predicting agronomic performance of barley using canopy reflectance data. *Canadian Journal of Plant Science*, *84*(1), 1–9. https://doi.org/10.4141/P02-195

Filella, I., Serrano, L., Serra, J., & Peñuelas, J. (1995). Evaluating Wheat Nitrogen Status with Canopy Reflectance Indices and Discriminant Analysis. *Crop Science*, *35*(5), 1400–1405. https://doi.org/10.2135/cropsci1995.0011183X003500050023x

Gao, B. C. (1996). NDWI—A normalized difference water index for remote sensing of vegetation liquid water from space. *Remote Sensing of Environment*, *58*(3), 257–266. https://doi.org/10.1016/S0034-4257(96)00067-3

Gitelson, A. A., Stark, R., Grits, U., Rundquist, D., Kaufman, Y., & Derry, D. (2002). Vegetation and soil lines in visible spectral space: A concept and technique for remote estimation of vegetation fraction. *International Journal of Remote Sensing*, *23*(13), 2537–2562. https://doi.org/10.1080/01431160110107806

Gitelson, Anatoly A., Kaufman, Y. J., & Merzlyak, M. N. (1996). Use of a green channel in remote sensing of global vegetation from EOS-MODIS. *Remote Sensing of Environment*, *58*(3), 289–298. https://doi.org/10.1016/S0034-4257(96)00072-7

Gregory, P. J., & Nortcliff, S. (2012). *Soil Conditions and Plant Growth*. John Wiley & Sons.

Hall, A. E. (Anthony E. (2000). *Crop responses to environment*. CRC Press. https://books.google.cz/books?id=cZTMBQAAQBAJ&dq=Crop+Responses+to+Environment&hl=cs&source=gbs_navlinks_s

Hnilička, F., & Středa, T. (2016). *Rostliny v podmínkách stresu - abiotické stresory* (F. Hnilička (Ed.)). Česká zemědělská univerzita v Praze.

Huete, A., Didan, K., Miura, T., Rodriguez, E. P., Gao, X., & Ferreira, L. G. (2002).

Overview of the radiometric and biophysical performance of the MODIS vegetation indices. *Remote Sensing of Environment*, *83*(1–2), 195–213. https://doi.org/10.1016/S0034-4257(02)00096-2

Hunt Jr, R., & Rock, B. (1989). Detection of changes in leaf water content using Near-and Middle-Infrared reflectances☆. *Remote Sensing of Environment*, *30*(1), 43–54. https://doi.org/10.1016/0034-4257(89)90046-1

Jain, H. K. (2010). *Green revolution : history, impact and future*. Studium Press LLC. https://books.google.de/books?id=0aC62aMi_ToC&dq=green+revolution&hl=cs&source=gbs_navlinks_s

Krzywy-Gawrońska, E. (2012). Enzymatic Activity of Urease and Degydrogenasein Soil Fertilized With GWDA Compostwith or without a PRPSOL Addition. *Polish Journal of Environmental Studies*, *21*(4), 949–955.

Kumhálová, J., & Moudrý, V. (2014). Topographical characteristics for precision agriculture in conditions of the Czech Republic. *Applied Geography*, *50*, 90–98. https://doi.org/10.1016/j.apgeog.2014.02.012

Kumhálová, J., Zemek, F., Novák, P., Brovkina, O., & Mayerová, M. (2014). Use of Landsat images for yield evaluation within a small plot. *Plant Soil Environment*, *60*(11), 501–506. http://glovis.usgs.gov

Lillesand, T. M., Kiefer, R. W., & Chipman, J. W. (2014). *Remote sensing and image interpretation*. John Wiley & Sons. https://books.google.cz/books?id=AFHDCAAAQBAJ&dq=remote+sensing+and+image+interpretation&hl=cs&source=gbs_navlinks_s

Lippitt, C. D., Stow, D. A., & Coulter, L. L. (2015). *Time-sensitive remote sensing*. Springer. https://books.google.cz/books?id=71DMCQAAQBAJ&dq=remote+sensing+temporal+resolution&hl=cs&source=gbs_navlinks_s

Liu, L., Ji, H., An, J., Shi, K., Ma, J., Liu, B., Tang, L., Cao, W., & Zhu, Y. (2019). Response of biomass accumulation in wheat to low-temperature stress at jointing and booting stages. *Environmental and Experimental Botany*, *157*, 46–57. https://doi.org/10.1016/j.envexpbot.2018.09.026

Loganathan, P. (1987). *Soil quality considerations in the selection of sites for aquaculture*. https://www.fao.org/3/ac172e/AC172E00.htm#TOC

Maat, H. (2011). The history and future of agricultural experiments. *NJAS -*

Wageningen Journal of Life Sciences, *57*(3–4), 187–195. https://doi.org/10.1016/J.NJAS.2010.11.001

Mäder, P., Fließbach, A., Dubois, D., Gunst, L., Fried, P., & Niggli, U. (2002). Soil fertility and biodiversity in organic farming. *Science*, *296*(5573), 1694–1697. https://doi.org/10.1126/SCIENCE.1071148/SUPPL_FILE/MAEDERSUPPL.PDF

Maheswari, M., Yadav, S. K., Shanker, A. K., Kumar, M. A., & Venkateswarlu, B. (2012). Overview of Plant Stresses: Mechanisms, Adaptations and Research Pursuit. In *Crop Stress and its Management: Perspectives and Strategies* (pp. 1–18). Springer Netherlands. https://doi.org/10.1007/978-94-007-2220-0_1

Meyer, G. E., & Neto, J. C. (2008). Verification of color vegetation indices for automated crop imaging applications. *Computers and Electronics in Agriculture*, *63*(2), 282–293. https://doi.org/10.1016/j.compag.2008.03.009

Minhas, P. S., Rane, J., & Pasala, R. K. (2017). Abiotic Stresses in Agriculture: An Overview. In *Abiotic Stress Management for Resilient Agriculture* (pp. 3–8). Springer Singapore. https://doi.org/10.1007/978-981-10-5744-1_1

Misra, T., Priyadarshini, S., Arora, A., Marwaha, S., Roy, H. S., & Ray, M. (2018). A comparative study of chlorophyll content estimation techniques through image analysis. In *Journal of Crop and Weed* (Vol. 14, Issue 3).

Mittler, R. (2006). Abiotic stress, the field environment and stress combination. *Trends in Plant Science*, *11*(1), 15–19. https://doi.org/10.1016/J.TPLANTS.2005.11.002

Moldan, B. (2015). *Podmaněná planeta*. https://books.google.de/books?id=OpWKCwAAQBAJ&dq=moldan+2015&hl=cs&source=gbs_navlinks_s

National Drought Mitigation Center. (2022). *Types of Drought*. https://drought.unl.edu/Education/DroughtIn-depth/TypesofDrought.aspx

Pathak, H. S., Brown, P., & Best, T. (2019). A systematic literature review of the factors affecting the precision agriculture adoption process. *Precision Agriculture*, *20*(6), 1292–1316. https://doi.org/10.1007/S11119-019-09653-X

Paxton, K. W., Mishra, A. K., Chintawar, S., Roberts, R. K., Larson, J. A., English, B. C., Lambert, D. M., Marra, M. C., Larkin, S. L., Reeves, J. M., & Martin, S. W. (2011). Intensity of Precision Agriculture Technology Adoption by Cotton Producers. *Agricultural and Resource Economics Review*, *40*(1), 133–144.

https://doi.org/10.1017/S1068280500004561

Penuelas, J., Filella, I., Biel, C., Serrano, L., & Savé, R. (1993). The reflectance at the 950–970 nm region as an indicator of plant water status. *International Journal of Remote Sensing*, *14*(10), 1887–1905. https://doi.org/10.1080/01431169308954010

Pérez-Patricio, M., Camas-Anzueto, J., Sanchez-Alegría, A., Aguilar-González, A., Gutiérrez-Miceli, F., Escobar-Gómez, E., Voisin, Y., Rios-Rojas, C., & Grajales-Coutiño, R. (2018). Optical Method for Estimating the Chlorophyll Contents in Plant Leaves. *Sensors*, *18*(2), 650. https://doi.org/10.3390/s18020650

Perkins, J. H. (1997). *Geopolitics and the green revolution : wheat, genes, and the cold war*. Oxford University Press. https://books.google.de/books?id=hRcwrm_YW2UC&dq=green+revolution&hl=cs&source=gbs_navlinks_s

Pham, X., & Stack, M. (2018). How data analytics is transforming agriculture. *Business Horizons*, *61*(1), 125–133. https://doi.org/10.1016/j.bushor.2017.09.011

Poonia, R. C., Gao, X.-Z., Raja, L., Sharma, S., & Vyas, S. (2018). *Smart farming technologies for sustainable agricultural development*. IGI Global. https://books.google.de/books?id=nG5lDwAAQBAJ&hl=cs&source=gbs_navlinks_s

Porro, D., & Pedò, S. (2016). Implication of nutrition on root development. *Acta Horticulturae*, *1136*, 193–200. https://doi.org/10.17660/ACTAHORTIC.2016.1136.26

Psomiadis, E., Dercas, N., Dalezios, N. R., & Spyropoulos, N. V. (2016). The role of spatial and spectral resolution on the effectiveness of satellite-based vegetation indices. *Remote Sensing for Agriculture, Ecosystems, and Hydrology XVIII*, *9998*, 99981L. https://doi.org/10.1117/12.2241316

Putman, R. J., & Wratten, S. D. (2012). *Principles of Ecology*. Springer Science & Business Media. https://books.google.cz/books?id=MTPpCAAAQBAJ&dq=tolerance+curve+ecology&hl=cs&source=gbs_navlinks_s

Qi, J., Chehbouni, A., Huete, A. R., Kerr, Y. H., & Sorooshian, S. (1994). A modified soil adjusted vegetation index. *Remote Sensing of Environment*, *48*(2), 119–126.

https://doi.org/10.1016/0034-4257(94)90134-1

Richards, J. A. (2013). *Remote Sensing Digital Image Analysis : An Introduction*. Springer Science & Business Media. https://books.google.cz/books?id=k9LqCAAAQBAJ&dq=Remote+sensing+digital+image+analysis&hl=cs&source=gbs_navlinks_s

Richardson, A. D., Duigan, S. P., & Berlyn, G. P. (2002). An evaluation of noninvasive methods to estimate foliar chlorophyll content. *New Phytologist*, *153*(1), 185–194. https://doi.org/10.1046/j.0028-646X.2001.00289.x

Rouse, R. W. H., Haas, J. A. W., Schell, J. A., & Deering, D. W. (1974). Monitoring Vegetation Systems in the Great Plains with ERTS. *Proceedings Third ERTS-1 Symposium*, 351. https://ntrs.nasa.gov/search.jsp?R=19740022614

Šařec, P., Látal, O., & Novák, P. (2017a). Technological and economic evaluation of manure production using an activator of biological transformation. *Research in Agricultural Engineering*, *63 (2017)*(Special Issue), S59–S65. https://doi.org/10.17221/50/2017-RAE

Šařec, P., Novák, P., & Kumhálová, J. (2017b). Impact of activators of organic matter on soil and crop stand properties in conditions of very heavy soils. *Engineering for Rural Development*, *16*, 486–491. https://doi.org/10.22616/ERDev2017.16.N095

Sulewska, H., Koziara, W., Szymańska, G., Niewiadomska, A., Majchrzak, L., & Panasiewicz, K. (2012). Potatoes reaction on PRP SOL fertilisation. *Journal of Research and Applications in Agricultural Engineering*, *Vol. 57*(nr 4), 116–121.

Tavakoli, H., & Gebbers, R. (2019). Assessing Nitrogen and water status of winter wheat using a digital camera. *Computers and Electronics in Agriculture*, *157*, 558–567. https://doi.org/10.1016/j.compag.2019.01.030

Thenkabail, P. S. (2015). *Remotely sensed data characterization, classification, and accuracies*. CRC Press. https://books.google.cz/books?id=3xyvCgAAQBAJ&dq=radiometric+resolution&hl=cs&source=gbs_navlinks_s

Tomera, A. N. (2001). *Understanding Basic Ecological concepts*. Walch Publishing. https://books.google.de/books?id=X_EVePtJVzMC&dq=ecology+food+pyramid&hl=cs&source=gbs_navlinks_s

USGS (2022). Landsat Satellite Missions. Retrieved January 18, 2022, from

https://www.usgs.gov/landsat-missions/landsat-satellite-missions

Uddling, J., Gelang-Alfredsson, J., Piikki, K., & Pleijel, H. (2007). Evaluating the relationship between leaf chlorophyll concentration and SPAD-502 chlorophyll meter readings. *Photosynthesis Research*, *91*(1), 37–46. https://doi.org/10.1007/s11120-006-9077-5

United Nations Department of Economic and Social Affairs Population Division. (2019). *Ten Key findings*.

Venkateswarlu, B., Shanker, A. K., Shanker, C., & Maheswari, M. (2012). *Crop stress and its management : perspectives and strategies*. Springer Science Business & Media B.V. https://books.google.cz/books?id=H7D0ps9SnE0C&dq=Crop+Stress+and+its+ Management:+Perspectives+and+Strategies&hl=cs&source=gbs_navlinks_s

Vesali, F., Omid, M., Kaleita, A., & Mobli, H. (2015). Development of an android app to estimate chlorophyll content of corn leaves based on contact imaging. *Computers and Electronics in Agriculture*, *116*, 211–220. https://doi.org/10.1016/j.compag.2015.06.012

Wagner, W., Francisco, J. P., Flumignan, D. L., Marin, F. R., & Folegatti, M. V. (2022). Optimized algorithm for evapotranspiration retrieval via remote sensing. *Agricultural Water Management*, *262*, 107390. https://doi.org/10.1016/j.agwat.2021.107390

Wang, J., Xu, R., & Yang, S. (2009). Estimation of plant water content by spectral absorption features centered at 1,450 nm and 1,940 nm regions. *Environmental Monitoring and Assessment*, *157*(1–4), 459–469. https://doi.org/10.1007/s10661-008-0548-3

Wani, S. H., & Kumar, V. (2020). *Heat stress tolerance in plants : physiological, molecular and genetic perspectives*.

Wilhite, D. A., & Glantz, M. H. (1985). Understanding: the Drought Phenomenon: The Role of Definitions. *Water International*, *10*(3), 111–120. https://doi.org/10.1080/02508068508686328

Xue, J., & Su, B. (2017). Significant Remote Sensing Vegetation Indices: A Review of Developments and Applications. *Journal of Sensors*, *2017*, 1–17. https://doi.org/10.1155/2017/1353691

Yost, M. A., Kitchen, N. R., Sudduth, K. A., Sadler, E. J., Drummond, S. T., &

Volkmann, M. R. (2017). Long-term impact of a precision agriculture system on grain crop production. *Precision Agriculture*, *18*(5), 823–842. https://doi.org/10.1007/S11119-016-9490-5/FIGURES/8

Žalud, Z., Trnka, M., & Hlavinka, P. (2020). *Zemědělské sucho v České Republice*. Agrární komora České republiky. https://www.intersucho.cz/userfiles/file/ZemedelskeSucho.pdf

Zhang, Q. (2016). *Precision agriculture technology for crop farming*. CRC Press, Taylor & Francis Group.

List of Appendices

Appendix 1

Křížová, K, & Kumhálová, J. (2017). Comparison of selected remote sensing sensors for crop yield variability estimation. *Agronomy Research, 15*(4), 1636–1645. https://doi.org/10.15159/AR.17.016

Appendix 2

Křížová, K., Haberle, J., Kroulík, M., Kumhálová, J., & Lukáš, J. (2018). Assessment of soil electrical conductivity using remotely sensed thermal data. *Agronomy Research, 16*(3), 784–793. https://doi.org/10.15159/AR.18.111

Appendix 3

Novák, V., Šařec, P., Křížová, K., Novák, P., & Látal, O. (2021). Soil physical properties and crop status under cattle manure and Z'Fix in Haplic Chernozem. *Plant, Soil and Environment, 67*(No. 7), 390–398. https://doi.org/10.17221/159/2021-PSE

Appendix 4

Novák, V., Šařec, P., Křížová, K., Novák, P., & Látal, O. (2022). Potential Impact of Biostimulator NeOsol and Three Different Manure Types on Physical Soil Properties and Crop Status in Heavy Soils Conditions. *Sustainability, 14*(1), 438. https://doi.org/10.3390/SU14010438

Appendix 5

Křížová, K., Kadeřábek, J., Novák, V., Linda, R., Kurešová, G., & Šařec, P. (2022). Using a single-board computer as a low-cost instrument for SPAD value estimation through colour images and chlorophyll-related spectral indices. *Ecological Informatics, 67*, 101496. https://doi.org/10.1016/j.ecoinf.2021.101496

Appendix 1

Comparison of selected remote sensing sensors for crop yield variability estimation

Křížová, K, & Kumhálová, J. (2017). Comparison of selected remote sensing sensors for crop yield variability estimation. *Agronomy Research, 15*(4), 1636–1645. https://doi.org/10.15159/AR.17.016

Comparison of selected remote sensing sensors for crop yield variability estimation

K. Křížová[1,*] and J. Kumhálová[2]

[1]Czech University of Life Sciences in Prague, Faculty of Engineering, Department of Agricultural Machines, Kamýcká 129, CZ165 21 Prague, Czech Republic
[2]Czech University of Life Sciences in Prague, Faculty of Engineering, Department of Machinery Utilization, Kamýcká 129, CZ165 21 Prague, Czech Republic
*Correspondence: krizovak@tf.czu.cz

Abstract. Currently, spectral indices are very common tool how to describe various characteristics of vegetation. In fact, these are mathematical operations which are calculated using specific bands of electromagnetic spectrum. Nevertheless, remote sensing sensors can differ due to the variations in bandwidth of the particular spectral channels. Therefore, the main aim of this study is to compare selected sensors in terms of their capability to predict crop yield by NDVI utilization. The experiment was performed at two locations (Prague-Ruzyně and Vendolí) in the year 2015 for both locations and in 2007 for Prague-Ruzyně only, when winter barley or spring barley grew on the plots. The cloud-free satellite images were chosen and normalised difference vegetation indices (NDVI) were calculated for each image. Landsat satellite images with moderate spatial resolution (30 m per pixel) were chosen during the crop growth for selected years. The other data sources were commercial satellite images with very high spatial resolution – QuickBird (QB) (0.6 m per pixel) in 2007 and WorldView-2 (WV-2) (2 m per pixel) in 2015 for Prague-Ruzyně location; and SPOT-7 (6 m per pixel) satellite image in 2015 for Vendolí location. GreenSeeker handheld crop sensor (GS) was used for collecting NDVI data for both locations in 2015 only. NDVI calculated at each of images was compared with the yield data. The data sources were compared with each other at the same term of crop growth stage. The results showed that correlation between GS and yield was relatively weak at Ruzyně. Conversely, significant relation was found at Vendolí location. The satellite images showed stronger relation with yield than GS. Landsat satellite images had higher values of correlation coefficient (in 30 m spatial resolution) at Ruzyně in both selected years. However, at Vendolí location, SPOT-7 satellite image has significantly better results compared to Landsat image. It is necessary to do more research to define which sensor measurements are most useful for selected applications in agriculture management.

Key words: Remote sensing, crop yield, satellite images, Greenseeker, NDVI.

INTRODUCTION

The concept of Precision Agriculture (PA) has developed as an indispensable reaction to higher population growth over recent decades (Zhang, 2015; United Nations, 2015). Up to 1960s, increasing crop production was enabled by expansion of agricultural areas, however, this trend slowed down when the percentage of arable land reached 9%

of total area worldwide (Moldan, 2015). Vegetation Indices (VI) are one of the tools by which it the concept of PA is currently fulfilled. These mathematical formulas are based on various combinations of reflectance values in specific bands of electromagnetic spectrum. Knowledge of spectral behaviour of vegetation is therefore essential for results interpretation. The method of evaluation canopy characteristics using VI has been gaining importance recently because the whole process operates in a non-destructive mode (Richards, 1993). It is therefore possible to carry out particular analysis repeatedly, for instance in different growth stages (Jones & Vaughan, 2010). A number of studies have been performed to prove the relation between VI and investigated vegetation characteristics, e.g. the study of Hunt Jr. et al. (2013), where triangular greenness index (TGI) was developed and successfully used to indicate leaf chlorophyll content. Prediction models for barley, canola and spring wheat yield were created by Johnson et al. (2016) using Normalized Difference Vegetation Index (NDVI) and Enhanced Vegetation Index (EVI) data. VI may be also utilized for comparison of different hybrids yield, as Marino et al. (2013) did when studying two hybrids of onion productivity.

NDVI is the basic representative of VI's. The algorithm for NDVI calculation was stated by Rouse et al. (1973) as the ratio of reflectance in near infrared (NIR) and red visible region. NDVI is considered as main indicator of greenness, e.g. of dense and healthy vegetation. Its values range from -1.0 to +1.0, where higher values (0.6–0.9) indicate denser vegetation cover (USGS, 2015). Nevertheless, Huete et al. (2002) stated, that NDVI tend to lose sensitivity as the vegetation cover becomes denser.

To acquire desired information about specific vegetation characteristic in form of VI, remotely sensed data are utilized. At present, there are a number of sources that provide such kind of imagery. The data may beacquired by spacecraft or aircraft. These carry devices onboard, that capture Earth's surface either actively or passively (Khorram et al., 2016), therefore remote sensing sensors are divided into active and passive as well. Passive sensors exploit the electromagnetic radiation emitted or reflected from Earth's surface, thus the signal detected comes from outside a sensor. Conversely, active sensors collect information per an artificial signal. Energy is emitted from within the sensor and detected after it is reflected from the surface (Wang & Weng, 2013). In literature, differences between active and passive sensors have been intensively studied. Erdle et al. (2011) tested one passive and three active reflectance sensors to examine how they provide the information about nitrogen content and crop biomass. Another study (Elsayed et al., 2015) dealt with the capability of both types of sensor to estimate Normalized Relative Canopy Temperature (NRCT). GS is a representative of the active sensors. Its signal is emitted towards the target and the amount of reflected radiation is detected. GS convert such data into NDVI directly (Trimble, 2017). On the other hand, satellite data in this study were all acquired by passive sensors. There are differences in desired wavelengths between particular sensors.

It is clear from the above literature review that different methods and sensors can be used for crop yield prediction. Therefore, this study aims to compare selected sensors in terms of their capability to predict crop yield by NDVI utilization.

MATERIALS AND METHODS

Study area

The data for this study were obtained from two experimental fields. The first one (Ruzyně) was situated in Prague-Ruzyně (50°05'N, 14°17'30"E), Czech Republic. A larger part of the field has a southern aspect and the elevation ranges from 338.5 to 357.5 m above average sea level (a.s.l). The size of area is 11.5 ha. The average slope of the field is approximately 6%. The soil of this experimental plot can be classified as Haplic Luvisols partially covering fine calcareous sandstones with higher content of coarse silt and lower content of clay particles and clay. The value of cation exchange capacity in the top layer containing clay is 20–35%. The soil profile is neutral and the sorption capacity is from saturated to fully saturated. Content of available minerals is from good to very good. In the slope positions and in loess loam profiles of Luvisols with remnants of alluvial horizon can be found. Some parts where the topsoil directly overlays the parent material of loess loam are strongly eroded. The average precipitation is 526 mm per year and the average temperature is 7.9 °C.

The second field (Vendolí) was located near to Vendolí in Eastern Bohemia (49°43' 47.94"N, 16°24' 14.21"E), Czech Republic, and it has 26.4 ha. The plot is undulated with the average slope approximately 6%. The elevation ranges from 543 to 571 m a.s.l. The soil of this experimental plot can be classified as modal cambisols lying on calcareous sandstone. Some parts, on sloppy terrain especially, are strongly eroded, while big amount of stones is lying on the top parts of the field. The average precipitation is 700 mm per year and the average temperature is between 6–7 °C.

Conventional arable soil tillage technology based on ploughing was used on these fields. Crop rotation system, based on wheat, barley and oilseed rape crops alternation, is common practice in the Czech Republic. Our experiment included the data from the year 2007 and 2015 for Ruzyně with winter barley and 2015 only for Vendolí with spring barley.

Field data

A combine harvester Sampo 2070 equipped with an LH 500 yield monitor (LH Agro, Denmark) with a DGPS receiver with EGNOS correction measured yield in Ruzyně location. The horizontal and vertical accuracy of this system was ± 0.1 to 0.3 m and ± 0.2 to 0.6 m, respectively. Measured yield data were processed by an on-board computer on the combine harvester and saved together with the location data every 3 s. An axial combine harvester New Holland CR9080 equipped with New Holland factory yield monitor and DGPS receiver with correction measured yield in Vendolí location. The precision of this system horizontally was ± 0.1 to 0.3 m and vertically it was ± 0.2 to 0.6 m. The data were saved with the coordinates every 1 s. The grain moisture content was measured continuously in the case of both fields and the yield was recalculated to 14% moisture content. The yield values were corrected using a common statistical procedure; all values that exceeded the range defined as mean ± 3 standard deviations were removed. Because of the large amount of data for both location studied (more than 8,000), the Method of Moments (MoM) was used to compute the experimental variograms. Experimental variograms of yield were computed and modelled by weighted least-squares approximation in GS+ software (Gamma Design Software, St. Painwell, MI, USA). A detailed description of this method can be found in

1638

Kumhálová et al. (2011). Ordinary punctual kriging was done using the relevant data and exponential variogram model parameters for yield data visualisation.

NDVI values from GS handheld crop sensor were collected during the winter barley growth in April 23rd, and May 19th 2015 at Ruzyně location, and May 8th, May 30th and June 30th at Vendolí location. Experimental variograms of NDVI values were computed by common procedures using an exponential and spherical model (see Table 1). The data were processed in ArcGIS 10.3.1 software (Esri, Inc., Redlands, CA, USA).

Table 1. Summary statistics, variogram model parameters and the methods of interpolation used for yield and GS in the experimental field

	Yield			GS – NDVI				
Crop	Winter barley		Spring barley	Winter barley		Spring barley		
Location	Ruzyně		Vendolí	Ruzyně		Vendolí		
				2015		2015		
				23-april	19-may	8-may	30-may	20-june
Count	8,808.0	10,974.0	18,537.0	103.0	103.0	110.0	110.0	110.0
Mean	5.618	5.322	4.049	0.779	0.802	0.321	0.697	0.672
Median	5.481	5.385	4.111	0.790	0.810	0.310	0.715	0.680
Standard deviation	1.373	0.836	1.377	0.062	0.030	0.076	0.083	0.068
Minimum	1.109	1.391	0.204	0.390	0.670	0.190	0.440	0.510
Maximum	10.149	9.254	8.733	0.890	0.850	0.580	0.850	0.830
Skewness	0.015	-0.666	-0.025	-2.946	-2.206	0.458	-0.693	-0.567
Methodofinterpolation	Kriging							
Methodofestimation	Method of Moments (MoM)							
Variogram model	Exponential				Spherical			
Distance parameter (r)	22.9	11.0	72.30	205.7	610.9	210.9	297.0	215.9
Approximaterange = 3 x r	68.7	33.0	216.9	617.1	-	-		-
Nugget variance	0.3170	0.4200	0.5390	0.0025	0.0005	0.0044	0.0038	0.0047
Sill variance	1.0100	0.5900	1.9140	0.0051	0.0012	0.0063	0.0077	0.0026

Total monthly precipitation and temperature data were provided by the agro-meteorological station at the Crop Research Institute in Prague-Ruzyně and from weather station Davis in Vendolí. Precipitation and temperatures for the observed year are also provided in Table 2.

Table 2. Precipitation and temperatures in different growth stages by BBCH scale recorded on the experimental fields in the year 2015 for winter and spring barley

	Precipitation (mm)			Temperature (°C)		
	2007	2015	2015	2007	2015	2015
	Ruzyně		Vendolí	Ruzyně		Vendolí
Plant	Winter barley		Spring barley	Winter barley		Spring barley
BBCH 0-19	32.0	48.7	30.4	10.9	11.0	5.5
BBCH 20-29	90.4	100.4	7.6	5.7	3.8	9.7
BBCH 30-59	2.4	43.7	35.8	12.8	12.3	13.0
After BBCH 60	146.6	64.6	132.6	18.1	17.1	18.6
Sum	271.4	189.5	206.4	-	-	-
Mean	90.5	63.2	51.6	12.6	10.9	11.7

Remote sensing data

Landsat satellite images were downloaded directly from the USGS Global Visualization Viewer (http://earthexplorer.usgs.gov/), as free remotely sensed data.Images from Landsat 5 (L-5), Landsat 7 (L-7) and Landsat 8 (L-8) were used for this study. WV-2, QB and SPOT-7satellite images were purchased from the ArcDATA Company. Table 3 provides the bandwidths of red visible (RED) and near infrared (NIR) range of sensors used in this study. For atmospheric correction, the Fast Line-of-sight Atmospheric Analysis of Hypercubes was used (Li et al., 2014; Dominguez et al., 2015). All image pre-processing was implemented with ENVI SW (ENVI; version 5.3, Excelis, Inc., McLean, VA, USA).

NDVI were computed for every image with ENVI SW. All images were then exported into ArcGIS SW for further processing. Very high resolution (VHR) images (WV-2, QB and SPOT-7) were resampled according to Landsat satellite image outputs to 30 m. Yield data were resampled according to satellite images to spatial resolution of 0.6 m, 2 m, 6 m and 30 m. Data from GS were resampled according to Landsat images to 30 m spatial resolution for further processing.

Pearson's correlations between the yield maps and NDVI derived from satellite images and GS sensor were calculated using Statistica 13 (StatSoft Inc., Tulsa, USA) procedure.

Table 3. Bandwidths of red visible (RED) and near infrared (NIR) range of selected satellites and sensors

Satellite	Sensor	RED range (nm)	NIR range (nm)
L-5	TM	630–690	760–900
L-7	ETM+	630–690	750–900
L-8	OLI	640–670	850–880
QB		590–710	715–918
SPOT-7		625–695	760–890
WV-2		630–690	705–895
	GS	660, ~25 nm FWHM	780, ~25 nm FWHM

RESULTS AND DISCUSSION

Correlation coefficients (R) between NDVI (from original and resampled data sets of Landsat, QB, WV-2 and SPOT-7 satellite images) and yield were calculated for individual image data and plant species in selected locations (see Table 4). Correlation matrices between NDVI from GS crop sensor, Landsat satellite images and yield were then calculated for individual data sets (see Table 5). Summary statistics for NDVI calculated from original and resampled satellite images for selected crops are in Table 6. Summary statistics of crop yield and GS for selected dates only for 2015 provides Table 1.

Winter barley was grown in 2007 and 2015 in Ruzyně location. The year 2007 was drier up to BBCH 60 phenological stage in comparison with the year 2015 in Ruzyně location (see Table 2). Low precipitation in the growth stage BBCH 30-59 (2.4 mm) can cause a significant displacement of relatively higher yield to water-accumulating depressions. This fact is confirmed also by correlations presented in Table 4, where R between NDVI a yield had average value 0.856. The movement of higher yield to

terrain concave areas in 2007 was also validated by summary statistics presented in Table 1, whereby both standard deviation and min-max range were higher than in 2015. In our previous articles (Kumhálová et al., 2011; Kumhálová et al., 2014), the influence of topography to yield in drier years was also found.

Table 4. Correlation coefficients between normalised difference vegetation index (NDVI) (from original and resampled L, QB and WV-2 satellite images with different spatial resolution (SR)) and yield of selected crops and years (levels of statistical significance: * $p < 0.05$; ** $p < 0.01$; *** $p < 0.001$)

Year	Yield		Growth stage	NDVI	
2007	Ruzyně		BBCH 59	Winter barley	
Satellite	L-5 TM	QB	L-5	QB	QB
SR	30 m	0.6 m	30 m	0.6 m	30 m
Date	May 24	May 22	May 24	May 22	May 22
Yield	1	1	0.861***	0.861***	0.835***
2015			BBCH 21-22		
Satellite	L-8 OLI	WV-2	L-8	WV-2	WV-2
SR	30 m	2 m	30 m	2 m	30 m
Date	March 18	March 23	March 18	March 23	March 23
Yield	1	1	0.264**	0.133***	-0.018
2015	Vendolí		BBCH 75	Spring barley	
Satellite	L-8 OLI	SPOT	L-8	SPOT-7	SPOT-7
SR	30 m	6 m	30 m	6 m	30 m
Date	July 1	July 4	July 1	July 4	July 4
Yield	1	1	0.341**	0.565***	0.501***

The year 2015 was drier year in sum of precipitation than the year 2007, but the precipitation distribution was more balanced during the growth stages (see Table 2). On the contrary, the precipitation distribution in BBCH 30–59 (43.7 mm) could probably cause the later crop beaten. In this year, harvesting losses caused by crop beating decreased the yield (see Table 1). This fact was confirmed by low R values between yield and NDVI (see Table 5); although the NDVI values were relatively high during BBCH 21–22 and crops were in a good condition (see Table 6). GS measurements on April 23rd (BBCH 31) and May 19th (BBCH 55) and comparisons between NDVI from GS and Landsat images and yield in Table 5 are in good accordance with previous statements. Nevertheless, R between NDVI from GS and Landsat images were weak (see Table 5).

Spring barley was grown in 2015 in Vendolí location. The precipitation distribution during the growth stages were balanced except the BBCH 20–29. The precipitation distribution was lower during these growth stages (7.6 mm) – see Table 2. Nevertheless, this weather running could lead to higher R (0.613) between yield and NDVI calculated from Landsat image in 30th May (see Table 5). It is validated by summary statistics presented in Table 1 as well, whereby standard deviation reached higher value. The precipitation distribution over the all growth stages could cause displacement of higher yield to places with better growth conditions. GS measurements were carried out on May8[th] (BBCH 35), May 30th (BBCH 55) and June 20th (BBCH 65). R between NDVI from GS and Landsat images was weak in early growth stage (8th May). On the contrary, the R value reached 0.679 between these two (GS and Landsat satellite) measurement methods in 30th May. The last measurements NDVI on 20th June with GS and on 20th

with Landsat were similar in comparison with yield, but the *R* between the measurement methods reached the value 0.453 only. These differences can be caused by other measurement method used and other spatial distribution of values measured. SPOT-7 image, acquired on 1st July, was chosen for crop evaluation. Very high resolution image in late date was available only, because of very cloudy scene during the crop growth. The *R* between yield and Landsat and SPOT-7 images was different. The Landsat image was cloudy in northern part of the experimental field. That is why 38 pixels from this part of field had to be removed (see Table 6).

Table 5. Correlation coefficients between normalised difference vegetation index (NDVI) from GS sensor, Landsat images and crop yield (levels of statistical significance: *$p < 0.05$; ** $p < 0.01$; *** $p < 0.001$)

2015	Date/SR	GS NDVI	GS NDVI	L-8 NDVI	L-8 NDVI		
		Winter barley – Ruzyně					
Date		April 23	May 19	April 19	May 14		
Yield	30m	0.011	0.022	0.260**	0.145		
L-8 NDVI	April 19	0.310*	-	-	-		
L-8 NDVI	May 14	-	0.359***	-	-		
		Spring barley – Vendolí					
2015	Date/SR	GS NDVI	GS NDVI	GS NDVI	L-7 NDVI	L-8 NDVI	L-8 NDVI
Date		May 8	May 30	June 20	April 29	May 30	June 24
Yield	30m	0.323***	0.458***	0.387***	0.001	0.613***	0.415**
L-7 NDVI	April 29	0.035	-	-	-	-	-
L-8 NDVI	May 30	-	0.679***	-	-	-	-
L-8 NDVI	June 24	-	-	0.453***	-	-	-

L-8 – Landsat 8 OLI image; L-7 – Landsat 7 ETM+; SR – spatial resolution.

Table 6. Summary statistics for NDVI calculated from original and resampled satellite images for selected years and crops

Year	2007 – winter barley			2015 – winter barley			2015 – spring barley		
	Ruzyně						Vendolí		
Satellite	L-5	QB	QB	L-8	WV-2	WV-2	L-8	SPOT-7	SPOT-7
SR	30 m	0.6 m	30 m	30 m	2 m	30 m	30 m	6 m	30 m
Count	115	306704	115	102	26684	102	231	6311	269
Mean	0.756	0.635	0.635	0.528	0.414	0.418	0.888	0.802	0.797
Median	0.759	0.638	0.635	0.532	0.416	0.418	0.901	0.809	0.809
Standard deviation	0.077	0.041	0.039	0.046	0.057	0.056	0.095	0.044	0.055
Minimum	0.556	0.477	0.544	0.315	0.185	0.269	0.519	0.623	0.531
Maximum	0.876	0.799	0.721	0.626	0.619	0.559	1.087	0.886	0.876
Skewness	-0.664	-0.401	-0.138	-1.047	-0.153	-0.353	-0.413	-0.732	-0.763

Summary statistics in Table 6 show that NDVI derived from Landsat images had higher mean and maximum values than NDVI derived from other satellites used in this study. This fact may support the conclusion, that Landsat images are more sensitive to crop biomass content. It can be explained by the differences in RED and NIR bandwidth among the sensors (see Table 3). QB, WV-2 and SPOT-7 have wider band range, than any of Landsat sensors. When comparing available Landsat sensors, L-5 and L-7 have similar calibration in contrast with L-8 (see Table 3). Studies dealing with this different

L-8 setting were also performed (Holden et al., 2016; Roy et al., 2016).GS handheld sensor and L-7 provide data in approximately same wavelengths. Nevertheless, there is a difference between GS and L-8. Despite this fact, L-8 data are very well correlated both with GS NDVI ($R = 0.679$, 30th May 2015 at Vendolí) and also with yield ($R = 0.613$, 30th May at Vendolí). However, this may be also caused by measuring date accordance. Differences in red band wavelengths are not so substantial in any case.

Another cause of differences may be input data resampling. Apart from Landsat, all satellite data were resampled to 30 m spatial resolution. Table 6 shows summary statistics for both, original and resampled data. Resampling seems to have no influence on QB data, all categories of summary statistics differ very slightly and mean values are even equal. WV-2 and SPOT-7 original and resampled data differ more in summary statistics than other sources. Each sensor was used to evaluate different dataset. Results that are more accurate may be gained when evaluating selected sensors by calculating NDVI from the same dataset. In addition, Bégué et al. (2008) stated that single date images may be unsatisfactory for yield prediction.

As mentioned above, there is the opinion that NDVI may be poor indicator of crop biomass when the canopy becomes denser (Huete et al., 2002). Gao et al. (2000) stated, that Enhanced Vegetation Index (EVI) tend not to be saturated over dense vegetation, like NDVI does, and seems to be sensitive enough to plant structural characteristics.In study by Zhu et al. (2016) similar issue was studied. L-5, L-7 and L-8 imagery were used to calculate NDVI and EVI for land cover changes evaluation in the city of Guangzhou, China. Due to the different wavelength setting, EVI was chosen as better indicator of greenness. Erdle et al. (2011) compared utilization of active and passive sensors. According to their study, made on seven wheat cultivars, active sensors disadvantage is that they are capable to measure limited number of VI. Conversely, passive sensors perform a possibility to develop different VI. Above that, GS measures only two fixed bands, while another active sensor Crop Circle is capable to capture three user configurable bands, e.g. green, red edge and NIR.As stated in Cao et al. (2015) study, indices derived from Crop Circle perform significantly better, than indices acquired by GS. Ali et al. (2014) examined the potential of yield prediction on dry direct-seeded rice using GS and then chlorophyll meter (SPAD) and simple leaf colour chart. Their result allegation was that all of these methods can be used for in-season yield prediction. Thus, according to that, GS is comparable with more simple measurement methods.

CONCLUSION

The results showed that all satellite images used in this study can sufficiently explain crop variability in given dates and can be used for yield prediction and crop growth evaluation. NDVI spectral index seemed to be good tool for simple and fast evaluation of the agriculture crop, because several data sourceswere possible to use for its calculation. Passive remote sensing sensors were compared with GS active sensor. Nevertheless, not very consistent results were acquired. VHR images were resampled to 30 m spatial resolution according to Landsat images in order to examine possible influence of spatial resolution on information evaluated. However, various bandwidths in RED and NIR region of selected images made the correlations between yield and NDVI different. The greatest difference in such evaluation was found between L-8 OLI sensor and WV-2 and SPOT-7 sensors. On the base of the results obtained in this study,

it is necessary to undertake more research to define which of selected sensors is the most capable for yield prediction under conditions of the Czech Republic.

REFERENCES

Bégué, A., Todoroff, P. & Pater, J. 2008. Multi-time scale analysis of sugarcane within-field variability: improved crop diagnosis using satellite time series? *Precis Agric.* **9**, 161–171.

Cao, Q., Miao, Y., Feng, G., Gao, X., Li, F., Liu, B., Yue, S., Cheng, S., Ustin, S.L. & Khosla, R. 2015. Active canopy sensing of winter wheat nitrogen status: An evaluation of two sensor systems. *Comput Electron Agr.* **112**, 54–67.

Dominguez, J.A., Kumhálová, J. & Novák, P. 2015. Winter oilseed rape and winter wheat growth prediction using remote sensing methods. *Plant Soil Environ* **74**(2), 229–239.

Elsayed, S., Rischbeck, P. & Schmidhalter, U. 2015. Comparing the performance of active and passive reflectance sensors to assess the normalized relative canopy temperature and grain yield of drought-stressed barley cultivars. *Field Crop Re.s* **177**, 148–160.

Erdle, K., Mistele, B. & Schmidhalter, U. 2011. Comparison of active and passive spectral sensors in discriminating biomass parameters and nitrogen status in wheat cultivars. *Field Crop Res* **124**, 74–84.

Gao, X., Huete, A.R., Ni, W. & Miura, T. 2000. Optical-biophysical relationships of vegetation spectra without background contamination. *Remote Sens Environ* **74**, 609–620.

Holden, Ch.E. & Woodcock, C. 2016. An analysis of Landsat 7 and Landsat 8 under flight data and the implications for time series investigations. *Remote Sens Environ* **185**, 16–36.

Huete A., Didan K., Miura T., Rodriguez E.P., Gao X. & Ferreira L.G. 2002. Overview of the radiometric and biophysical performance of the MODIS vegetation indices. *Remote Sens Environ* **83**, 195–213.

Hunt, Jr. E.R., Doraiswamy, P.C., McMurtrey, J.E., Daughtry, C.S.T., Perry, E.M. & Akhmedov, B. 2013. A visible band index for remote sensing leaf chlorophyll content at the canopy scale. *Int J Appl Earth Obs.* **21**, 103–112.

Johnson, M.D., Hseih, W.W., Cannon, A.J., Davidson, A. & Bédard, F. 2016. Crop yield forecasting on the Canadian Prairies by remotely sensed vegetation indices and machine learning methods. *Agr Forest Meteorol.* **218-219**, 74–84.

Jones, H.G. & Vaughan, R.A. 2010. *Remote Sensing of Vegetation: Principles, techniques and applications*. Oxford University Press, Oxford, 353 pp.

Khorram, S., Van der Wiele, C.F., Koch, F.H., Nelson, S.A.C. & Potts, M.D. 2016. *Principles of Applied Remote Sensing,* Khorram, Springer-Verlag, Berlin, 307 pp.

Kumhálová, J. & Moudrý, V. 2014. Topographical characteristics for precision agriculture in conditions of the Czech Republic. *Appl Geogr.* **50**, 90–98.

Kumhálová, J., Kumhála, F., Kroulík, M. & Matějková, Š. 2011. The impact of topography on soil properties and yield and the effects of weather conditions. *Precis Agric* **12**, 813–830.

Li, P., Jiang, L. & Feng, Z. 2014. Cross-Comparison of Vegetation Indices Derived from Landsat-7 Enhanced Thematic Mapper Plus (ETM+) and Landsat-8 Operational Land Imager (OLI) Sensors. *Remote Sens Basel* **6**, 310–329.

Marino, S., Basso, B., Leon, A.P. & Alvino, A. 2013. Agronomic traits and vegetation indices of two onion hybrids. *Sci Hortic Amsterdam* **155**, 56–64.

Moldan, B. 2015. *Podmaněná planeta*. Karolinum. Praha, 511 pp. (in Czech).

Richards, J.A. 1993. *Remote Sensing Digital Image Analysis: An Introduction.* Springer-Verlag, Berlin, 340 pp.

Rouse, J., Haas, R., Schnell, J. & Deering, D. 1973. Monitoring Vegetation Systems in the Great Plains with ERTS. *Third ERTS Symposium, NASA*, 309–317

Roy, D.P., Kovalskyy, V., Zhang, H.K., Vermote, E.F., Yan, L., Kumar, S.S. & Egorov, A. 2016. Characterization of Landsat-7 to Landsat-8 reflective wavelength and normalized difference vegetation index continuity. *Remote Sens Environ* **185**, 57–70.

Satellite Imaging Corporation 2017. *SPOT-7 Satellite Sensor.* Satellite Imaging Corporation, online: http://www.satimagingcorp.com/satellite-sensors/spot-7/ (accessed 22.1.2017).

Trimble 2017. *GreenSeeker handheld crop sensor.* Trimble Inc., online: http://www.trimble.com/Agriculture/gs-handheld.aspx?tab=Product_Overview (accessed 20.1.2017).

United Nations Department of Economic and Social Affairs/Population Division 2015. *World Population Prospects: The 2015 Revision, Key Findings and Advance Tables*. United Nations, New York, 59 pp.

USGS 2015. *NDVI, the Foundation for Remote Sensing Phenology.* United States Geological Survey, online: https://phenology.cr.usgs.gov/ndvi_foundation.php (accessed 20.1.2017).

Wang, G. & Weng, Q. 2013. *Remote Sensing of Natural Resources*. CRC Press, 580 pp.

Zhang, Q. 2015. *Precision Agriculture Technology for Crop Farming.* CRC Press, 360 pp.

Zhu, Z., Fu, Y., Woodcock, C.E., Olofsson, P., Vogelmann, J.E., Holden, Ch., Wang, M., Dai, S. & Yu, Y. 2016. Including land cover change in analysis of greenness trends using all available Landsat 5, 7, and 8 images: A case study from Guangzhou, China (2000–2014). *Remote Sens Environ* **185**, 243–257.

Appendix 2

Assessment of soil electrical conductivity using remotely sensed thermal data

Křížová, K., Haberle, J., Kroulík, M., Kumhálová, J., & Lukáš, J. (2018). Assessment of soil electrical conductivity using remotely sensed thermal data. *Agronomy Research, 16*(3), 784–793. https://doi.org/10.15159/AR.18.111

Assessment of soil electrical conductivity using remotely sensed thermal data

K. Křížová[1,2,*], J. Haberle[3], M. Kroulík[1], J. Kumhálová[4] and J. Lukáš[2]

[1]Czech University of Life Sciences Prague, Faculty of Engineering, Department of Agricultural Machines, Kamýcká 129, CZ16500 Prague, Czech Republic
[2]Crop Research Institute, Division of Crop Protection and Plant Health, Drnovská 507/73, CZ 16106 Prague, Czech Republic
[3]Crop Research Institute, Division of Crop Management Systems, Drnovská 507/73, CZ16106 Prague, Czech Republic
[4]Czech University of Life Sciences Prague, Faculty of Engineering, Department of Machinery Utilization, Kamýcká 129, CZ16500 Prague, Czech Republic
[*]Correspondence: krizovak@tf.czu.cz

Abstract. Detection of heterogeneity (crop, soil, etc.) gained a lot of importance in the field of site-specific farming in recent years and became possible to be measured by different sensors. The thermal spectrum of electromagnetic radiation has a great potential today and experiments focused on describing a relation between canopy temperature and various vegetation characteristics are conducted. This paper was aimed to examine the relation between canopy temperature and electrical conductivity as one of staple soil characteristics. The related experiment was undertaken in Sojovice, Czech Republic, within an agricultural plot where winter wheat was grown in 2017 growing season. The examined plot was composed of three sub plots and 35 control points were selected within this area which the data were related to. A canopy was sensed by UAV (eBee carrying thermoMAP (FLIR TAU2) camera). Soil conductivity data were collected by terrestrial sampling using EM38-MK2 Ground Conductivity Meter in 1 m depth and 2 m sampling point distance. This dataset was later interpolated using the kriging method. The correlation analysis results showed a strong negative correlation between conductivity and thermal data (-0.82; $p < 0.001$). When comparing conductivity with NDVI representing the aboveground biomass, there was an opposite trend but also strong result (0.86; $p < 0.001$). Correlation coefficient of thermal data and NDVI comparison was -0.86; ($p < 0.001$). These preliminary results have a potential for further research in terms of soil characteristics studies.

Key words: precision agriculture, winter wheat, heterogeneity, UAV, kriging.

INTRODUCTION

The concept of Precision Agriculture (PA) has developed rapidly in recent decades. As the population grows and the field of specialized technologies are enhanced, the methods of site-specific farming more or less engage the common practice. Many studies are conducted with the aim to describe relations between various soil and vegetation characteristics and different kind of remotely sensed (RS) data. Such knowledge is essential to obtain a complex overview of how the natural processes may be explained

by spectral imagery. The major advantage of such approach is especially the fact that the research may be carried out in a non-destructive mode. Related analyses may be thus undertaken repeatedly during one growing season, i.e. it is possible to evaluate crops on particular plot in different growth stages (Richards, 1993; Jones & Vaughan, 2010). It was determined that the spectral characteristics are related to various vegetation characteristics such as biochemical composition, physical structure or plant status (Sahoo et al., 2015). Based on this knowledge there is not only the possibility to evaluate the crop status at the canopy scale, but it is also possible to detect some within-field heterogeneity. This heterogeneity may be caused by variability of elevation or soil texture that in both cases affects at most the water distribution (Kumhálová et al., 2011; Sassenrath & Kulesza, 2017). Detecting of the within-field heterogeneity may be utilized to adjust the agricultural management and delineate so-called production zones. Initially, the concept of PA was based on responses in the visible and near-infrared (NIR) regions of the electromagnetic spectrum. Plenty of vegetation indices (VI) were developed as the ratios of reflectance in different wavelengths. Although many of them are considered to be very effective indicator of soil and vegetation characteristics, the research is focused on thermal infrared region of the spectrum in recent years. The major difference between these two approaches is that optical RS exploits the radiation reflected from the investigated surface, whereas thermal RS methods work with the amount of radiation that is emitted by the particular surface or object (Sabins Jr., 1997). As the temperature is such characteristic that is not visible under standard conditions, the thermal RS converts this information and displays the patterns as the visible image (Ishimwe et al., 2014). According to Khanal et al. (2017) this is especially useful for early detection of stressed vegetation based on the crop temperature on the contrary to optical RS methods, where the stress may be indicated only when visible symptoms appear. This statement is supported also by study of Camoglu et al. (2017), where thermal and hyperspectral data were analyzed to detect four levels of water stress on peppers (*Capsicum annuum L.*). Whereas spectral indices did not indicate the difference between 100% and 75% irrigated vegetation, thermal indices provided significant results. Initially, the obtaining of high resolution thermal imagery was limited by high acquisition costs. However, recently the low-costs platforms were developed. Especially, the utilization of Unmanned Aerial Vehicles (UAV) has lowered the costs and thus the thermal imagery became more accessible for various branches of agricultural research such as nursery and greenhouse monitoring, irrigation management, plant disease detection or yield prediction (Ishimwe et al., 2014). A number of studies focus on fruit trees yield prediction. An algorithm was developed by Stajnko et al. (2004) to estimate apple tree yield prediction using thermal data. Moreover, Bulanon et al. (2008) demonstrated the method how to estimate citrus fruit yield based on the fact that the fruits have approximately 1.6 °C higher temperature than leaves during the night. Nevertheless, the utilization of thermal imagery to predict cereals yield has still some limits in scientific literature. However, there are also studies describing the relation of thermal imagery and soil characteristics. Soil texture was found to be strongly related to a land surface temperature (Mattikalli et al., 1998). It is a factor that besides the others affects the amount of water held in soil profile that on the rebound influences the surface temperature. Soil electrical conductivity (EC) is considered to be a staple soil property. It determines capability of soil to transmit an electrical charge (Logsdon, 2008). According to various studies EC is associated to other soil attributes

such as soil texture or soil water content (Corwin & Lesch, 2003; Logsdon, 2008; Malin & Faulin, 2013). Exploration of physical and chemical soil properties within examined area is often expensive and time consuming procedure. Therefore, in terms of PA applications EC became useful and most frequently obtained measurements to determine soil properties. Obtained values of EC are usually processed and thereafter presented as a map. This kind of map thus gives approximate information about soil texture and soil water distribution. It may be utilized not only for appropriate crop selection, but also for evaluation of drainage and irrigation management or spatio-temporal changes in soil properties.

Since thermal RS methods gained attention in recent years and the soil EC is considered to be a staple soil factor, this study aimed to describe the relation between these two variables. Experimental data presented in this paper are aimed to be analysed to determine the level of association of canopy temperature (T_c) and soil EC as the staple soil factor.

MATERIALS AND METHODS

Experimental Site

The experiment was conducted within an agricultural plot near the Sojovice town in Czech Republic. It is located approximately 25 km north-east from Prague [50°13'45"N, 14°45'54"E]. The whole experimental area has nearly 25 ha and it is composed of three smaller plots marked by numbers (Fig. 1). The west side plot [7] has 8.4 ha and there are cambisols as a staple soil type. The northern part of plot [9] has 10.0 ha and the southern one [5] has 5.8 ha. There are regosols as the staple soil type within both of these plots. According to the DEM the elevation ranges between 175–184 m a.s.l. thus there is no significant elevation variability over the area. This agricultural plot has already been monitored in recent years. Certain pattern in crop heterogeneity is observable on different kind of imagery during the growing season (Fig. 2).
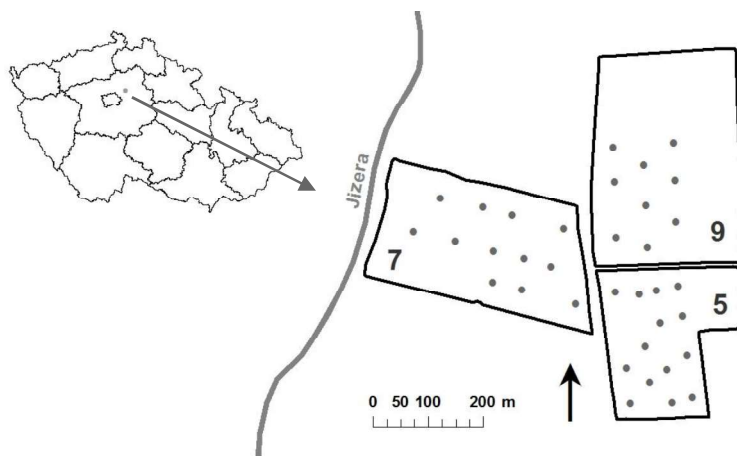

Figure 1. Experimental plot localization and composition (subplots marked by numbers 5, 7, 9) with 35 control points depicted within the field and Jizera river flow on the west side.
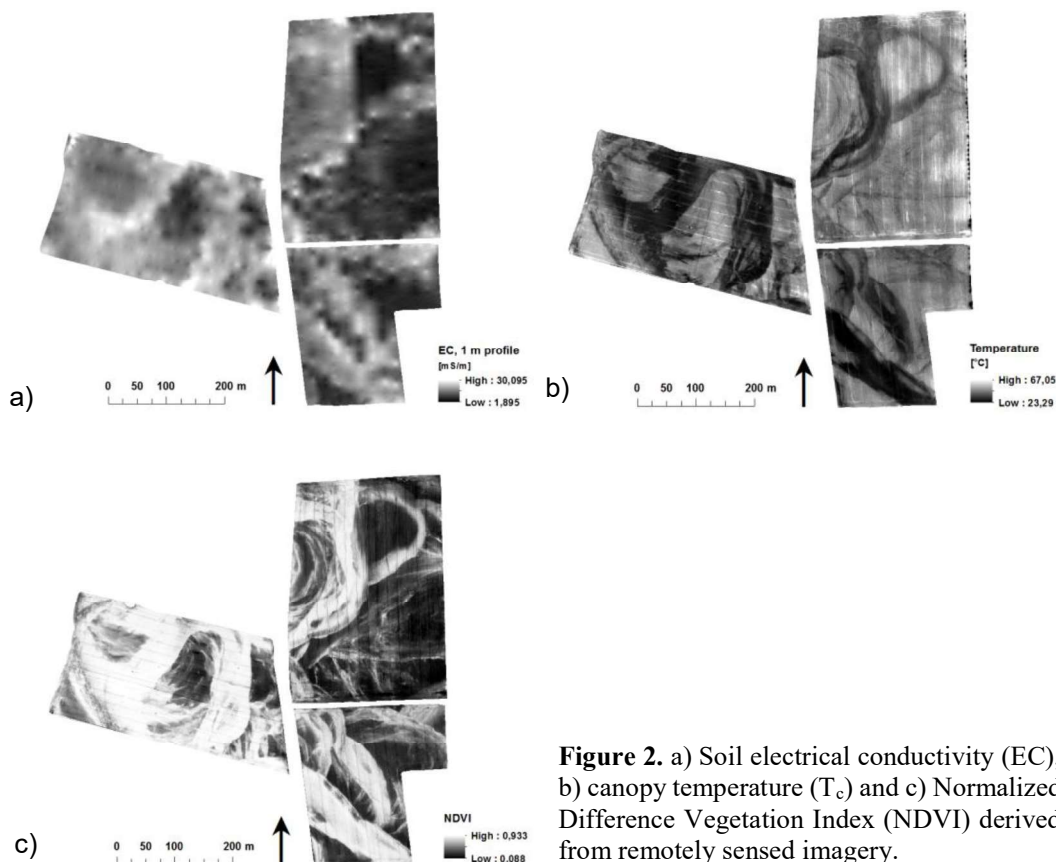
Figure 2. a) Soil electrical conductivity (EC), b) canopy temperature (T_c) and c) Normalized Difference Vegetation Index (NDVI) derived from remotely sensed imagery.

This heterogeneity is very likely influenced by the nearby flow of Jizera river and it is planned to be examined also in upcoming growing season. For a purpose of pedological research in total 35 control points were selected (Fig. 1). This control points selection was based on remotely sensed data from years 2015 and 2016 that were generally poor on precipitation. Therefore, zones of crops stressed by insufficient amount of water appeared in certain pattern during both examined growing season. Thus, points were selected to represent zones with different rate of crop water stress.

Agricultural management of the examined plot works with crop rotation of winter wheat and potato with one-year period. In 2017 growing season there was a winter wheat grown in two varieties. Variety *Patras* was sown on the southern part of the plot [5], while the other two parts were sown with *Epos* variety. Consequently all data analysis and results interpretation are related to winter wheat as one of the staple agricultural crops.

Remotely sensed Data
To obtain spectral data in sufficient spatial resolution the canopy of the experimental plot was sensed using UAV on 19th June 2017. A fully autonomous drone eBee (senseFly, Cheseaux-Lausanne, Switzerland) was utilized to carry two different types of camera. Canopy temperature data were obtained using thermal camera senseFly thermoMap. The images were processed and composed using specialized SW. In order

787

to calculate Normalized Difference Vegetation Index (NDVI) sensing with multispectral camera senseFly multiSPEC 4C was done as well. To acquire absolute reflectance measurements the calibration with calibration target was necessary to be done before flight. This multispectral camera contains four separate sensors that acquire data in four bands – green, red, red-edge and NIR. Based on multispectral imagery NDVI index was calculated using ENVI 5.4 (Exelis Visual Information Solutions, Boulder, Colorado, USA). This index was derived and used in the analysis as the indicator of aboveground biomass. Technical specifications of utilized cameras and their settings for this particular sensing are given by Table 1, whereas Table 2. describes meteorological conditions during the process of data acquisition.

Table 1. Technical parameters of canopy remote sensing at 80 above ground level

	Thermal camera	MS camera
Typ of device	thermoMap	multiSPEC 4C
Sensor	FLIR TAU2, 640 × 512 px	4×1/3" CMOS
Ground resolution at 100 m, cm/px	19	10
Velocity, m s^{-1}	12–13	
Vertical overlap, %	80	
Horizontal overlap, %	80	
SW	eMotion, Pix4D	

Soil Electrical Conductivity Data

In order to gain the soil EC data, a terrestrial sampling was carried out using widely known probe for electromagnetic induction (EMI) (Corwin and Lesch, 2005) measurement EM38 MK2 (Geonics Limited, Ontario, Canada) on 13th September 2017. Weather conditions during the process of measurement are given in Table 2. The probe was pulled by quad by the speed approximately 2.8 m s^{-1}, while the data were acquired in the soil profile 0–1 m. The measurement was performed as the set of points with the distance of 2 m in the direction of quad motion. Weather conditions

Table 2. Meteorological conditions by data collection

	T_c	EC
Date of sensing	19.6.2017	13.9.2017
Time of sensing	2–3 PM	2–4 PM
Aerial temperature, °C	29	16.4
Precipitation, mm	0.0	0.0
Wind velocity, k h^{-1}	8.6	18
Air pressure, hPa	1,020.3	1,005.8

during the process of measurement are given in Table 2. The probe was pulled by quad by the speed approximately 2.8 m s^{-1}, while the data were acquired in the soil profile 0–1 m. The measurement was performed as the set of points with the distance of 2 m in the direction of quad motion. The distance between particular trajectories was approximately 20 m. Data from probe was recorded to the measuring unit together with DGPS signal each second. In order to eliminate recorded errors, some modifications on the original EC values were performed before processing. Data were treated at the extreme values. Data of conductivity were processed using statistical and geostatistical methods. The set of 7,428 points was interpolated in order to get coherent map

representing the EC values distribution within the examined area. The maps were created using the kriging interpolation method (see Table 3). Software Microsoft office (Microsoft Corporation, Redmond, USA) and ArcGIS 10.5 (ESRI, Redlands, California, USA) were used.

Table 3. Parameters of Kriging as a method of interpolating the point electrical conductivity (EC) data

Method of estimation	Method of Moments (MoM)
Method of interpolation	Kriging
Variogram model	Spherical
Nugget variance	0.776
Distance parameter (r)	43.471
Partial sill	12.349

Data Analysis

Since the data were acquired and processed, it was possible to display numerical values of examined vegetation and soil characteristics in form of raster layer. This kind of visualisation showed certain pattern of data variability within examined agricultural plot. Nevertheless, the analysis needed to be done to describe the relation between T_c and EC more precisely. In addition, analysis of the relation between EC and NDVI, respectively T_c and NDVI was done as well to obtain complex information about the dataset. Since there was set of 35 control points selected within the experimental area, the other data analysis was related to those points. Values from raster layers (T_c, EC and NDVI) were extracted using the *Extract Multi Values to Points* tool in ArcMap 10.5 SW and added to the attribute table of 35 control point vector layer. Thus, the result was the table with in containing exact numerical information about T_c, the soil EC and NDVI at the particular point. Statistical analysis process was done in R Studio SW (RStudio Team, Boston, Massachusetts, USA). Pearson's correlation coefficient was calculated at three levels. At first the relation T_c and EC was evaluated, followed by the calculations for T_c and NDVI and also EC and NDVI.

RESULTS AND DISCUSSION

First, summary statistics of examined variables was done to acquire complex information about the dataset intended to be analysed. Results of the summary are given by Table 4. Mean value of EC was 10.306 mS m^{-1}, whereas median reached only 9.310 mS m^{-1}. These values were in accordance with possitive skewness (0.403) that indicated the data are more distributed on the right side of the mean value, i.e. the field is mostly characterized by lower values of EC, however the mean value is influenced by several parts with higher EC values. Mean canopy temperature was calculated to be 30.4 °C, median 31.6 °C. Negative skewness indicated higher vaules dominating among the dataset. NDVI mean value was 0.66 and slightly negative skewness showed on more values distributed on the left side of the mean.

Table 4. Summary statistics of soil electrical conductivity (EC), canopy temperature (T_c) and Normalized Difference Vegetation Index (NDVI)

	EC	T_c	NDVI
Count	35	35	35
Mean	10.306	30.440	0.660
Median	9.310	31.600	0.679
Sample variance	14.621	5.825	0.040
Standard deviation	3.824	2.413	0.199
Minimum	4.280	26.440	0.323
Maximum	18.048	33.910	0.901
Skewness	0.403	-0.215	-0.179

Relation of soil EC and T_c was evaluated within selected agricultural plot. Additionally, the NDVI was added to the analysis as the aboveground biomass indicator. The analysis was concentrated in 35 control points selected in terms of previous research. Correlation coefficients were calculated for combinations of three examined variables, however, the relation of EC and T_c was the most required one. Fig. 3 gives a complex overview of correlation analysis results. Significantly strong correlation was detected at all levels. Soil EC and T_c were negatively correlated with the correlation coefficient value -0.82. Even stronger negative correlation was observed by T_c and NDVI relation (-0.86), while conversely very strong positive correlation was found by EC and NDVI (0.86). Fig. 4 gives detailed information about the relation of EC and other two examined variables (T_c and NDVI).

Figure 3. Results of correlation analysis presented as correlogram, where the dark grey colour within a pie chart represents a positive trend of correlation coefficient, while the light grey indicates a negative trend (*p-value < 0.001*). Confidence intervals are given in round brackets.

Based on the results of correlation analysis the relation of soil property and canopy temperature may be described. The negative value of correlation coefficient is the indicator of indirect proportion. In fact, with lower values of EC the canopy temperature tends to increase. It is generally known that plant temperature is associated with the stomatal conductance that further links to the nutrient uptake and therefore it influences actual biomass of the crop (Cai & Cespedes, 2012). This fact is also in accordance with result of analysis of thermal data and NDVI representing aboveground biomass, where the correlation coefficient indicated indirect proportion as well.
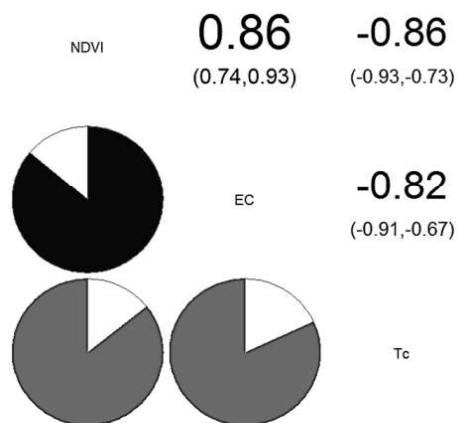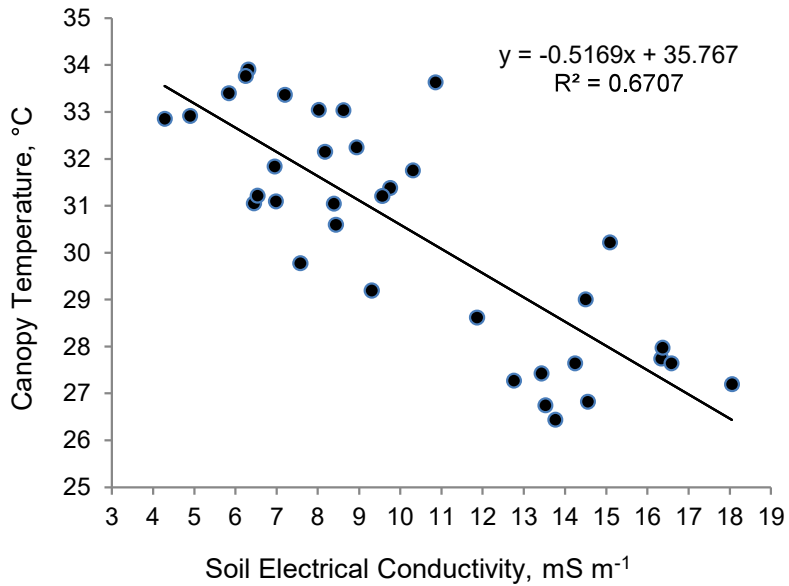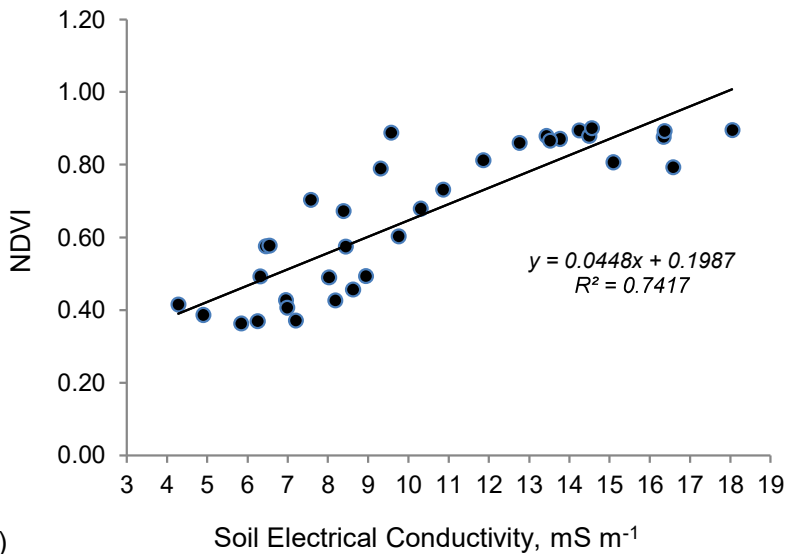
a)

b)

Figure 4. a) Trend of T_c and EC and b) trend of NDVI and EC relation based on the data from 35 control points.

Multispectral imagery can provide quick information about crop biomass within the field by calculating particular VI. In this case, NDVI values ranges from 0.323 to 0.901 and the heterogeneity is apparent also from attached map (Fig. 2, c). When having such information about the crop vegetation status, the cause of such differences should be determined. Various factors may influence the crop growth, e.g. topography (Kumhálová et al., 2011), soil properties variability or presence of pests or effect of plant disease. As was stated above, the elevation variability is not significant within the examined plot. Very likely the heterogeneity is caused by variable soil properties, but

the soil sampling is difficult to be conducted during growing season. On the contrary, evaluation of vegetation cover using thermal RS techniques may be carried out regardless of time. T_c and EC correlation analysis showed the value -0.89 and thus the EC may be very likely explained by remotely sensed thermal data. There are studies that describe very tight correlation of EC and other soil properties (Corwin & Lesch, 2003). However, other studies were conducted with different results. Malin & Faulin (2013) evaluated two agricultural plots to determine the relation of EC and clay and water content. Significant results were found only on one of two evaluated plots, where spatial variability of soil texture was higher. Moreover, the study of Valente et al. (2012) found no significant results when evaluating EC and soil texture and moisture, respectively various chemical properties. It is clear that conclusions differ across the scientific literature, so the particular limiting soil factor may not be always identified precisely without soil sampling.

CONCLUSIONS

A number of studies were conducted to describe possible utilization of recently enhanced thermal RS data to predict yield of agricultural plot. However, the potential of thermal data to explain the soil properties that are a major factor influencing the crop growth, i.e. yield as well, is not described yet. In order to determine some basic relation of thermal response and soil characteristics this study was conducted. Soil electrical conductivity was chosen to be analysed as the factor subsuming most of other soil properties. At first, correlation analysis showed that aboveground biomass (presented by NDVI) is strongly influenced by EC (0.86). Based on this piece of information the correlation of canopy temperature and EC was examined and provided significant results, respectively close negative correlation (-0.82) was indicated. Such conclusion may be considered as some preliminary result supporting the thesis on possibility of soil properties to be explained by thermal RS. Further research may be conducted based on this conclusion to explore how are the thermal data capable to explain other soil properties.

REFERENCES

Bulanon, D.M., Burks, T.F. & Alchantis, V. 2008. Study on temporal variation in citrus canopy using thermal imaging for citrus fruit detection. *Biosystems Engineering* **101**, 161–171.

Cai, J. & Cespedes, M. 2012. Plant temperature measurement and analysis from infrared images. In: *27th Conference on Image and Vision Computing New Zealand.* IVCNZ, Dunedin, pp. 406–411.

Camoglu, G., Demirel, K. & Levent, G. 2017. Use of infrared thermography and hyperspectral data to detect effects of water stress on pepper. Quantitative InfraRed Thermography Journal, DOI: 10.1080/17686733.2017.1331008.

Corwin, D.I. & Lesch, S.M. 2003. Applicaion of Soil Electrical Conductivity to Precision Agriculture: Theory, Principles, and Guidelines. *Agronomy Journal* **95**, 445–471.

Corwin, D.L. & Lesch, S.M. 2005. Apparent soil electrical conductivity measurements in agriculture. *Computers and Electronics in Agriculture* **46**, 11–43.

Ishimwe, R., Abutaleb, K. & Ahmed, F. 2014. Applications of Thermal Imaging in Agriculture – A Review. *Advances in Remote Sensing* **3**, 128–140.

Jones, H.G. & Vaughan, R.A. 2010. *Remote Sensing of Vegetation: Principles, techniques and applications*. Oxford University Press, Oxford, 353 pp.

Khanal, S., Fulton, J. & Shearer, S. 2017. An overview of current and potential applications of thermal remote sensing in precision agriculture. *Computer and Electronics in Agriculture* **139**, 22–32.

Kumhálová, J., Kumhála, F., Kroulík, M. & Matějková, Š. 2011. The impact of topography on soil properties and yield and the effects of weather conditions. *Precision Agriculture* **12**, 813–830.

Logsdon S.D. 2008. *Soil Science: Step-by-step Field Analysis*. ASA-CSSA-SSSA, Madison, 251 pp.

Malin, J.P. & Faulin, G.CH. 2013. Spatial and Temporal variability of soil electrical conductivity related to soil moisture. *Scientia Agricola* **70**, 1–5.

Mattikalli, N.M., Engman, E.T., Jackson, T.J. & Ahuja, L.R. 1998. Microwave remote sensing of temporal variations of brightness temperature and near-surface soil water content during a watershed-scale field experiment and its application to the estimation of soil physical properties. *Water Resources Research* **34**, 2289–2299.

Richards, J.A. 1993. *Remote Sensing Digital Image Analysis: An Introduction.* Springer-Verlag, Berlin, 340 pp.

RStudio Team 2016. RStudio: Integrated Development for R. RStudio, Inc., Boston, MA URL http://www.rstudio.com/.

Sabbins, Jr. F.F. 1997. *Remote Sensing: Principles and Interpretation, 3rd Edition*. W.H. Freeman, New York, 494 pp.

Sahoo, R.N., Ray, S.S. & Manjunath, K.R. 2015. Hyperspectral remote sensing of agriculture. *Current Science* **108**, 848–859.

Sassenrath, G.F. & Kulesza, S. 2017. Measuring Soil Electrical Conductivity to Delineate Zones of Variability in Production Fields. In: *SEARC Agricultural Research 2017*. Kansas State University, Manhattan, pp. 64–72.

Stajnko, D., Lakota, M. & Hočevar, M. 2004. Estimation of number and diameter of apple fruits in an orchard during the growing season by thermal imaging. *Computer and Electronics in Agriculture* **42**, 31–42.

Valente, D.S.M., DeQueiroz, D.M., Pinto, F.A.C., Santos, N.T. & Santos, F.L. 2012. The relationship between apparent soil electrical conductivity and soil properties. *Revista Ciência Agronômica* **43**, 683–690.

Appendix 3

Soil physical properties and crop status under cattle manure and Z'Fix in Haplic Chernozem

Novák, V., Šařec, P., Křížová, K., Novák, P., & Látal, O. (2021). Soil physical properties and crop status under cattle manure and Z'Fix in Haplic Chernozem. *Plant, Soil and Environment*, *67*(No. 7), 390–398. https://doi.org/10.17221/159/2021-PSE

Soil physical properties and crop status under cattle manure and Z'Fix in Haplic Chernozem

Václav Novák[1]*, Petr Šařec[1], Kateřina Křížová[1,2], Petr Novák[3], Oldřich Látal[4]

[1]*Department of Machinery Utilisation, Faculty of Engineering, Czech University of Life Sciences Prague, Prague, Czech Republic*

[2]*Division of Crop Protection and Plant Health, Crop Research Institute, Prague, Czech Republic*

[3]*Department of Agricultural Machines, Faculty of Engineering, Czech University of Life Sciences, Prague, Czech Republic*

[4]*Department of Agrochemistry, Soil Science, Microbiology and Plant Nutrition, Faculty of Agrisciences, Mendel University in Brno, Brno, Czech Republic*

*Corresponding author: novakvaclav@tf.czu.cz

Abstract: A three-year experiment was conducted to investigate the effect of Z'Fix on soil physical properties and crop status. Z'Fix is an agent recommended as an addition to animal bedding to prolong its function and to lower ammonia emissions in stables. Concurrently, a positive effect on organic matter transformation in resulting manure is claimed. The experiment involved control, farmyard manure (FYM), and farmyard manure with Z'Fix (FYM_ZF) as variants. In-field sampling was conducted for cone index, water infiltration and implement a unit draft, where the latter two showed significant differences in favour of FYM_ZF. Also, concerning crop yields, FYM_ZF consistently attained the highest values, followed by FYM throughout all three seasons. Furthermore, remotely sensed data were analysed to describe crop status *via* normalised difference vegetation index where significant differences were found across all variants. Based on the study, FYM_ZF demonstrated positive effects both on soil properties and crop conditions.

Keywords: organic fertiliser; biological transformation; field experiment; pedocompaction; remote sensing

The positive effect of soil organic matter (SOM) on the physical, chemical and biological soil properties has already been well described. A high SOM level is related to improved soil properties resulting in higher water infiltration and nutrients accessibility. According to Lal (2020), SOM increases the available water capacity for all soil types. Besides others, such a list of benefits leads to increased biomass and eventually crop yields (Bauer and Black 1994, Berzsenyi et al. 2000, Önemli 2011). Farmyard manure is one of the most common ways to reintroduce quality organic matter to the soil. Compared to synthetic fertilisers, manure application strongly and positively affects the relative yield by increasing soil organic carbon storage, soil nutrients, and soil pH (Cai et al. 2019, Voltr et al. 2021). However, due to various socio-economic changes over the recent 30 years, there has been a significant decrease in animal husbandry in the Czech Republic. The numbers of cattle were reduced by 60% (Czech Statistical Office 2021). Therefore, the amount of produced organic fertiliser is limited nowadays. Together with still more intensive agricultural practice, it results in a serious lack of SOM that is further related to a number of other environmental issues, for example, to low water infiltration ability leading to surface

runoff and related soil erosion (Matula 2003). In contrast with the benefits in the form of quality organic matter, it is necessary to pay attention to the negative aspects of livestock breeding as well. According to the estimates, livestock farming accounts for 18% of greenhouse gases. The largest source of these gases is cattle breeding, which accounts for about 65% (Gerber et al. 2013). The optimisation of organic fertiliser production with respect to their environmental footprint is therefore undeniably necessary. Manure agents are the substances that are used by farmers to enhance the welfare of animals, control produced odours, and eventually increase fertiliser value (Cluett et al. 2020). Z'Fix (Olmix Group, Bréhan, France) is one representative of such agents. It is a dust-free pearled pellet, which can be added to deep animal bedding, but it is applicable to all types of farm fertilisers (manure, slurry, compost). Some studies already evaluated the effect of Z'Fix both on animal welfare and organic fertiliser properties. When applied directly to straw bedding, the fermentation process is enhanced, resulting in better manure quality. The higher nutrient content was also determined (Šařec et al. 2017a). In combination with pig slurry, it is trusted to increase crop yield and micronutrients content (Mozdzer and Chudecka 2017). Nevertheless, the exact impact on major soil physical properties was not yet sufficiently described. Reduced bulk density after application of manure treated by Z'Fix was examined by Šařec et al. (2017b), where the conclusion confirmed the positive effect of Z'Fix compared to control (NPK) on heavy soils. Since this activator is claimed to positively influence SOM, the objective of this study is to verify this statement in a three-year study conducted in real conditions. Hypotheses that are about to be verified are related to (a) reduction of cone index and implement a unit draft, and (b) increase of the infiltration ability of the soil. Moreover, the secondary impact of Z'Fix on crop status is about to be examined *via* spectral index derived from remotely sensed data.

MATERIAL AND METHODS

Farmyard manure agent Z'Fix. Z'Fix is an activator of the biological transformation used in stables to enhance the quality of bedding by controlling the fermentation process of organic matter. The primary benefit here is animal welfare; the manufacturer, however, claims that there is also a secondary effect for resulting organic fertiliser. Z'Fix is produced in

the form of granules based on calcium and magnesium carbonates with an admixture of micro- and macro-elements (potassium, sodium, sulphur, iron, manganese), which is designed to regulate fermentation processes in manure and compost. The composition of Z'Fix is: organic matter – 5%, Ca – 26.8%, Mg – 2.7%, Na – 2.88%, S – 0.28%, K – 0.42%, P – 0.04%, Fe – 2 000 ppm; Mn – 150 ppm, Zn – 30 ppm. The patented MIP (mineral inducer process) technology uses bioactive properties of minerals and specific trace elements in order to stimulate the biological reactions of the plant and the microflora within the soil.

The site and crop management. The field experiment was conducted near the town of Městec Králové, Central Bohemian Region, Czech Republic (50°12'56.8''N, 15°19'50.6''E, 235 m a.s.l.) during 2018–2020 cropping seasons. The experimental field of the farm company ZS Sloveč, a.s. involved three smaller plots according to the agricultural management. The area of the control variant (C) was 1 ha, while the variant with pure farmyard manure (FYM) and farmyard manure treated by Z'Fix (FYM_ZF) had 5 ha. The distribution of experimental variants was performed with respect to the dimensions of the field.

According to the national system, the soil type is Haplic Chernozem. According to the USDA triangle diagram, it is clay loam soil. Selected chemical properties of the soil on the monitored plot are shown in Table 1.

NPK fertiliser was applied at the rate corresponding to the farm-specific agricultural standards concerning crop demand for pure nutrients. Cattle manure (FYM and FYM_ZF) dosages were as follows: 2017 – 50 t/ha; 2019 – 30 t/ha. Concerning the FYM_ZF variant, Z'Fix was applied at the rate of 1 kg/head/week directly to deep bedding. The composition characteristics of manure and manure treated by

Table 1. Chemical soil properties

		Soil depth (cm)	
		0–30	30–60
C	(%)	3.1	2.7
C/N ratio		9.7	6.9
pH_{KCl}		7.1	7.2
K		797	697
Ca	(ppm)	7 532	8 036
Mg		350	337
P		159	123

Table 2. Cattle manure chemical analysis for variants FYM (farmyard manure) and FYM_ZF (farmyard manure with Z'Fix)

Variant	Dry matter	N	C:N	P	K	Ca	Mg	pH
	(%)			(%)				
FYM	23.1	0.56	22.3:1	0.162	0.573	0.35	0.096	8.4
FYM_ZF	23.6	0.69	18.1:1	0.179	0.739	0.458	0.12	9.4

Z'Fix are shown in Table 2. The crop rotation system during the investigated seasons was as follows: sugar beet (2018), poppy (2019), and winter wheat (2020). Since soil properties are strongly influenced by water content, the information about precipitation is given in Figure 1.

Data acquisition and processing. To assess the physical soil properties, two field visits were accomplished each year. Cone index (CI), water infiltration (WI), and implement unit draft (IUD) were investigated. CI was measured in spring terms when the soil profile was more likely to have been evenly saturated with water. The measurements of the IUD and WI took place in the autumn terms, i.e., it followed the crop harvest, as it was a common practice for this kind of measurements.

CI is a staple indicator of pedocompaction, where higher values negatively impact the crop's ability to penetrate the soil profile and thus create a rich root system. CI is basically a measure of soil resistance against a cone with precisely described geometric properties (angle, area). To obtain such data, the penetrometer PN70 was developed at the Czech University of Life Sciences Prague. This custom-made device meets all requirements of the agriculture normative ASAE S313.3 (ASABE). Measurements of CI

were conducted in the spring term of each cropping season with ten repetitions per variant.

WI was examined using a rain simulator. This instrument was designed to measure not only parameters of erosion but also soil infiltration characteristics using a color dye. Usually, blue dye as a solution of water and brilliant blue (E 133) is used to spray the surface by the rain simulator for a period of 1 h. Such an application is followed by a 5 h break, during which the blue dye penetrates the soil profile. Afterwards, the soil profile is removed to a depth of approximately 40 cm and photographed. This method of infiltration characteristics assessment is based on image analysis (Figure 2). In the case of this study, the measurement was repeated three times per each variant. The soil profile was captured by a digital camera and further analysed by computer software Gwyddion 2.30 (Brno, Czech Republic). The pre-processing procedure involved cutting the image according to precisely located pins in order to analyse the exact same area recurrently, determining colour zones, and eliminating low-size soil particles to avoid errors caused by reflection. Further, the image was converted to a binary image, where the black colour defined the soil profile, and the white colour indicated the infiltrated area. In
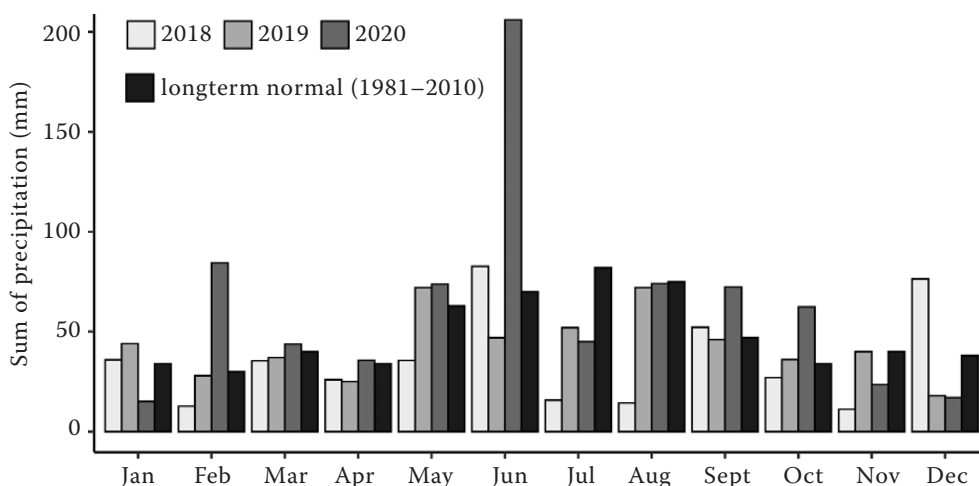

Figure 1. Rainfall conditions during investigated cropping seasons compared to a long-term normal
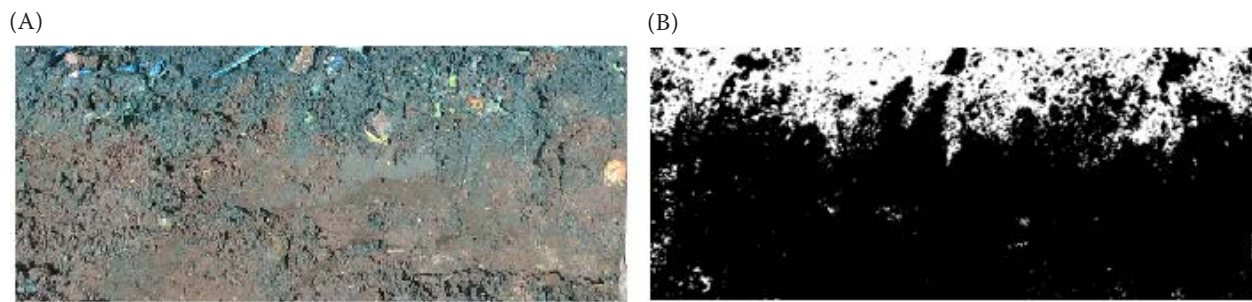
(A)

(B)

Figure 2. Water infiltration assessed by the rainfall simulator *via* (A) a digital image converted to (B) a binary image

this format, the image was also processed in ImageJ software (LOCI, Madison, USA), where the total image area was calculated together with the determination of percentages representing soil profile (black) and infiltrated part of it (white).

Energy demand for soil tillage is commonly described by the IUD. The IUD was determined using a drawbar dynamometer with strain gauge S-38/200kN (Lukas, Prague, Czech Republic) placed between the towing and the towed tractor. The IUD was measured using a tine cultivator Köckerling Vario 480 (Verl, Germany), during several passes of the machinery across each variant. The measurement was conducted under a constant speed and at a set tillage depth (2018 – 11 cm; 2019 – 17 cm; 2020 – 7 cm). The tillage depth was checked after each pass. In order to determine the potential influence of terrain slope and the rolling resistance of the towed tractor, machinery passes were repeated with the tillage implement, not in work. Data was collected using the system NI CompactRIO (National Instruments Corporation, Austin, USA), the sampling rate frequency was 0.1 s. GPS location was assigned to measured values using Trimble Business Center 2.70 (Trimble, Sunnyvale, USA).

Crop yields were measured using three separate passes of a harvester per each variant. The yield was weighed after each pass. When relevant, samples were taken to ascertain representative characteristics of the harvested product.

Since the set of soil properties has a direct impact on cropped vegetation, crop status within investigated variants was also evaluated. In the presented study, freely available Sentinel-2 satellite images (European Space Agency) with atmospheric correction and 10 m spatial resolution were collected and processed to obtain the normalised difference vegetation index (NDVI). NDVI is considered as a common indirect indicator of vegetation greenness and health (Rouse et al. 1974) and is often used to describe actual crop

status. Each variant was then described by the mean value of NDVI of all pixels within its boundary.

Statistics. The acquired dataset of all investigated soil and crop properties was eventually statistically analysed with the aim to describe potential differences between investigated variants. The required homogeneity of variances for ANOVA utilisation was not met in the case of soil physical properties; therefore, a non-parametric Kruskal-Wallis test of variance was applied. Nevertheless, remotely sensed data met the ANOVA requirements, and so NDVI variance was evaluated using a standard parametric test (ANOVA with random effect of the term) followed by Tukey *HSD* (honestly significant difference) test for multiple comparisons. For all the computations, the R version 4.0.4 (R Core Team 2021) with packages *readexcel*, *tidyverse*, and *reshape2* was utilised. Plots were further generated using the *ggplot* package (Vienna, Austria).

RESULTS AND DISCUSSION

Table 3 provides the results of the Kruskal-Wallis variance test for all investigated soil properties. CI was monitored in soil profile depths of 4, 8, 12, 16, and 20 cm. Although there was no statistically significant difference between variants, the trend depicted in Figure 3 shows the lowest values within FYM_ZF compared to the other two variants almost at all depth levels. In terms of WI, FYM_ZF performed the best since the analysis showed a significant difference compared to C in 2018 and 2020, i.e., in the years straight after the manure application. The situation in particular soil profile levels is presented in Figure 4, where FYM_ZF shows the best infiltration characteristics at all depths and years. Eventually, IUD results indicated significant differences in FYM and FYM_ZF compared to C in seasons 2018 and 2020, i.e., again instantly after the manure application. Figure 5 provides the overview

Table 3. Descriptive statistics of investigated physical soil properties within variants C (control), FYM (farmyard manure), and FYM_ZF (farmyard manure with Z'Fix)

Variant	2018			2019			2020		
	mean ± SD	C	FYM	mean ± SD	C	FYM	mean ± SD	C	FYM
CI (MPa)									
4 cm									
C	0.35 ± 0.334	–	–	0.43 ± 0.134	–	–	0.55 ± 0.127	–	–
FYM	0.422 ± 0.406	0.8	–	0.4 ± 0.125	0.97	–	0.55 ± 0.085	0.91	–
FYM_ZF	0.39 ± 0.281	0.8	0.84	0.42 ± 0.123	0.97	0.97	0.58 ± 0.199	0.91	0.91
8 cm									
C	1.17 ± 0.587	–	–	0.83 ± 0.125	–	–	0.99 ± 0.247	–	–
FYM	1 ± 0.568	0.68	–	0.83 ± 0.2	0.72	–	0.89 ± 0.233	0.45	–
FYM_ZF	0.94 ± 0.712	0.59	0.68	0.77 ± 0.067	0.72	0.72	0.8 ± 0.125	0.13	0.48
12 cm									
C	2.04 ± 0.532	–	–	1.07 ± 0.267	–	–	1.33 ± 0.424	–	–
FYM	1.289 ± 0.528	0.4	–	0.94 ± 0.158	0.53	–	1.12 ± 0.355	0.36	–
FYM_ZF	1.2 ± 0.506	0.4	0.54	0.9 ± 0.141	0.32	0.53	1.07 ± 0.350	0.2	0.62
16 cm									
C	2.04 ± 0.532	–	–	1.45 ± 0.493	–	–	1.62 ± 0.450	–	–
FYM	1.744 ± 0.332	0.45	–	1.09 ± 0.238	0.092	–	1.53 ± 0.291	0.91	–
FYM_ZF	1.75 ± 0.453	0.45	1	1.01 ± 0.166	0.058	0.509	1.45 ± 0.328	0.91	0.91
20 cm									
C	2.36 ± 0.497	–	–	1.71 ± 0.547	–	–	1.99 ± 0.482	–	–
FYM	2.011 ± 0.289	0.42	–	1.25 ± 0.242	0.054	–	2.03 ± 0.416	0.62	–
FYM_ZF	2.25 ± 0.54	0.73	0.45	1.24 ± 0.299	0.054	0.787	1.8 ± 0.422	0.57	0.57
UID (kN/m^2)									
C	105.11 ± 4.131	–	–	170.8 ± 5.376	–	–	246.571 ± 14.095	–	–
FYM	104.62 ± 5.833	0.82	–	172.77 ± 4.973	0.29	–	243.47 ± 14.340	0.26	–
FYM_ZF	97.86 ± 6.713	**< 0.001**	**< 0.001**	168.82 ± 6.766	0.29	0.1	233.43 ± 15.319	**< 0.001**	**< 0.001**
WI (%)									
C	22.724 ± 8.566	–	–	22.34 ± 3.195	–	–	12.76 ± 3.163	–	–
FYM	30.243 ± 13.447	0.325	–	36.827 ± 4.853	0.0591	–	22.253 ± 5.003	0.198	–
FYM_ZF	48.975 ± 18.093	**0.034**	0.146	53.02 ± 5.256	0.0097	0.0591	34.82 ± 5.391	**0.013**	0.198

Results of Kruskal-Wallis variance test (significance level $P < 0.05$ in bold). SD – standard deviation; CI – Cone index; IUD – implement unit draft; WI – water infiltration

for all three seasons. Furthermore, vegetation status expressed by means of NDVI was evaluated, and results are presented in Table 4. Even though three different crops were evaluated, statistically significant differences were indicated by ANOVA in all levels ($P < 0.01$). The secondary impact of a particular treatment on crop status is also demonstrated by yield information provided in Table 5. The best yields were consistently attained by FYM_ZF, followed by FYM throughout all three seasons. As demonstrated
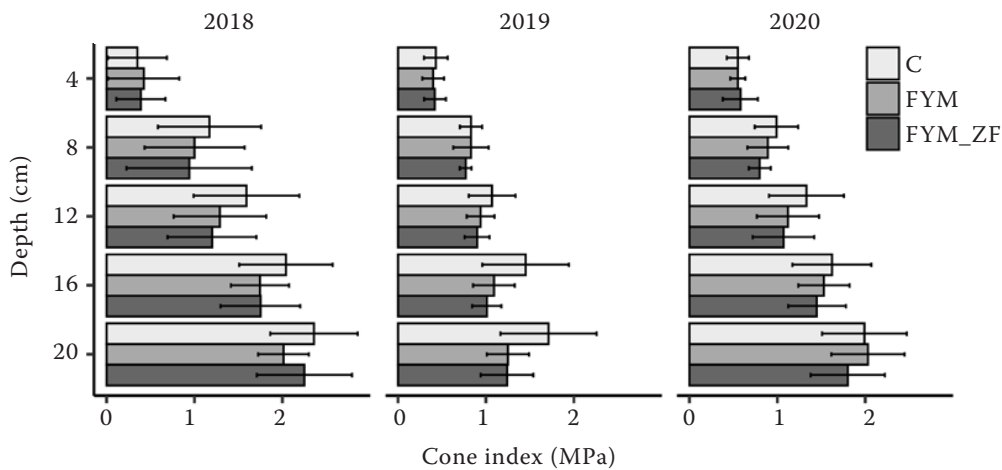
Figure 3. Cone index acquired by the penetrometer PN70, error bars representing standard deviation. C – control; FYM – farmyard manure; FYM_ZF – farmyard manure with Z'Fix

in Table 5, the differences in yields were significant between FYM_ZF and C in the case of sugar beet and winter wheat. Also, the sugar content reached by FYM and FYM_ZF was significantly higher than the one attained by C.

CI represents a staple soil property since it is closely related to root architecture and thus also a water uptake (Colombi et al. 2018). CI around 2.5 MPa is considered the threshold where higher values directly restrict the plant growth (Whalley et al. 2007). In the case of this study, this threshold was not reached within any variant, nor depth. However, positive effects of Z'Fix treatment may be observed through the reduced CI values in comparison with control and pure manure. The study of Celik et al. (2010) confirms that the application of organic fertilisers leads to a reduction in CI. In our study, FYM_ZF

performs even better than FYM in most of the cases, and this beneficial effect, even though not significant, is likely to be supported by Z'Fix addition. The reduction of CI in upper layers of the soil profile is in line with findings of the study of Čermáková et al. (2019). When CI was lower when using Z'Fix.

The results of WI using a rain simulator showed a trend that was maintained during all monitored seasons. These results seem to be very interesting, as they do not provide a simple point information since the area under investigation involves approx. 4 square meters of the soil profile. The highest WI was always achieved by the FYM_ZF variant. In addition, there were statistically significant differences between C and FYM_ZF each season following manure application. The results clearly show an improvement of infiltration conditions for the FYM_ZF variant,
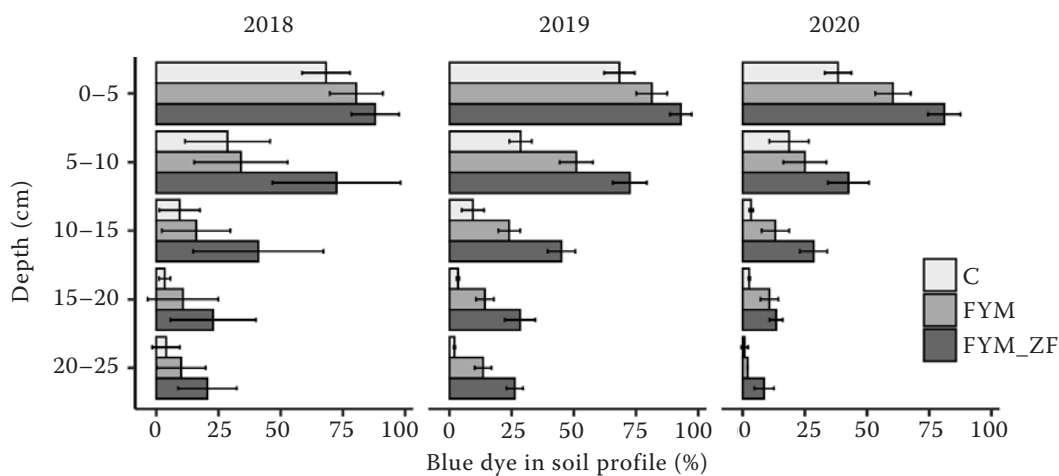

Figure 4. Percentage of infiltrated area (WI) using rainfall simulator in specific levels error bars representing the standard deviation. C – control; FYM – farmyard manure; FYM_ZF – farmyard manure with Z'Fix

Table 4. Descriptive statistics of normalised difference vegetation index (NDVI) (best performing variant in bold) and results of ANOVA with random effect (term) through Tukey *HSD* (honestly significant difference) test (*sowing date; ×harvest date)

Sugar beet — 31. 3. 2018*; 23. 10. 2018×

	Tukey *HSD*	19. 4.	21. 4.	29. 4.	4. 5.	21. 5.	26. 5.	3. 7.	5. 7.	22. 8.	27. 8.	29. 8.	18. 9.	28. 9.	11. 10.
FYM	b	0.231 ± 0.010	0.225 ± 0.008	0.219 ± 0.009	0.276 ± 0.010	0.635 ± 0.052	0.742 ± 0.034	0.883 ± 0.006	0.823 ± 0.007	0.577 ± 0.026	0.593 ± 0.026	0.602 ± 0.025	0.640 ± 0.031	**0.663** ± 0.035	**0.672** ± 0.035
FYM_ZF	c	**0.234** ± 0.010	**0.231** ± 0.009	**0.226** ± 0.009	**0.286** ± 0.010	**0.705** ± 0.062	0.781 ± 0.040	**0.886** ± 0.009	**0.827** ± 0.012	**0.605** ± 0.045	**0.627** ± 0.045	**0.626** ± 0.041	**0.646** ± 0.051	0.651 ± 0.045	0.648 ± 0.038
C	a	0.227 ± 0.010	0.223 ± 0.008	0.219 ± 0.009	0.280 ± 0.008	0.700 ± 0.024	**0.781** ± 0.013	0.881 ± 0.007	0.819 ± 0.010	0.556 ± 0.022	0.569 ± 0.024	0.581 ± 0.022	0.597 ± 0.031	0.603 ± 0.030	0.610 ± 0.028

Poppy — 1. 3. 2019*; 26. 7. 2019×

	Tukey *HSD*	1. 4.	4. 4.	21. 4.	26. 5.	3. 6.	5. 6.
FYM	b	0.213 ± 0.014	0.181 ± 0.016	0.254 ± 0.020	**0.859** ± 0.008	**0.929** ± 0.004	**0.908** ± 0.005
FYM_ZF	c	0.222 ± 0.011	0.195 ± 0.011	0.265 ± 0.013	0.857 ± 0.008	0.927 ± 0.004	0.904 ± 0.006
C	a	**0.227** ± 0.009	**0.206** ± 0.011	**0.271** ± 0.009	0.857 ± 0.011	0.925 ± 0.008	0.904 ± 0.010

Winter wheat — 4. 10. 2019*; 23. 7. 2020×

	Tukey *HSD*	31. 10.	30. 11.	24. 3.	29. 3.	5. 4.	8. 4.	20. 4.	23. 4.	28. 4.	8. 5.	18. 5.
FYM	b	0.395 ± 0.056	0.661 ± 0.065	0.801 ± 0.039	0.755 ± 0.038	0.723 ± 0.034	0.751 ± 0.029	0.824 ± 0.017	0.846 ± 0.015	0.835 ± 0.015	0.856 ± 0.012	0.897 ± 0.011
FYM_ZF	c	**0.454** ± 0.025	**0.738** ± 0.030	**0.852** ± 0.022	**0.815** ± 0.022	**0.783** ± 0.023	**0.803** ± 0.022	**0.838** ± 0.016	**0.855** ± 0.015	**0.840** ± 0.015	**0.864** ± 0.011	**0.898** ± 0.008
C	a	0.351 ± 0.030	0.584 ± 0.031	0.761 ± 0.032	0.738 ± 0.038	0.712 ± 0.035	0.746 ± 0.033	0.811 ± 0.021	0.834 ± 0.018	0.826 ± 0.018	0.853 ± 0.013	0.890 ± 0.011

C – control; FYM – farmyard manure; FYM_ZF – farmyard manure with Z'Fix
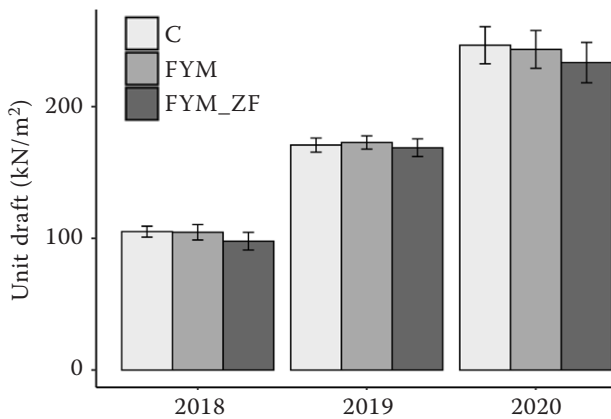
Figure 5. Implement unit draft obtained by dynamometer with strain gauge S-38/200kN, error bars representing the standard deviation. C – control; FYM – farmyard manure; FYM_ZF – farmyard manure with Z'Fix

as well as the general effect of manure and other organic matter, but to a lesser extent than when using activators. Concerning the fact that the WI is influenced by the bulk density (Chyba et al. 2017), WI results of the present study concurrently confirm the conclusions of the study of Šařec et al. (2017b), which described the favourable effect of Z'Fix on soil properties, bulk density, respectively.

The reduction in IUD within FYM_ZF is in line with the results obtained in previous small-plots one-year studies on two different soil types, where cattle manure treated by Z'Fix was applied (Šařec and Žemličková 2016, Žemličková and Šařec 2016). Tillage is one of the most energy-intensive operations in agriculture. The implement draft of FYM_ZF decreased by 4.5% (three-years average) compared to FYM. This decrease might result in fuel savings of about 0.45 L/ha (assuming average power delivery efficiency of around 50% and the fuel requirements of tillage operations at the level of 20 L/ha). However, the benefit is not only linked directly to fuel consumption and costs but also to the reduced emissions produced during tillage (Lal et al. 2019). Finally, vegetation conditions were evaluated. A total of 31 satellite images between 2018–2020 were analysed to derive the NDVI index. The beneficial effect of the Z'Fix during the emergence phase could be observed by sugar beet (2018) and wheat (2020). However, the effect was uncertain in 2019 (Table 4). Z'Fix seemed to maintain beneficial even during the drought periods. Although the months of July and August were really dry in 2018 (Figure 1), FYM_ZF kept showing the highest NDVI values. This observation is in line with the statement of Šařec et al. (2017b), which declares that Z'Fix can alleviate the stress of vegetation in the dry season.

Table 5. Descriptive statistics of yield parameters during the period of field experiment and results of one-way ANOVA through Tukey *HSD* (honestly significant difference) test (statistically significant results with *P* < 0.05 marked as bold)

Year	Variable	Variant	Mean ± SD	C	FYM
2018	sugar beet yield (t/ha)	C	55.19 ± 2.38	–	–
		FYM	58.60 ± 1.84	0.150	–
		FYM_ZF	61.17 ± 1.33	**0.020**	0.295
	sugar content (%)	C	19.00 ± 0.46	–	–
		FYM	21.80 ± 0.70	**0.002**	–
		FYM_ZF	22.20 ± 0.30	**0.001**	0.629
2019	poppy yield (t/ha)	C	0.82 ± 0.10	–	–
		FYM	0.89 ± 0.06	0.555	–
		FYM_ZF	0.97 ± 0.07	0.126	0.473
	poppy seed and straw mix yield (t/ha)	C	1.41 ± 0.09	–	–
		FYM	1.49 ± 0.07	0.496	–
		FYM_ZF	1.56 ± 0.09	0.141	0.576
2020	winter wheat yield (t/ha)	C	7.60 ± 0.27	–	–
		FYM	8.13 ± 0.20	0.322	–
		FYM_ZF	8.66 ± 0.62	**0.044**	0.322

SD – standard deviation; C – control; FYM – farmyard manure; FYM_ZF – farmyard manure with Z'Fix

Eventually, based on the above-described results, the following conclusions can be drawn. CI and IUD were mostly reduced when using agent Z'Fix for manure treatment. Concurrently, WI status was found to be superior over the other variants. All those described effects on the soil environment also positively influenced the plant status indicated by NDVI and finally resulted in higher yields during investigated cropping seasons, especially in drought periods. With respect to the sustainability of agricultural production, these findings are directly applicable to the agricultural practice; nevertheless, it is necessary to verify them further under different conditions (various soil types, manures, and climatic conditions, etc.).

REFERENCES

Bauer A., Black A.L. (1994): Quantification of the effect of soil organic matter content on soil productivity. Soil Science Society of America Journal, 58: 185–193.

Berzsenyi Z., Győrffy B., Lap D.Q. (2000): Effect of crop rotation and fertilisation on maize and wheat yields and yield stability in a long-term experiment. European Journal of Agronomy, 13: 225–244.

Cai A.D., Xu M.G., Wang B.R., Zhang W.J., Liang G., Hou E., Luo Y. (2019): Manure acts as a better fertilizer for increasing crop yields than synthetic fertilizer does by improving soil fertility. Soil and Tillage Research, 189: 168–175.

Celik I., Gunal H., Budak M., Akpinar C. (2010): Effects of long-term organic and mineral fertilizers on bulk density and penetration resistance in semi-arid Mediterranean soil conditions. Geoderma, 160: 236–243.

Čermáková N., Šařec P., Látal O. (2019): Impact of manure and selected conditionners on physical properties of clay soil. In: TAE 2019 – Proceeding of 7th International Conference on Trends in Agricultural Engineering. Prague, Czech University of Life Sciences Prague, 93–98. ISBN 978-80-213-2953-9

Chyba J., Kroulik M., Krištof K., Misiewicz P.A. (2017): The influence of agricultural traffic on soil infiltration rates. Agronomy Research, 15: 664–673.

Cluett J., VanderZaag A.C., Baldé H., McGinn S., Jenson E., Hayes A.C., Ekwe S. (2020): Effects of two manure additives on methane emissions from dairy manure. Animals, 10: 807.

Colombi T., Torres L.C., Walter A., Keller T. (2018): Feedbacks between soil penetration resistance, root architecture and water uptake limit water accessibility and crop growth – a vicious circle. Science of The Total Environment, 626: 1026–1035.

Czech Statistical Office (2021): Czech Statistical Office. Prague, Czech Statistical Office.

Gerber P.J., Steinfeld H., Henderson B., Mottet A., Opio C., Dijkman J., Falcucci A., Tempio G. (2013): Tackling Climate Change Through Livestock – A Global Assessment of Emissions and Mitigation Opportunities. Rome, Food and Agriculture Organisation of the United Nations.

Lal B., Gautam P., Nayak A.K., Panda B.B., Bihari P., Tripathi R., Shahid M., Guru P.K., Chatterjee D., Kumar U., Meena B.P. (2019): Energy and carbon budgeting of tillage for environmentally clean and resilient soil health of rice-maize cropping system. Journal of Cleaner Production, 226: 815–830.

Lal R. (2020): Soil organic matter and water retention. Agronomy Journal, 112: 3265–3277.

Matula S. (2003): The influence of tillage treatments on water infiltration into soil profile. Plant, Soil and Environment, 49: 298–306.

Mozdzer E., Chudecka J. (2017): Impact of natural fertilization using PRP fix on some soil fertility indicators. Journal of Ecological Engineering, 18: 137–144.

Önemli F. (2011): The effects of soil organic matter on seedling emergence in sunflower (*Helianthus annuus* L.). Plant, Soil and Environment, 50: 494–499.

R Core Team (2021): R: A Language and Environment for Statistical Computing. Vienna, R Foundation for Statistical Computing.

Rouse R.W.H., Haas J.A.W., Deering D.W. (1974): Monitoring Vegetation Systems in the Great Plains with ERTS. In: Proceedings of a Symposium Held – Third Earth Resources Technology Satellite-1 Symposium. Washington, NASA SP-351, 309–317.

Šařec P., Látal O., Novák P. (2017a): Technological and economic evaluation of manure production using an activator of biological transformation. Research in Agricultural Engineering, 63: S59–S65.

Šařec P., Novák P., Kumhálová J. (2017b): Impact of activators of organic matter on soil and crop stand properties in conditions of very heavy soils. In: Proceedings of the 16th International Scientific Conference Engineering for Rural Development, Jelgava.

Šařec P., Žemličková N. (2016): Soil physical characteristics and soil-tillage implement draft assessment for different variants of soil amendments. Agronomy Research, 14: 948–958.

Voltr V., Menšík L., Hlisnikovský L., Hruška M., Pokorný E., Pospíšilová L. (2021): The soil organic matter in connection with soil properties and soil inputs. Agronomy, 11: 779.

Whalley W.R., To J., Kay B.D., Whitmore A.P. (2007): Prediction of the penetrometer resistance of soils with models with few parameters. Geoderma, 137: 370–377.

Žemličková N., Šařec P. (2016): Influence of application of organic matter and its activators on soil-tillage implement draft on Modal Luvisol. In: Proceedings of the 6th International Conference on Trends in Agricultural Engineering. Prague, 736–742.

Appendix 4

Potential Impact of Biostimulator NeOsol and Three Different Manure Types on Physical Soil Properties and Crop Status in Heavy Soils Conditions

Novák, V., Šařec, P., Křížová, K., Novák, P., & Látal, O. (2022). Potential Impact of Biostimulator NeOsol and Three Different Manure Types on Physical Soil Properties and Crop Status in Heavy Soils Conditions. *Sustainability, 14*(1), 438. https://doi.org/10.3390/SU14010438

Article

Potential Impact of Biostimulator NeOsol and Three Different Manure Types on Physical Soil Properties and Crop Status in Heavy Soils Conditions

Václav Novák [1], Petr Šařec [1,*], Kateřina Křížová [1,2], Petr Novák [3] and Oldřich Látal [4]

[1] Department of Machinery Utilization, Faculty of Engineering, Czech University of Life Sciences Prague, 165 00 Prague, Czech Republic; novakvaclav@tf.czu.cz (V.N.); krizovak@tf.czu.cz (K.K.)

[2] Division of Crop Protection and Plant Health, Crop Research Institute, 161 06 Prague, Czech Republic

[3] Department of Agricultural Machines, Faculty of Engineering, Czech University of Life Sciences, 165 00 Prague, Czech Republic; novakpetr@tf.czu.cz

[4] Department of Agrochemistry, Soil Science, Microbiology and Plant Nutrition, Faculty of AgriSciences, Mendel University in Brno, 613 00 Brno, Czech Republic; oldrich.latal@mendelu.cz

* Correspondence: psarec@tf.czu.cz

Abstract: This study was conducted to understand the long-term influence of biostimulator NeOsol in combination with different manure types on soil's physical properties and crop status. NeOsol is a soil biostimulator that should stimulate the biological reactions of the soil profile and improve the soil's physical and chemical properties. A six-year experiment was conducted with eight treatments: NPK, cattle manure, pig manure, poultry manure, and the same four treatments with the NeOsol added on top. The in situ sampling of soil properties provided data on unit draft (UD), bulk density (BD), and saturated hydraulic conductivity (SHC). Furthermore, remotely sensed data were analyzed to describe crop status via three selected vegetation indices (VI), and crop yields were assessed last. The variants treated with NeOsol demonstrated decreases in UD over time; BD, SHC, and VI did not significantly change. The impact on yield was significant and increased over time. When comparing the variants with manure application to those without one, the cattle manure led to significantly higher SHC; the pig manure led to significantly lower UD and BD but significantly higher SHC and yield; and the poultry manure led to significantly lower UD and BD but higher yield.

Keywords: bulk density; unit draft; saturated hydraulic conductivity; yield; Sentinel-2

1. Introduction

The growing population and the impacts of climate change are the major drivers of a significant revolution in current agriculture. Today, farmers around the globe are under substantial pressure to ensure still-higher yields in a limited area. In doing so, they must adjust their common management to actual environmental policies. Although the impacts of changing climate vary among regions and by crop, it is clear that responsible strategies must be adopted on a global scale [1]. Research-based technologies began to be implemented in the 1950s [2]. Collecting, processing, and transferring data into practice are some of the cornerstones of precision agriculture, one of the staple concepts of the ongoing Agriculture 4.0 [3]. Properly interpreted results then enable practitioners to (a) increase productivity, (b) reasonably allocate sources, (c) adapt agricultural management, and (d) avoid food waste [4]. Along with the rapid development in technology over recent decades, significant efforts have been undertaken to design and apply technologies helping to fight emerging food production issues [5].

Soil fertility is a major factor for sustainable agriculture [6]. Soil properties, including infiltration and soil structure stability may be improved with manure application. The

method, rate, and timing of manure application should be considered to reduce environmental impacts, e.g., soil erosion [7]. Soil erosion by water is an outcome of two main processes: firstly, the detachment of soil particles from the soil surface by raindrop impact, and secondly, the transport of the detached particles by raindrop splash or surface runoff. Hence, the structure stability of the soils affects the rate of soil erosion. Management practices [8] used to control runoff include contouring, strip cropping, conservation tillage, terraces, and buffer strips. More than one runoff-control practice may be necessary for protection in areas with high runoff potential. Current intensive agricultural management often fatigues the soil to an extreme extent in some regions, so fertility has to be restored by a fertilizer supply [9]. Generally, organic fertilizers act as natural products while manufactured mineral fertilizers mostly consist of ideal combinations of NPK nutrients. Although mineral fertilizers appear to be an easy solution to soil fertility issues, it concurrently has many other negative impacts on the surrounding environment as a whole. Thus, properly managed organic fertilizers are the preferable option, since it is commonly known that they positively influence both chemical and physical soil properties [10]. Nevertheless, the amount of produced organic fertilizers has decreased in Europe over recent decades as animal husbandry (such as cattle and pigs) has been significantly reduced [11]. Therefore, new approaches are being researched and tested to exploit the positive features of organic fertilizers as much as possible. NeOsol (previously PRP SOL) is manufactured by Olmix Group (France) as a soil microbial biomass activator. When applied to a soil profile, it is supposed to stimulate soil biological activity and hence promote hummus synthesis. Various studies have already been conducted to describe NeOsol's actual impact on (a) soil properties, (b) plant status, (c) crop yields, and (d) compost properties. According Spychalski et al. [12], PRP SOL significantly influenced the chemical properties of soil by increasing pH and available form of magnesium, as well as by decreasing available forms of potassium. Enhanced water and nutrient uptake [13], favorable effects on soil compaction and the moisture status of the top layer [14], and reductions in the force required by soil tillage [15] were observed. Furthermore, beneficial impacts on the enzymatic activity of sand and clay soils were described by Bielińska et al. [16]. Naturally, enhanced soil properties directly impact crop growth. This was the subject of a study by Borowiak et al. [17], where PRP SOL had a positive effect on the photosynthesis rate and plant growth of spring barley and maize. PRP SOL was found to significantly enhance chlorophyll content in the leaf blades of ryegrass [18]. Various studies have also described higher yields of soybean [19], potatoes [20], and the dry matter of calendula [21] with the use of PRP SOL. Porro and Pedò [22] found that grape vines on vineyards treated with PRP SOL were in better physiological and eco-physiological condition than controls, and the taste of the final products was fruitier and more floral. The biostimulative potential of the PRP SOL was studied in combination with municipal compost, where the total contents of nickel, manganese, lead, and their soluble forms in soil were observed [23]. Furthermore, the application of compost in combination with PRP SOL had a significantly positive impact on wheat grain yield [24].

Although the above-mentioned studies addressed the topic of the biostimulator NeOsol, this study was aimed at verifying the effectiveness of this soil agent and its effect on enhancing the outcome of the three types of manure in a six-year experiment in real agricultural conditions. The hypotheses to be verified are as follows: the use of this soil agent would lead to a) reductions in implement unit draft and bulk density, (b) increase in saturated hydraulic conductivity, (c) enhancement of crop growth, and (d) increase in crop yield.

2. Materials and Methods

2.1. Biostimulator NeOsol

NeOsol is manufactured by Olmix Group (Bréhan, France) as a granular biostimulator of vital soil functions. This soil agent uses the patented technology MIP (Mineral Inducer Process). It exploits the bioactive properties of minerals and specific trace elements to stimulate the biological reactions within the soil profile. More specifically, it uses iron, manganese, copper, and boron to stimulate enzymatic reactions involved in the transformation of raw organic matter, especially humification (α-glucosidase, ß-glucosidase, etc.). In addition to MIP technology, NeOsol also uses SEAweed DRY algae extracts, which are rich in nutrients, for soil biota stimulation.

This biostimulator is declared to contain 28.0% *w/w* of CaO, 15.9% *w/w* of MgO, and 98.9% *w/w* of dry matter, from which the combustible substances create 7% w/DMw. The pH varies from 8 to 10, i.e., it is strongly alkaline.

The recommended dose ranges between 100 and 200 kg ha^{-1}, depending on crop and local soil conditions. The application is conducted after harvest in the same manner as granular mineral fertilizers, i.e., it is sprinkled on a soil's surface.

2.2. Site and Crop Management

A six-year study was undertaken within the experimental field near the town of Městec Králové in Central Bohemia of the Czech Republic (50°14.256′ N, 15°20.705′ E, 235 masl.). In terms of soil conditions, initial sampling was conducted at the beginning of the experiment in 2014 after the harvest of barley, and the characteristics are given in Table 1. The experiment was based on heavy soil (Gleyic Phaeozem), often referred to as difficult in terms of soil tillage management. In terms of texture, the soil fell into the clay category according to the USDA texture triangle.

Table 1. Analysis of the chemical and physical composition of the soil conducted at the beginning of the experiment in 2014.

	Soil Profile Depth (m)		Unit
	0.00–0.30	0.30–0.60	
Clay (<0.002 mm)	48	60	% *w/w*
Silt (0.002–0.05 mm)	32	39	% *w/w*
Very fine sand (0.05–0.10 mm)	2	1	% *w/w*
Fine sand (0.10–0.25 mm)	18	0	% *w/w*
Bulk density	1.46	1.48	g cm^{-1}
Porosity	46.15	43.99	% *w/w*
Hummus content	3.89	1.44	% *w/w*
Cation exchange capacity	278	272	mmol kg^{-1}
Volumetric moisture	35.65	40.20	% *v/v*
pH (KCl)	7.18	7.21	

The experimental field was divided into smaller plots with a rectangular area of 45 × 140 m (0.63 ha) per variant. These small plots were arranged with respect to the shape of the experimental field, and the headlands were left out. The characteristics of the treatments of particular variants with manure of different origin or with NeOsol are depicted in Table 2. Standard NPK mineral fertilizer was applied during vegetation to top up the nutrients contained in manure so that the recommended [25] full dose of nutrients for a specific crop grown was attained. Of course, the variant NPK, i.e., the control variant, was left without any additional treatment and the recommended full NPK dose including ground fertilization in autumn. This complex of treatments finally provided a set of eight variants, where all the subsequent samplings were undertaken.

Table 2. Treatment of individual variants during the experimental period (2014–2020).

Variant	Treatment		
	NPK [1]	Manure	NeOsol
NPK	Yes—full rate	No	No
NPKSOL	Yes—full rate	No	Yes
catt	Yes—top-up rate	Yes—cattle	No
cattSOL	Yes—top-up rate	Yes—cattle	Yes
pig	Yes—top-up rate	Yes—pig	No
pigSOL	Yes—top-up rate	Yes—pig	Yes
pou	Yes—top-up rate	Yes—poultry	No
pouSOL	Yes—top-up rate	Yes—poultry	Yes

[1] NPK application rate was calculated to top up the nutrients contained in manure so that the recommended [25] full dose of nutrients was attained in kg ha^{-1}: corn (N 185; P 30; K 190); winter wheat (N 180; P 35; K 95); spring barley (N 140; P 30; K 80).

The crop rotation system in the experimental field was carried out according to standard local practice. The agricultural business was located in a sugar beet production region with the crop rotation of cereals, corn, and either oilseed rape, or sugar beet. The latter two should not rotate in the same field. The standard crop rotation of the trial field included oilseed rape. The schedule of each field management practice during the experiment period is presented by Table 3. All types of manure were applied in fall using a manure spreader, while the NeOsol application proceeded immediately after harvest by a fertilizer spreader.

Table 3. Crop rotation and agricultural management during the experimental period (2014–2020).

Season	Sowing Date	Harvest Date	Crop	NeOsol (kg ha^{-1})	Cow Manure (t ha^{-1})	Pig Manure (t ha^{-1})	Poultry Manure (t ha^{-1})
2014	-	-	Barley	200	50	40	10
2015 Term I	14.4.2015	27.8.2015	Corn	200	-	-	-
2016	23.3.2016	5.8.2016	Spring barley	200	50	20	8
2017 Term II	2.11.2016	4.8.2017	Winter wheat	150	-	-	-
2018	10.4.2018	3.8.2018	Corn	150	-	-	-
2019	5.10.2018	24.7.2019	Winter wheat	150	30	20	10
2020 Term III	15.10.2019	30.7.2020	Winter wheat	150	-	-	-

2.3. Data Acquisition and Processing

Data assessment was performed for three terms selected to follow in the same interval after the manure application, i.e., in 2015 (Term I), 2017 (Term II), and 2020 (Term III). Hereby, the potential influence of uneven interval between the treatment and measurements was eliminated. The soil's physical properties were sampled by in situ measurements performed either in spring (bulk density and saturated hydraulic conductivity) or autumn (unit draft). To acquire data on unit draft (UD), a dynamometer with S-38/200 kN strain gauges (Lukas, Prague, the Czech Republic) was placed in a horizontal position between two tractors. Firstly, measurements were accomplished with the tillage implement at a working depth and a constant speed in order to measure the overall draft of the pulled tractor and the working implement. The working depth was verified by measurement after each pass. Secondly, the not-working implement was used to measure the rolling resistance and the force induced by the potential field gradient. These were deduced from the overall draft in order to calculate the implement draft. The direction of passes was also taken into account. With regard to common agricultural practices, measurements were made with different types of implements and at different depths of soil tillage. A Köckerling Vario 480 tine cultivator was operated at depths of 11 cm (2015—Term I) and 7 cm (2020—Term III). Furthermore, a Horsch Terrano 8 FG tine cultivator was operated

at 15 cm (2017—Term II). There were several passes done with each variant and the non-working and working implements, and GPS data were recorded by Trimble Business Center 2.70 (Trimble, Sunnyvale, California, USA). Simultaneously, raw UD data were collected using the NI CompactRIO system (National Instruments Corporation, Austin, Texas, USA). The sampling frequency for both GPS and UD was 0.1 s.

Furthermore, bulk density (BD) was determined via soil samples obtained using a soil sample ring kit (Eijkelkamp, Giesbeek Netherlands). The volume of each ring was 100 cm^3, and sampling was performed in three repetitions per variant. Further BD soil sample processing involved analysis in the laboratories of the Engineering Faculty of the Czech University of Life Sciences in Prague according to the national standard CSN EN ISO 17892-2.

Saturated hydraulic conductivity (SHC) was measured according to the simplified Falling-head method of Bagarello et al. [26]. It uses circular infiltrometers (in this case, 0.15 m diameter) and a known amount of water (0.5 l), which is subsequently poured on the soil surface in the area of the infiltrometer. Volumetric soil moisture was measured with a Theta Probe (Delta-T Devices, Ltd., UK) before and after water application. The time of water infiltration was measured for the later calculation of the final SHC value K_{fs} (Equation (1).

$$K_{fs} = \frac{(\Delta\theta)}{(1 - \Delta\theta)t_\alpha}\left[\frac{D}{\Delta\theta} - \frac{\left(D + \frac{1}{\alpha^*}\right)}{(1 - \Delta\theta)}\ln\left(1 + \frac{(1 - \Delta\theta)D}{(\Delta\theta)\left(D + \frac{1}{\alpha^*}\right)}\right)\right] \tag{1}$$

here: $\Delta\theta$ = difference between initial soil moisture content and saturated soil moisture content; D = the ratio of V (volume of water) and A (area of a cylinder), which is the water level corresponding to the water volume; t_α = infiltration time; and α = constant according to Elrick et al. [27].

Potential differences in the soil's physical properties between investigated treatments were determined through one-way (factor: term) or factorial (factors: term; manure type; NeOsol treatment) analyses of variance (ANOVA) and Tukey HSD post-hoc tests.

2.4. Crop Status

A secondary effect of the investigated treatments on crops within selected variants was further determined. For this purpose, remotely sensed data were utilized because they result from a simple and widely used non-destructive method used to acquire spatial data of crop status.

The European Space Agency (ESA) provides freely available remotely sensed imagery taken by the constellation of Sentinel satellites. In this case, cloud-free multispectral data of the Sentinel-2 were utilized. Basic vegetation indices, namely the Normalized Difference Vegetation Index (NDVI) as a basic indicator of plant health and greenness [28], the Normalized Difference Water Index (NDWI) that provides information on water contents in plant tissues [29], and the Leaf Area Index (LAI) that describes the robustness of vegetation canopy [30], were calculated. This set of indicators complexly describes a canopy in terms of nutrient and water saturation. Since the Sentinel-2 data were not yet available in 2015 and 2016, the above-mentioned indices were calculated only for the following cropping seasons: 2017, 2018, 2019, and 2020.

The whole process of indices calculation was carried out in the Google Earth Engine (GEE), as it provides a convenient online environment where every step is controlled by JavaScript code. This saves a user from time-consuming, one-by-one image processing and ensures the repeatability of the same processing steps for every image in a collection. Using GEE, pre-processed and ready-to-use imagery does not have to be downloaded to a local computer because they are directly processed on the server. For the purpose of this study, a zonal statistics summary of three vegetation indices was exported in a text file and further processed in RStudio 1.4.1717, with R version 4.1.0 [31]. Potential differences in crop performance between investigated treatments were determined through analysis

of variance (ANOVA) with the random effect of the image acquisition date to minimize the influence of varying index values through the cropping season.

Finally, crop yield was recorded using a combine harvester and a trailer positioned on a DINI ARGEO WWSB 16t portable static axle scale (DINI ARGEO S.r.l., Modena, Italy). The grain yield was weighed after each of set of three passes of the combine harvester per variant.

3. Results

3.1. Unit Draft

UD results are given in Figure 1, which also shows the multiple comparison analysis results based on Tukey's HSD test. The differences among investigated seasons were highly influenced by varying soil moisture during soil tillage, the type of the tillage implement used, and the depth of tillage. Therefore, comparisons of variants' UD were performed separately according to the particular terms by the one-way ANOVA. Statistically significant differences were detected for both pig manure variants, i.e., pig and pigSOL. Compared to NPK, NPKSOL, catt, and cattSOL, the pig manure variants attained considerably lower UD at Terms II and III. Pure pig manure variant (pig) values significantly differed from those obtained by NPK, NPKSOL, and catt at Term I. Otherwise, no notable differences were found. In the case of pigSOL, there was a gradual reduction in UD (relative to the NPK variant), overall reaching more than 10%. This decrease could result in fuel savings of about 1 L ha⁻¹ (assuming an average power delivery efficiency of around 50% and the fuel requirements of tillage operations at a level of 20 L ha⁻¹).
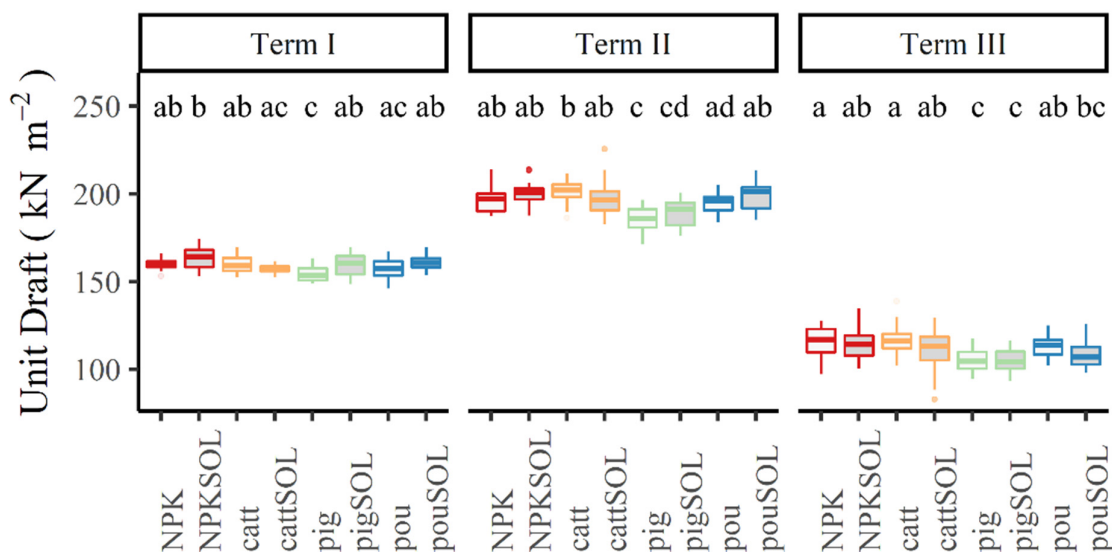

Figure 1. Unit draft within variants during the three investigated seasons. Error bars indicate the standard deviation, and letters represent multiple comparisons according to the results of Tukey's HSD test.

Additionally, the factorial (manure type; NeOsol treatment) ANOVA was employed separately for each of the terms. Concerning NeOsol treatment, Terms I and III presented significantly different results. Though variants treated with NeOsol attained higher UD values at Term I, the values become significantly lower at Term III. This fact suggests the favorable influence of the NeOsol activator on UD over a prolonged period of time. Regarding manure type, Term I presented significantly better (i.e., lower) UD values for the variants where cattle and particularly pig manure had been applied compared to the variants without any manure. At Term II, only both pig manure variants presented significantly lower UD values compared to all the other variants. The same outcome regarding

the pig manure variants was present at Term III. Moreover, both variants with poultry manure showed significant and favorable differences compared to the variants without manure application.

3.2. Bulk Density

Figure 2 shows the results of soil bulk density analysis after calculating the final values. In general, BD is a relatively constant indicator that has a key effect on, for example, soil infiltration. At Term I, relatively homogeneous values could be observed, though they changed during the following years. In this regard, the overall difference between Term I and II was found to be statistically significant. A degressive reduction in BD could be observed, particularly with the application of poultry manure and pigSOL. The importance of organic matter in soil is reflected in the highest BD values of variants without any type of manure supply, i.e., NPK and NPKSOL. Furthermore, the NPKSOL variant demonstrated a gradual increase in values during the monitored periods. The pig variant always presented higher BD values than the pigSOL variant. Applying the factorial (term; manure type; NeOsol treatment) analysis of variance though the factor of NeOsol, i.e., regardless of manure type and term, demonstrated no significant differences. Concerning manure type, pig and poultry showed significantly lower BD values than variants where no manure was applied, with the poultry manure's BD values significantly differing compared to the cattle manure. Regarding individual terms, Term II provided significant decreases in BD compared to Term I.
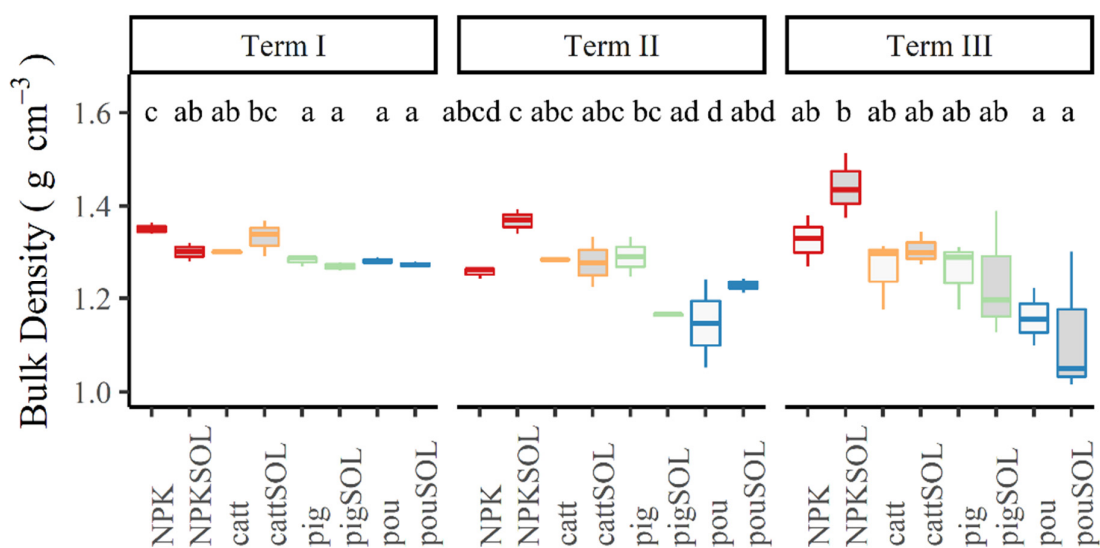

Figure 2. Bulk density within variants during the three investigated seasons. Error bars indicate the standard deviation, and letters represent multiple comparisons according to the results of Tukey's HSD test.

3.3. Saturated Hydraulic Conductivity

SHC results are presented in Figure 3. The values significantly differed among the terms, since the SHC was strongly influenced by the condition of the upper layer of the soil. Within the factorial (term; manure type; NeOsol treatment) analysis of variance, no significantly different values could be observed over the trial period between the variants, including those with/without the NeOsol biostimulator, although certain trends could be observed regarding the type of manure. The long-term use of pig manure and (particularly) cattle manure led to significantly improved SFH values compared to the variants without manure treatment. The SHC of both variants with cattle manure significantly sur-

passed the SHC values of variants with poultry manure. An adverse trend could be observed for the NPKSOL variant, where there was a constant decrease in SHC compared to the NPK variant. The addition of SOL to poultry manure increased the SHC value at each term, but this difference was not statistically significant.
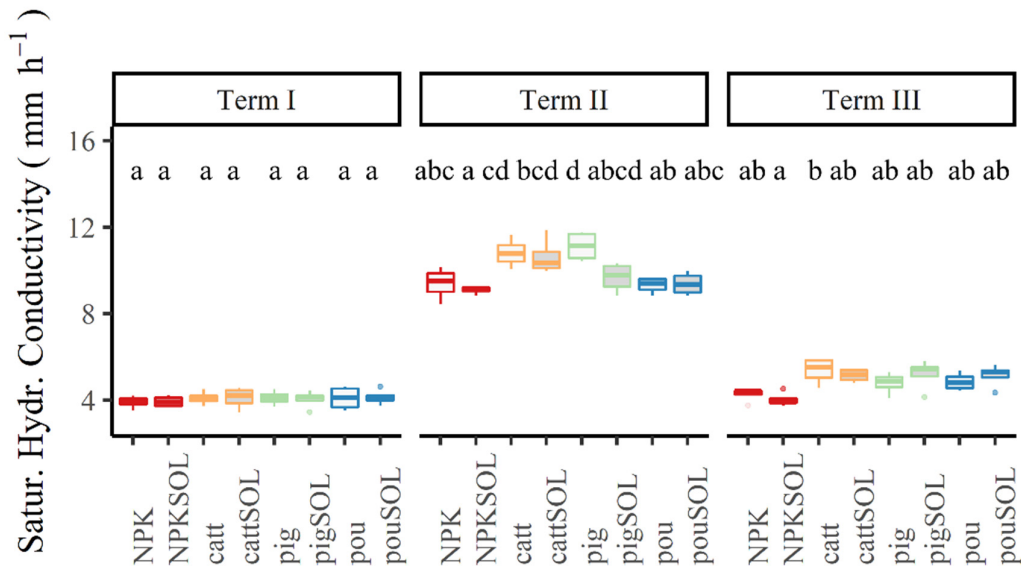

Figure 3. Saturated hydraulic conductivity within variants during the three investigated seasons. Error bars indicate the standard deviation, and letters represent multiple comparisons according to the results of Tukey's HSD test.

3.4. Vegetation Indices

The NDVI, NDWI, and LAI were generated from as many cloud-free Sentinel-2 images as there were available. These indexes introduced the spatial information of crop status in terms of (a) plant health, (b) water content, and (c) leaf area. Figure 4 depicts trends of the chosen indices through investigated cropping seasons that brought an overview information of the crop development, mostly in terms of the time effect of the used treatments.

ANOVA with the random effect of the date was performed to examine the potential diverse impact of treatments on both soil and crop status. Multiple comparisons are given in Table 4, where the gray highlighted lines represent the results of paired variants. These comparisons were supposed to answer the question of whether the NeOsol addition to the usual treatment was beneficial in terms of crop growth. It can be seen that no significant difference was found in any of these paired groups in any season. Some significant differences were observable for other variants. Those, however, appeared mostly between the control variant (NPK and NPKSOL) and variants enriched by organic matter of any kind. Hence, the effect of NeOsol addition was not verified when evaluating crop status. When focusing on the latest season (2020), the LAI was probably the most sensitive indicator, since it was also able to detect the differences among various manure types (e.g., poultry manure performed better than cattle).

Table 4. Multiple comparisons of crop status derived from three selected vegetation indices based on Tukey's HSD test. Paired variants (with/without NeOsol) are highlighted by gray color, and statistical significance levels are in bold as follows: $p < 0.05$ (*), $p < 0.01$ (**), and $p < 0.001$ (***).

	NDVI				NDWI				LAI			
	2017	**2018**	**2019**	**2020**	**2017**	**2018**	**2019**	**2020**	**2017**	**2018**	**2019**	**2020**
NPK–NPKSOL	−0.0049	−0.0037	0.0007	−0.0040	−0.0074	0.0062	−0.0018	−0.0069	−0.1032	0.1544	−0.0075	−0.0427
NPK–catt	−0.0126	−0.0159	−0.0125	**−0.0328 ***	−0.0225	−0.0225	**−0.0243 **	**−0.0493 ***	−0.2705	−0.0196	−0.1401	**−0.3302 ***
NPK–cattSOL	−0.0121	−0.0107	−0.0087	**−0.0256 ***	−0.0218	−0.0144	−0.0195	**−0.0385 ***	−0.2154	0.1198	−0.1054	**−0.2519 **
NPK–pig	−0.0107	**−0.0368 *	**−0.0173 *	**−0.0352 ***	−0.0232	−0.0312	**−0.0291 ***	**−0.0529 ***	−0.2540	−0.4654	−0.2331	**−0.4828 ***
NPK–pigSOL	**−0.0182 *	**−0.0410 **	**−0.0191 **	**−0.0384 ***	**−0.0333 *	−0.0338	**−0.0284 **	**−0.0554 ***	−0.3051	−0.9308	**−0.3241 **	**−0.5624 ***
NPK–pou	−0.0125	**−0.0403 **	**−0.0226 ***	**−0.0384 ***	**−0.0291 *	−0.0206	**−0.0290 **	**−0.0545 ***	−0.1564	−0.8391	**−0.3627 ***	**−0.5481 ***
NPK–pouSOL	−0.0129	−0.0316	**−0.0188 **	**−0.0354 ***	**−0.0289 *	−0.0215	**−0.0249 **	**−0.0519 ***	−0.1757	−0.6348	**−0.3284 **	**−0.5207 ***
NPKSOL–catt	−0.0077	−0.0123	−0.0132	**−0.0288 ***	−0.0150	−0.0287	**−0.0225 *	**−0.0425 ***	−0.1673	−0.1739	−0.1325	**−0.2874 ***
NPKSOL–cattSOL	−0.0072	−0.0070	−0.0094	**−0.0216 ***	−0.0144	−0.0206	−0.0178	**−0.0316 ***	−0.1122	−0.0346	−0.0979	**−0.2092 *
NPKSOL–pig	−0.0059	**−0.0331 *	**−0.0180 *	**−0.0312 ***	−0.0158	**−0.0374 *	**−0.0273 **	**−0.0460 ***	−0.1508	−0.6198	−0.2256	**−0.4401 ***
NPKSOL–pigSOL	−0.0133	**−0.0373 *	**−0.0198 **	**−0.0343 ***	−0.0259	**−0.0400 *	**−0.0266 **	**−0.0485 ***	−0.2019	**−1.0852 *	**−0.3165 **	**−0.5197 ***
NPKSOL–pou	−0.0076	**−0.0366 *	**−0.0233 ***	**−0.0344 ***	−0.0217	−0.0268	**−0.0273 **	**−0.0476 ***	−0.0532	**−0.9935 *	**−0.3551 **	**−0.5054 ***
NPKSOL–pouSOL	−0.0081	−0.0279	**−0.0195 **	**−0.0314 ***	−0.0214	−0.0277	**−0.0231 *	**−0.0450 ***	−0.0725	−0.7892	**−0.3209 **	**−0.4780 ***
catt–cattSOL	0.0005	0.0053	0.0038	0.0072	0.0006	0.0081	0.0048	0.0109	0.0551	0.1393	0.0347	0.0783
catt–pig	0.0018	−0.0209	−0.0048	−0.0024	−0.0007	−0.0087	−0.0048	−0.0035	0.0165	−0.4458	−0.0931	−0.1526
catt–pigSOL	−0.0056	−0.0251	−0.0066	−0.0056	−0.0108	−0.0113	−0.0040	−0.0060	−0.0346	−0.9113	−0.1840	**−0.2323 **
catt–pou	0.0001	−0.0243	−0.0101	−0.0056	−0.0067	0.0019	−0.0047	−0.0051	0.1142	−0.8196	−0.2226	**−0.2179 *
catt–pouSOL	−0.0003	−0.0156	−0.0063	−0.0027	−0.0064	0.0010	−0.0006	−0.0026	0.0949	−0.6153	−0.1884	−0.1905
cattSOL–pig	0.0013	−0.0261	−0.0086	−0.0096	−0.0014	−0.0168	−0.0096	−0.0144	−0.0386	−0.5851	−0.1278	**−0.2309 **
cattSOL–pigSOL	−0.0061	−0.0303	−0.0103	−0.0127	−0.0115	−0.0194	−0.0088	−0.0169	−0.0897	**−1.0506 *	−0.2187	**−0.3105 ***
cattSOL–pou	−0.0004	−0.0296	−0.0139	−0.0128	−0.0073	−0.0062	−0.0095	−0.0160	0.0590	**−0.9589 *	**−0.2573 *	**−0.2962 ***
cattSOL–pouSOL	−0.0009	−0.0209	−0.0101	−0.0098	−0.0070	−0.0071	−0.0054	−0.0134	0.0397	−0.7546	−0.2231	**−0.2688 **
pig–pigSOL	−0.0074	−0.0042	−0.0017	−0.0031	−0.0101	−0.0026	0.0008	−0.0025	−0.0511	−0.4655	−0.0909	−0.0796
pig–pou	−0.0017	−0.0034	−0.0053	−0.0032	−0.0059	0.0106	0.0001	−0.0016	0.0977	−0.3738	−0.1295	−0.0653

pig–pouSOL	−0.0022	0.0053	−0.0015	−0.0002	−0.0057	0.0097	0.0042	0.0010	0.0783	−0.1695	−0.0953	−0.0379
pigSOL–pou	0.0057	0.0007	−0.0035	0.0000	0.0042	0.0132	−0.0007	0.0009	0.1488	0.0917	−0.0386	0.0143
pigSOL–pouSOL	0.0052	0.0094	0.0002	0.0029	0.0044	0.0123	0.0035	0.0035	0.1295	0.2960	−0.0044	0.0417
pou–pouSOL	−0.0005	0.0087	0.0038	0.0029	0.0003	−0.0009	0.0042	0.0026	−0.0193	0.2043	0.0342	0.0274
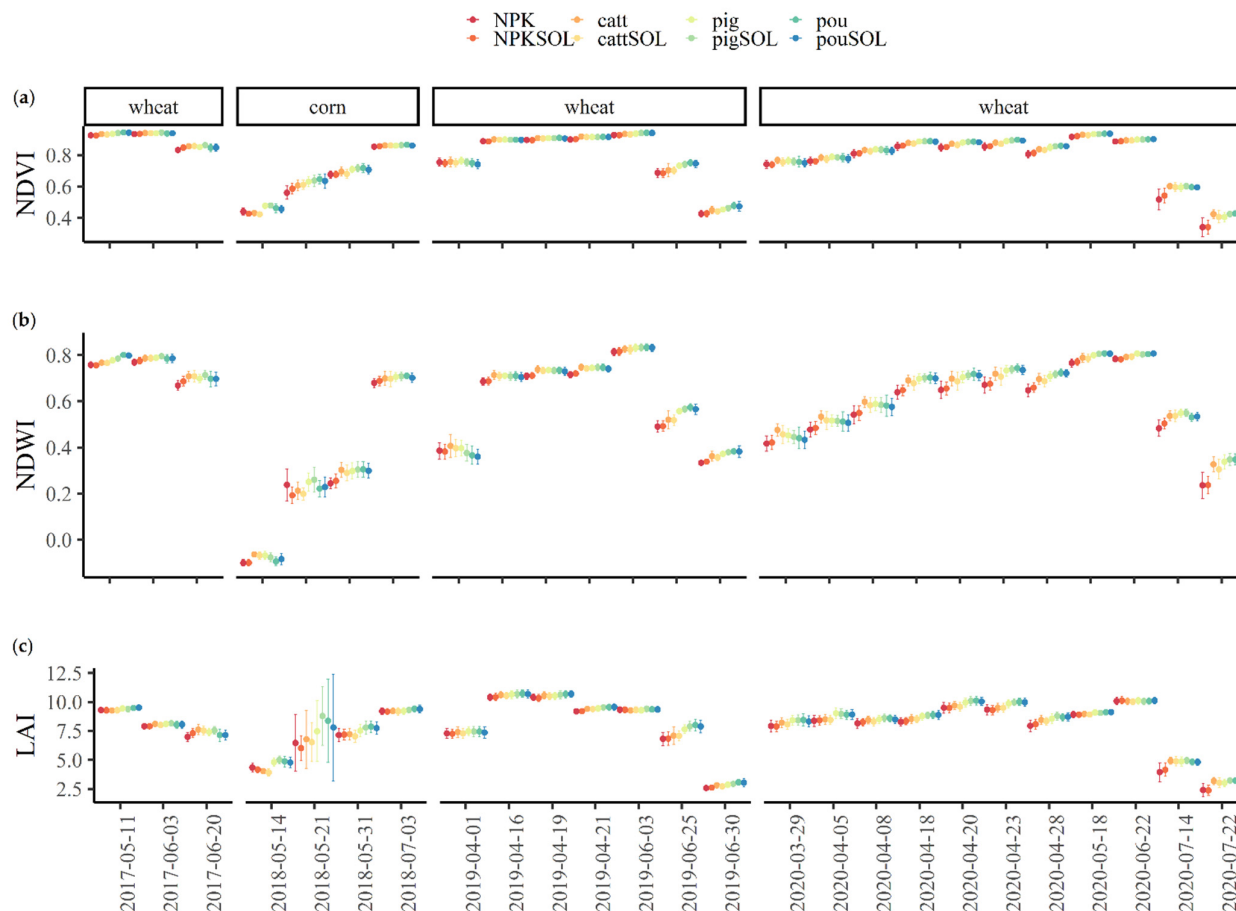
Figure 4. Crop status in terms of (**a**) crop health and biomass represented by the Normalized Difference Vegetation Index (NDVI), (**b**) crop water content status represented by the Normalized Difference Water Index (NDWI), and (**c**) canopy leaf area represented by the Leaf Area Index (LAI). Indices were derived from Sentinel-2 satellite imagery during the 2017-2020 cropping seasons. Error bars represent the standard deviation of index (pixel) values within each investigated small plot.

3.5. Yield

Table 5 presents the results of crop yields. When primarily focusing on variations between paired variants differing only in NeOsol content, higher yields were clearly obtained by the variants enriched with NeOsol, particularly at Terms II and III. This was also the case for cattle and pig manure in all three terms. Regarding poultry manure, the effect was observed at Terms II and III. NeOsol addition also had a beneficial effect on yield in the case of the NPK variant at Terms II and III. When applying the factorial (term; manure type; NeOsol treatment) analysis of variance, the overall difference between variants treated with NeOsol and the untreated variants was found to be significant. At the last term, the difference was most profoundly demonstrated. The pig and poultry manure types showed significantly higher yields than the variants where no manure was applied. When assessing the results separately within individual terms, the corn yields of the pigSOL and pou variants were significantly higher than most of the others. Term II did not demonstrate any significant differences among winter wheat yields. At Term III, however, almost all the variants reached significantly higher yields than the NPK variant.

Table 5. Descriptive statistics of yield (Mean ± Std. Dev.) during the terms of the field experiment and the results of one-way ANOVA through Tukey's HSD test.

Variant.	Term I	Term II	Term III
	Corn (t ha^{-1})	Winter Wheat (t ha^{-1})	Winter Wheat (t ha^{-1})
NPK	32.9 ± 0.7 (a)	7.71 ± 0.35 (a)	7.36 ± 0.33 (a)
NPKSOL	32.3 ± 0.8 (a)	7.95 ± 0.33 (a)	8.11 ± 0.32 (b)
catt	32.5 ± 0.7 (a)	8.43 ± 0.42 (a)	7.93 ± 0.21 (ab)
cattSOL	33.1 ± 0.7 (ab)	8.48 ± 0.42 (a)	8.29 ± 0.40 (b)
pig	32.1 ± 1.0 (a)	7.71 ± 0.36 (a)	8.11 ± 0.18 (b)
pigSOL	35.7 ± 0.6 (c)	8.10 ± 0.46 (a)	8.38 ± 0.22 (b)
pou	34.8 ± 0.8 (bc)	7.62 ± 0.30 (a)	8.11 ± 0.19 (b)
pouSOL	32.3 ± 0.9 (a)	7.90 ± 0.41 (a)	8.32 ± 0.19 (b)

4. Discussion

UD is a commonly used metric for assessing energy demand during soil tillage, since it gives the information about the energy necessary for tillage tools to loosen the topsoil. Soil tillage is the most energy-demanding operation in the crop production process, and a decrease in fossil fuel usage should be the crucial goal in sustainable crop production [32]. UD is highly influenced by soil moisture content, tillage depth, and operation speed [33]. The study of Liang et al. [34] concluded that the application of manure has reduced the energy demand of tillage. In case of our study, the results regarding pig and poultry manure confirm Liang's results, though less so for cattle manure. The results regarding the pig manure are in line with the work of Mclaughlin et al. [35], who reported that repeated applications of manure are reflected in reduced tillage energy. The results concerning cow manure with NeOsol are, however, not in line with the work of Žemličková and Šařec [36], who reported an increase in unit draft at one year after application. Urbanovičová et al. [15] described a decrease in tension force at ploughing by 5.71% after three applications of NeOsol compared to an untreated plot. All three applications were carried out within the years 2015–2016, and the draft of a plough was only measured at the end of the experiment. Tuba et al. [37] also reported a considerable decrease in plough draft after NeOsol treatment in their three-year experiment. In this study, we only observed a significant decrease in UD by 2.9% after six years of NeOsol treatment.

BD is an important indicator of soil compaction. BD values vary with the time delay from soil tillage. Immediately after tillage, values are lowest and tend to increase during the season due to climatic factors and mechanical load exerted on the soil surface [38,39]. According to the USDA [40], the ideal bulk density for optimal plant growth on soils with a clay content of more than 45% is lower than 1.1 g cm^{-3}. In case of this study, this threshold was exceeded for each term. The pigSOL variant achieved better results in comparison to the pure pig manure. Schjonning et al. [41] reported that long-term cattle manure application led to the decline in soil BD, and Hemmat et al. [42] reported that different BD values were more influenced by the application rate of manure than the manure origin. The results regarding the NPKSOL variant in our study are in line with Urbanovičová et al. [15], who found an increase in BD in the topsoil with NeOsol. The long-term results regarding the pigSOL variant also confirm the results of Šařec and Žemličková [43], who found that the application of NeOsol in combination with pig manure led to an improvement in BD in the topsoil.

SHC is a staple hydrogeological parameter that describes a soil's ability to infiltrate water and distribute it further to the crop root system. Our observations concerning SHC or infiltration rate in general are by and large consistent with past ones [44,45], which have shown improvements in infiltration processes and reductions in surface runoff rates and soil loss for soils with various organic soil treatments from livestock production. Apart from different types of organic matter, some activators have also been examined. Particu-

larly, biochar [46] was found to significantly increase the final infiltration rate and significantly reduce soil loss. However, in our study, NeOsol did not demonstrate any such effect.

The major advantage of the utilization of remote sensing data in agriculture is the fact that a canopy can be easily observed in a non-destructive manner with a high temporal resolution (5 days for Sentinel-2 at the equator in ideal meteorological conditions). This results in a complex set of data that provides information about crop development during the cropping season. Figure 4 and Table 4 illustrate this kind of information, and even though no significant difference between paired variants has so far been observable, the timeline shows a clear trend. Starting at the 2017 season with almost no difference between treatments, the significance increased over time. In 2020, strong differences between NPK, NPKSOL, and the variants with any manure can be clearly observed in every comparison level by all three indices. NeOsol's contribution to higher chlorophyll content has already been described in several studies [17,18,20,47]. It is therefore likely that the desired impact of the management of crop status might be detected in the following seasons, e.g., over a longer time span after NeOsol application.

The NDWI was calculated to gain information regarding crop water content, which was closely related to the SHC soil property. Šindelková, Badalíková, and Kubíková [13] stated that improvements in soil properties using activators leads to preferable utilization of water and nutrient uptake by plants. Nonetheless, though SHC results (Figure 3) demonstrate the only difference between the NPKSOL and the catt variant at Term III, crop water status via the NDWI differed on several more levels. Here again, the major advantage of spatial data is noticeable, as they provide more accurate information than point sampled data.

Sustainable agriculture is necessary to provide careful nutrient management, which is important for increasing soil organic carbon due to improving agricultural productivity and maintaining ecosystem health [48]. One of the possibilities may be the application of manure, which improves soil fertility even in combination with mineral fertilizers [49]. On the other hand, the application of inorganic fertilizers directly leads to higher yields by providing nutrients that encourage crop growth [50]. In both years of the mentioned experiment, the yield of winter wheat grain significantly increased and almost proportionally to the increasing doses of compost. The application of the soil improver on the background of compost further significantly increased the grain yield. However, the soil improver applied in the control treatment, without compost, had an insignificant impact on the wheat yield [24]. Several experiments were conducted to verify the effect of PRP SOL (now NeOsol) on yields with diverse outcomes. The PRP SOL activator proved to be a useful soil additive for calendula growing, as it was found to increase the yield of dry matter of flowerheads [21]. PRP SOL can also replace the inorganic fertilizing of spring barley with phosphorus and potassium without grain yield losses [51]. Another study [52] of a two-year soybean experiment did not show any statistically significant increase in yields when using the SOL activator. Conversely, PRP SOL in combination with urea was found to have a positive effect in terms of increased soybean yield [19]. Our observations have proven the significant effects of NeOsol on yield, which were intensified after a prolonged application, i.e., at the last term of the experiment.

This experiment verified beneficial effect of the NeOsol activator on crop yield and the unit draft of tillage implements after a prolonged application. In an agricultural practice, this may manifest in higher revenues from crops and lower fuel consumption of soil tillage.

5. Conclusions

We carried out a six-year experiment on the biostimulator NeOsol and three manure types of different origin (cattle, pig, and poultry) that were applied either alone or in a combination in order to assess their influence on soil's physical properties and crop status

in real agricultural conditions. The evaluation focused on three terms when manure had been applied beforehand.

Concerning unit draft (UD), the overall influence of NeOsol regardless of time development was not significant. However, though at Term I, variants treated with NeOsol attained higher UD values, the values become significantly lower at Term III (by 2.9%). This fact suggests the favorable influence of the NeOsol activator on UD over a prolonged period of time. The variants with manure application, particularly pig manure (by 6.5%) and poultry manure to some extent (by 2.1%), attained significantly lower UD values than those without treatment. Regarding soil bulk density (BD), NeOsol did not show any significant influence, whereas pig manure (by 6.7%) and particularly poultry manure (by 10.3%) presented significantly lower values compared to the variants without any manure.

No significantly different values of saturated hydraulic conductivity (SHC) could be observed between the variants including those with/without the NeOsol biostimulator over the whole trial period. On the other hand, pig manure (by 12.4%) and particularly cattle manure (by 15.9%) application led to significantly decreased SFH values compared to the variants without manure treatment.

NeOsol's effect on several vegetation indices (VI) proved inconclusive as opposed to the variants enriched by the manure of any origin. When assessing yield, however, NeOsol's effect was significant. At the last term of the experiment, the difference in winter wheat yield reached 5.0%. A similar outcome was produced by manure application, where the variants with pig and poultry manure presented 3.8% and 2.7% higher average yields, respectively, than the other treatments. At Term III, the difference was significant even for all three manure types, i.e., cattle, pig, and poultry manure surpassed the yields of variants without manure by 4.8%, 6.6%, and 6.2%, respectively.

References

1. Anderson, R.; Bayer, P.E.; Edwards, D. Climate Change and the Need for Agricultural Adaptation. *Curr. Opin. Plant Biol.* **2020**, *56*, 197–202. https://doi.org/10.1016/j.pbi.2019.12.006.
2. Jain, H.K. *The Green Revolution History, Impact and Future*; Studium Press LLC: Houston, Texas, USA, 2010; ISBN 1933699639.
3. Pham, X.; Stack, M. How Data Analytics Is Transforming Agriculture. *Bus Horiz.* **2018**, *61*, 125–133. https://doi.org/10.1016/j.bushor.2017.09.011.
4. Zhai, Z.; Martínez, J.F.; Beltran, V.; Martínez, N.L. Decision Support Systems for Agriculture 4.0: Survey and Challenges. *Comput. Electron. Agric.* **2020**, *170*, 105256. https://doi.org/10.1016/j.compag.2020.105256.

5. Klerkx, L.; Rose, D. Dealing with the Game-Changing Technologies of Agriculture 4.0: How Do We Manage Diversity and Responsibility in Food System Transition Pathways? *Glob. Food Sec.* **2020**, *24*. https://doi.org/10.1016/j.gfs.2019.100347.

6. Maeder, P.; Fliessbach, A.; Dubois, D.; Gunst, L.; Fried, P.; Niggli, U. Soil Fertility and Biodiversity in Organic Farming. *Science* **2002**, *296*, 1694–1697. https://doi.org/10.1126/science.1071148.

7. Goldberg, N.; Nachshon, U.; Argaman, E.; Ben-Hur, M. Short Term Effects of Livestock Manures on Soil Structure Stability, Runoff and Soil Erosion in Semi-Arid Soils under Simulated Rainfall. *Geosciences* **2020**, *10*, 213. https://doi.org/10.3390/GEOSCI-ENCES10060213.

8. Gilley, J.E.; Risse, L.M.; Eghball, B. Managing Runoff Following Manure Application. *J. Soil Water Conserv.* **2002**, *57*, 530–533.

9. Badalucco, L.; Rao, M.; Colombo, C.; Palumbo, G.; Laudicina, V.A. Reversing Agriculture from Intensive to Sustainable Improves Soil Quality in a Semiarid South Italian Soil. *Biol. Fertil Soils* **2010**, *46*, 481–489. https://doi.org/10.1007/s00374-010-0455-y.

10. Menšík, L.; Hlisnikovský, L.; Pospíšilová, L.; Kunzová, E. The Effect of Application of Organic Manures and Mineral Fertilizers on the State of Soil Organic Matter and Nutrients in the Long-Term Field Experiment. *J. Soils Sediments* **2018**, *18*, 2813–2822.

11. Food and Agriculture Organizations of the United Nations Food and Agriculture Data Available online: http://www.fao.org/faostat (accessed on 22 October 2021).

12. Spychalski, W.; Sulewska, H.; Ratajczak, K.; Kaczmarek, T. Composition of Soil Solution after 10 Years of PRP SOL Fertilization Based on the Selected Chemical Properties. *J. Res. Appl. Agric. Eng.* **2017**, *62*, 139–143.

13. Šindelková, I.; Badalíková, B.; Kubíková, Z. The Soil Biostimulant Usage Effect on Soil Properties in Dry Area. In Proceedings of the International Multidisciplinary Scientific GeoConference Surveying Geology and Mining Ecology Management, SGEM, Albena, Bulgaria, 28 June–7 July 2019; Volume 19, pp. 561–568.

14. Szűcs, L.; Tuba, G.; Zsembeli, J. Effect of PRPSOL Soil Conditioner on the Physical Status of the Soil in Conventional and Reduced Tillage Systems. *Acta Agraria Debreceniensis* **2014**, *55*, 109–113. https://doi.org/10.34101/actaagrar/55/1919.

15. Urbanovičová, O.; Krištof, K.; Findura, P.; Mráz, M.; Jobbágy, J.; Križan, M. The Effect of Soil Conditioner on the Spatial Variability of Soil Environment. *Agron. Res.* **2018**, *16*, 2197–2210. https://doi.org/10.15159/AR.18.184.

16. Bielińska, E.J.; Futa, B.; Bik-Mołodzińska, M.; Szewczuk, C.; Sugier, D. The Impact of Fertilizing Agents on the Enzymatic Activity of Soils (Wpływ preparatów użyźniających na aktywność enzymatyczną gleb). *J. Res. Appl. Agric. Eng.* **2013**, *58*, 15–19.

17. Borowiak, K.; Niewiadomska, A.; Sulewska, H.; Szymanska, G. Effect of PRP SOL and PRP EBV Nutrition on Yield, Photosynthesis Activity and Soil Microbial Activity of Three Cereal Species. *Fresenius Environ. Bull.* **2016**, *25*, 2026–2035.

18. Swędrzyńska, D.; Zielewicz, W.; Swędrzyński, A. Comparison of Soil Bioconditioners and Standard Fertilization in Terms of the Impact on Yield and Vitality of Lolium Perenne and Soil Biological Properties. *Open Life Sci.* **2019**, *14*, 666–680.

19. Jukić, G.; Šunjić, K.; Varnica, I.; Gašo, D.; Labudović, B. Effect of Different Kinds of Fertilizer on Soybean Yield. In 8th International Scientific/Professional Conference, Agriculture in Nature and Environment Protection, Vukovar, Croatia, 1–3 June 2015; pp. 110–115.

20. Sulewska, H.; Niewiadomska, A.; Majchrzak, L.; Panasiewicz, K. Potatoes Reaction on PRP SOL Fertilisation. *J. Res. Appl. Agric. Eng.* **2012**, *57*, 116–121.

21. Ratajczak, K.; Sulewska, H.; Szymańska, G.; Wolna-Maruwka, A.; Faligowska, A. The Effect of Soil Type and Soil Additives on the Selected Growth Parameters and Yield of Flowerheads of *Calendula Officinalis* L. *Herba Polonica* **2016**, *62*, 17–30.

22. Porro, D.; Pedò, S. Implication of Nutrition on Root Development. In Proceedings of the I International Symposium on Grapevine Roots, Rauscedo, Italy, 16–17 October 2014; pp. 193–200.

23. Krzywy-Gawrońska, E. Enzymatic Activity of Urease and Degydrogenase in Soil Fertilized with GWDA Compost with or without a PRP SOL Addition. *Pol. J. Environ. Stud.* **2012**, *21*, 949–955.

24. Krzywy-Gawrońska, E.; Woloszyk, C. Effect of Compost Produced by the GWDA Method and PRP SOL on the Yield of Winter Wheat and Soil Properties. *Fertilizers and Fertilization* **2011**, *43*, pp. 29–38.

25. Klír, J.; Kunzová, E.; Cermák, P. *Frame Methodics of Plant Nutrition and Fertilization (Rámcová metodika výživy rostlin a hnojení)*, 2nd ed.; Crop Research Institute: Prague, the Czech Rep., 2008; ISBN 78-80-87011-61-4.

26. Bagarello, V.; Iovino, M.; Elrick, D. A Simplified Falling-Head Technique for Rapid Determination of Field-Saturated Hydraulic Conductivity. *Soil Sci. Soc. Am. J.* **2004**, *68*, 66–73, doi:10.2136/sssaj2004.6600.

27. Elrick, D.E.; Reynolds, W.D.; Tan, K.A. Hydraulic Conductivity Measurements in the Unsaturated Zone Using Improved Well Analyses. *Groundw. Monit. Remediat.* **1989**, *9*, 184–193. https://doi.org/10.1111/j.1745-6592.1989.tb01162.x.

28. Rouse, R.W.H.; Haas, J.A.W.; Deering, D.W. Monitoring Vegetation Systems in the Great Plains with ERTS. In Proceedings of the Third Earth Resources Technology Satellite-1 Symposium, NASA SP-351, Washington, DC, USA, 10–14 December 1973; Volume 1, Section A, pp. 309–317.

29. Gao, B.C. NDWI—A Normalized Difference Water Index for Remote Sensing of Vegetation Liquid Water from Space. *Remote Sens. Environ.* **1996**, *58*, 257–266. https://doi.org/10.1016/S0034-4257(96)00067-3.

30. Boegh, E.; Soegaard, H.; Broge, N.; Hasager, C.B.; Jensen, N.O.; Schelde, K.; Thomsen, A. Airborne Multispectral Data for Quantifying Leaf Area Index, Nitrogen Concentration, and Photosynthetic Efficiency in Agriculture. *Remote Sens. Environ.* **2002**, *81*, 179–193. https://doi.org/10.1016/S0034-4257(01)00342-X.

31. *RStudio Team RStudio: Integrated Deveopment for R*; R Foundation: Vienna, Austria, 2021.

32. Moitzi, G.; Neugschwandtner, R.W.; Kaul, H.; Wagentristl, H. Energy Efficiency of Winter Wheat in a Long-Term Tillage Experiment under Pannonian Climate Conditions. *Eur. J. Agron.* **2019**, *103*, 24–31. https://doi.org/10.1016/j.eja.2018.11.002.

33. Rashidi, M.; Najjarzadeh, I.; Jaberinasab, B.; Emadi, S.M.; Fayyazi, M. Effect of Soil Moisture Content, Tillage Depth and Operation Speed on Draft Force of Moldboard Plow. *Middle East J. Sci. Res.* **2013**, *16*, 245–249. https://doi.org/10.5829/idosi.mejsr.2013.16.02.11675.

34. Liang, A.; Mclaughlin, N.B.; Ma, B.L.; Gregorich, E.G.; Morrison, M.J.; Burtt, S.D.; Patterson, B.S.; Evenson, L.I. Changes in Mouldboard Plough Draught and Tractor Fuel Consumption on Continuous Corn after 18 Years of Organic and Inorganic N Amendments. *Energy* **2013**, *52*, 89–95. https://doi.org/10.1016/j.energy.2012.10.064.

35. Mclaughlin, N.B.; Gregorich, E.G.; Dwyer, L.M.; Ma, B.L. Effect of Organic and Inorganic Soil Nitrogen Amendments on Mouldboard Plow Draft. *Soil Tillage Res.* **2002**, *64*, 211–219.

36. Žemličková, N., Šařec, P. Influence of Application of Organic Matter and Its Activators on Soil-Tillage Implement Draft on Modal Luvisol. In Proceedings of the 6th International Conference on Trends in Agricultural Engineering, Prague, the Czech rep., 7–9 September 2016; pp. 736–742.

37. Tuba, G.; Kovács, G.; Sinka, L.; Nagy, P.; Rivera-Garcia, A.; Bajusová, Z.; Findura, P.; Zsembeli, J. Effect of Soil Conditioning on Soil Penetration Resistance and Traction Power Demand of Ploughing. *Agriculture* **2021**, *67*. https://doi.org/10.2478/AGRI-2021-0011.

38. Blanco-canqui, H.; Stone, L.R.; Schlegel, A.J.; Lyon, D.J.; Vigil, M.F.; Mikha, M.M.; Stahlman, P.W.; Rice, C.W. No-till Induced Increase in Organic Carbon Reduces Maximum Bulk Density of Soils. *Soil Sci. Soc. Am. J.* **2009**, *73*, 1871–1879. https://doi.org/10.2136/sssaj2008.0353.

39. Nouri, A.; Lee, J.; Yin, X.; Tyler, D.D.; Jagadamma, S.; Arelli, P. Soil Physical Properties and Soybean Yield as Influenced by Long-Term Tillage Systems and Cover Cropping in the Midsouth USA. *Sustainability* **2018**, *10*, 4696, https://doi.org/10.3390/su10124696.

40. United States Department of Agriculture. *Soil Bulk Density/Moisture/Aeration*; United States Department of Agriculture: Washington, DC, USA, 2019.

41. Schjønning, P.; Christensen, B.T.; Carstensen, B. Physical and Chemical Properties of a Sandy Loam Receiving Animal Manure, Mineral Fertilizer or No Fertilizer for 90 Years. *Eur. J. Soil Sci.* **1994**, *45*, 257–268. https://doi.org/10.1111/j.1365-2389.1994.tb00508.x.

42. Hemmat, A.; Aghilinategh, N.; Rezainejad, Y.; Sadeghi, M. Long-Term Impacts of Municipal Solid Waste Compost, Sewage Sludge and Farmyard Manure Application on Organic Carbon, Bulk Density and Consistency Limits of a Calcareous Soil in Central Iran. *Soil Tillage Res.* **2010**, *108*, 43–50. https://doi.org/10.1016/j.still.2010.03.007.

43. Šařec, P.; Žemličková, N. Soil Physical Characteristics and Soil-Tillage Implement Draft Assessment for Different Variants of Soil Amendments. *Agron. Res.* **2016**, *14*, 948–958.

44. Boyle, M.; Frankenberger, W.T.; Stolzy, L.H. The Influence of Organic Matter on Soil Aggregation and Water Infiltration. *J. Prod. Agric.* **1989**, *2*, 290–299. https://doi.org/10.2134/JPA1989.0290.

45. Tejada, M.; Gonzalez, J.L. Influence of Organic Amendments on Soil Structure and Soil Loss under Simulated Rain. *Soil Tillage Res.* **2007**, *93*, 197–205. https://doi.org/10.1016/J.STILL.2006.04.002.

46. Abrol, V.; Ben-Hur, M.; Verheijen, F.G.A.; Keizer, J.J.; Martins, M.A.S.; Tenaw, H.; Tchehansky, L.; Graber, E.R. Biochar Effects on Soil Water Infiltration and Erosion under Seal Formation Conditions: Rainfall Simulation Experiment. *J. Soils Sediments* **2016**, *16*, 2709–2719. https://doi.org/10.1007/S11368-016-1448-8.

47. Šařec, P.; Novák, P.; Kumhálová, J. Impact of Activators of Organic Matter on Soil and Crop Stand Properties in Conditions of Very Heavy Soils. In Proceedings of the Engineering for Rural Development, Jelgava, Latvia, 24–26 May 2017; Volume 16, pp. 486–491.

48. Li, T.; Zhang, Y.; Bei, S.; Li, X.; Reinsch, S.; Zhang, H.; Zhang, J. Contrasting Impacts of Manure and Inorganic Fertilizer Applications for Nine Years on Soil Organic Carbon and Its Labile Fractions in Bulk Soil and Soil Aggregates. *Catena* **2020**, *194*, 4739. https://doi.org/10.1016/j.catena.2020.104739.

49. Voltr, V.; Menšík, L.; Hlisnikovský, L.; Hruška, M.; Pokorný, E.; Pospíšilová, L. The Soil Organic Matter in Connection with Soil Properties and Soil Inputs. *Agronomy* **2021**, *11*, 779. https://doi.org/10.3390/agronomy11040779.

50. Liang, Q.; Chen, H.; Gong, Y.; Fan, M.; Yang, H.; Lal, R.; Kuzyakov, Y. Effects of 15 Years of Manure and Inorganic Fertilizers on Soil Organic Carbon Fractions in a Wheat-Maize System in the North China Plain. *Nutr Cycl Agroecosyst* **2012**, *92*, 21–33. https://doi.org/10.1007/s10705-011-9469-6.

51. Sulewska, H.; Koziara, W.; Szymańska, G.; Niewiadomska, A.; Panasiewict, K.; Ratajczak, K. Response of spring barley to prp sol application as a complex of mineral inducer prosess (MIP). *Nauka Przyroda Technologie* **2016**, *10*, 1–14. https://doi.org/10.17306/J.NPT.2016.2.17.

52. Kováč, L.; Jakubová, J.; Šariková, D. Effect of Tillage System and Soil Conditioner Application on Soybean (*Glycine Max* (L.) *Merrill*.) and Its Crop Management Economic Indicators. *Agriculture* **2014**, *60*, 60–69. https://doi.org/10.2478/agri-2014-0007.

Appendix 5

Using a single-board computer as a low-cost instrument for SPAD value estimation through colour images and chlorophyll-related spectral indices

Křížová, K., Kadeřábek, J., Novák, V., Linda, R., Kurešová, G., & Šařec, P. (2022). Using a single-board computer as a low-cost instrument for SPAD value estimation through colour images and chlorophyll-related spectral indices. *Ecological Informatics, 67*, 101496. https://doi.org/10.1016/j.ecoinf.2021.101496

Using a single-board computer as a low-cost instrument for SPAD value estimation through colour images and chlorophyll-related spectral indices

Kateřina Křížová [a,b,*], Jan Kadeřábek [c], Václav Novák [a], Rostislav Linda [d], Gabriela Kurešová [e], Petr Šařec [a]

[a] Department of Machinery Utilization, Faculty of Engineering, Czech University of Life Sciences Prague, Czech Republic
[b] Division of Crop Protection and Plant Health, Crop Research Institute in Prague, Czech Republic
[c] Department of Agricultural Machines, Faculty of Engineering, Czech University of Life Sciences Prague, Czech Republic
[d] Department of Silviculture, Faculty of Forestry and Wood Science, Czech University of Life Sciences Prague, Czech Republic
[e] Division of Crop Management Systems, Crop Research Institute in Prague, Czech Republic

ABSTRACT

The leaf chlorophyll content is a major indicator of plant stress. Therefore, it is often used for the evaluation of crop status to adjust agricultural management to ensure high quality yield while concurrently applying water and agrochemicals in a sustainable manner. Since laboratory procedures for their assessment are time-consuming and destructive, nondestructive methods have been developed recently based on known vegetation spectral response characteristics. In addition to various vegetation indices derived from remotely sensed data, hand-held sensors such as SPAD-502 are currently widely used for in-field sampling to gain precise information for decision-making in terms of best-fitting agricultural management. However, the costs of such commercial devices can be limiting for farmers. The low-cost alternatives that have been developed recently exploit widely accessible digital cameras with sensors sensitive to the visible region of the electromagnetic spectrum. Digital numbers extracted from colour images in RGB channels serve as the input for broadband "chlorophyll index" calculations. Major constraints regarding digital cameras are, however, the natural light illuminance and the necessity of data post-processing. In the framework of this study, a novel technological solution was developed to address these issues. A Raspberry Pi single-board computer together with a Pi Camera and a simple LED incorporated in a 3D print case created a prototype called Rasp2SPAD, which was programmed to acquire and analyse a colour image. The prototype and its setup were further tested on the experimental plant material of the winter rapeseed. A set of 22 chlorophyll-related parameters across various colour representation models were generated, from which an SPAD value was modelled using i) a simple linear model, ii) a generalized linear model, and iii) an artificial neural network. The blue (*Cb*) and red (*Cr*) chroma components of the YUV colour space were found to be most suitable for SPAD value modelling. Calibration equations were determined, and the results reached relatively high accuracy (mean absolute deviance 1.85 and R-squared 0.81 for simple linear model) while keeping the costs significantly low compared to the most commonly used commercial sensor. In this way, a simple and cheap methodology was introduced to bring the results of research closer to practice, which should help first spread the precision agriculture concept to a wider audience and second allow them to utilize with it.

1. Introduction

Leaf pigments are the essential plant cell components of all autotrophic organisms responsible for the conversion of solar energy into chemical bonds during the photosynthesis process. Among other pigments, green chlorophyll is considered the staple pigment since it facilitates the construction of glucose and carbohydrates from water and CO$_2$ (Mohr and Schopfer, 2012). In doing so, it determines the photosynthetic potential of a plant, while changes in chlorophyll arrangement or concentration reliably indicate crop stress (Pérez-Bueno et al., 2019). Since the vast amount of nitrogen is incorporated in the structure of green pigment, leaf chlorophyll content (LCC) provides an indirect measure of crop nutrient status (Filella et al., 1995). Therefore, LCC is the basic parameter that is being estimated when evaluating crop

conditions. The well-established method of LCC estimation involves a laboratory procedure, where leaf tissue is dissolved in an organic solvent and analysed in a spectrophotometer. Specific wavelengths are used to acquire the chlorophyll absorbance data that are used for chlorophyll content calculations (Porra et al., 1989). The results of such laboratory methods have shown to be accurate; however, drawbacks in addition to costs include time-consuming sampling collection and destruction of the investigated plant material. To address these issues, modern methods exploit the knowledge of the spectral response of vegetation to estimate LCC in a nondestructive manner. Plants are known to absorb and reflect specific parts of electromagnetic radiation according to their biophysical structure. The staple trait here is a high ratio of reflected radiation between the red- and near-infrared bands by healthy plants, while this ratio tends to decrease with higher plant stress. These traits are currently used to calculate various vegetation indices based on aerial images (satellites, UAVs), providing spatially related information on vegetation status (Domínguez et al., 2016; Kumhálová and Matějková, 2017). Concurrently, various hand-held instruments have recently been developed for direct in-field sampling based on a similar approach. Such devices are usually highly portable, eliminating the necessity of leaf tissue sampling, transport, and laboratory-based analysis. The desired information is obtained by inserting the intact leaf into a chamber, where specific wavelengths are emitted and recorded. Regarding a particular type of sensor, sample fluorescence (CCM-300, OptiSciences) or transmittance (CCM − 200, OptiSciences; SPAD-502, Konica Minolta) is recorded. Based on such data, optical methods generally calculate the "chlorophyll index" that has been shown to be related to relative chlorophyll content, and the relationship is described using a calibration equation (Richardson et al., 2002). Despite a variety of available portable instruments, SPAD-502 is the standard method of nondestructive LCC estimation. The SPAD-502 has been used in over 200 studies related to agricultural research purposes (Uddling et al., 2007). In practice, information about the actual plant status is often crucial for decision-making and scheduling agricultural operations, including fertilization, irrigation, or pest control. Properly interpreted results then enable a) increased primary productivity, b) allocation of sources reasonably, and c) adaptation of agricultural management to assure the highest crop yields (Wang et al., 2013; Zhai et al., 2020). In such practical cases, however, the affordability of the abovementioned instruments may be restrictive. Higher financial costs of commercial chlorophyll metres were the trigger for low-cost alternative development. Various in-house and research-based prototypes together with innovative techniques have emerged among studies. These low-cost methods generally benefit from scientific results and are convenient for end users. Mostly, the visible region of the electromagnetic spectrum is used to highlight vegetation properties, such as nitrogen status or chlorophyll content, since sensors sensitive to red, blue, green (RGB) bands are widely available among basic digital cameras or even current smartphones. These methods, similar to commercial handheld devices, generate basic indices, whose suitability for vegetation property estimates has been investigated by several studies, and have been summarized, for example, by Misra et al. (2018). To gain the actual data, several approaches have been described based on a) digital cameras and data postprocessing (Meyer and Neto, 2008; Tavakoli and Gebbers, 2019), b) smartphone cameras together with application development (Vesali et al., 2015), c) novel techniques through existing devices (Ali et al., 2012; Cortazar et al., 2015), or d) new prototypes with the data processing proposal (Pérez-Patricio et al., 2018). Naturally, every approach has both advantages and constraints. The weak spot of a particular solution is often related to either the noise induced by natural light (mostly concerning digital cameras, smartphones) or to the necessity of postprocessing the acquired data using some sort of computer software. Single-board computers (SBCs), such as Raspberry Pi (RPi), in various configurations have rapidly spread among many applications. In addition to traditional use in robotics, SBCs are now part of many solutions for medical (Kanani and Padole, 2020; Yildiz and Boyraz, 2019),

food production purposes (Osroosh et al., 2018; Vasishth and Bavarva, 2016), or even surveillance monitoring (Nasir et al., 2019; Prasad et al., 2017). When calibrated, RPi accompanied by the Pi Camera module is considered fully capable of producing scientific quality data to be used further, for example, in biophotonics or remote sensing applications (Pagnutti et al., 2017). Since such a configuration could be very easily combined with various other components, it has significant potential to create the foundation of very specific oriented devices.

Regarding sustainable crop production related to major climate change issues, collecting in-field data has become a crucial part of agricultural practice. Real-time quality data help farmers react promptly to unfavourable crop conditions, which is often connected to some kind of abiotic stress and might result in lower yield or quality of the product. This study aims to introduce a novel technological solution reflecting most of the abovementioned constraints of described low-cost handheld sensors while sustaining advantages, such as affordability, portability, and capability of providing data with a significant level of accuracy. Prototype development will leverage the latest advancements and trends of computer science, focusing particularly on SBC together with current knowledge of optical methods and their suitability for plant status description. Convenient properties of RPi will be utilized to construct a portable device for in-field chlorophyll-related index assessment. Based on these indices, a mathematical model for the prediction of the SPAD value will be derived.

2. Materials and methods

2.1. Prototype design

The main principle of this study was to construct a low-cost portable device that is able to capture a colour image using its own light emitter and a colour space camera under field conditions, perform image analysis according to the best fitting setup, and generate a set of most cited chlorophyll-related colour indices while finally demonstrating a so-called SPAD value estimate. Key features of the proposed device were low financial costs, the same as high-quality data acquisition. Such a seemingly complex task was based on simple technical and technological solutions supported by the latest scientific knowledge in the field of spectral response characteristics of plant material. By focusing on involving primarily free available SW features and low-cost HW components, the possibility of easily reproducing this so-called *Rasp2SPAD* prototype should be ensured.

As mentioned above, the chlorophyll metre SPAD-502Plus (Konica Minolta) is widely used for leaf chlorophyll content measurements both in research studies and practical applications focused on plant nutrition status determination. This common handheld sensor calculates the SPAD value, a numerical expression of the relation of spectral absorbance in two regions of the electromagnetic spectrum. It operates in the red band (600–700 nm) as one of the chlorophyll absorbance peaks and in the near-infrared band (700–1400 nm) with no absorbance declared. The high correlation of the SPAD value and LCC across the crop species and varieties ensured that the SPAD-502Plus sensor is currently considered a full-fledged nondestructive method of LCC indication. Thus, for the purpose of this study, SPAD-502Plus was assumed to provide accurate LCC data, which served as a reference for Rasp2SPAD setup evaluation.

SBCs have recently been utilized for a wide spectrum of purposes, including prototyping. RPi 3B+ was chosen to be a key component of Rasp2SPAD, as it is trusted to be a reliable prototyping platform (Johnston and Cox, 2017). Specific technical attributes of this particular model are described in detail in Table 1.

The SD card slot enables the user to insert any type of micro-SD card and thus to determine the storage memory with which the prototype can operate. Rasp2SPAD was equipped with a micro SDHC card SanDisk with 16 GB memory capacity to store acquired data.

Generally, the prototype consisted of two main parts that were

Table 1

Technical attributes of the single-board computer Raspberry Pi 3B+ used for Rasp2SPAD prototype development.

Processor	ARM Broadcom Quad-Core BCM2837B0, 1.4 GHz
Operating memory	1 GB RAM
Networking	GigaByte Ethernet/Wifi 802.11b/g/n/ac 2.4 and 5 GHz
Bluetooth	Bluetooth 4.2, Bluetooth Low Energy (BLE)
USB	4xUSB 2.0
GPIO	40-pin GPIO header, populated
SD card support	Micro SD formatted for loading operating system and data storage
Input power	5 V/2.5A DC via micro-USB connector, 5 V DC via GPIO header, Power over Ethernet (PoE)–enabled (requires separate PoE HAT)
Operating temperature	0 to 50 °C

designed and manufactured by 3D printing from thermoplastic material PLA using the 3D printer PrusaMK3S. First, a simple plastic case was printed to protect the RPi from mechanical damage. Second, a forceps-shaped 3D print (Fig. 1.1) was designed to create a specific environment for plant leaf insertion and for maintaining consistent light and sensing conditions when acquiring the image, which will be analysed later. The Forceps 3D print design was based first on the PLA material stiffness, which together with specifically placed material blocks helped to avoid mutual movement of individual forceps parts. This ensured the maximal deviation from the cut axis < 0.2 mm. The leaf insertion depth was regulated to the top 55 mm by a solid stopper.

Natural light is often considered a major limitation in vision-based LCC estimates because the acquired spectral reflectance/transmittance is very likely to be influenced by actual weather conditions, solar radiation, and leaf arrangement (Ali et al., 2012). As a reaction to this issue, Rasp2SPAD was equipped with its own light source (Fig. 1.2). Since white LEDs emit the full spectrum of wavelengths in the visible region, a circular 5 mm sunny white LED Yoldal YZ-WS5N40N was incorporated in the 3D forceps component. The specific range of wavelengths was checked by a Spectrometer VIS/NIR 380–950 nm (Ocean Optics, USA) spectrometer and is given in Fig. 2a. Light flux was scattered at 2 mm from the top of the LED by means of a single-layer textile diffuser Lastolite P15T TRANSLUCENT (Fig. 1.3) to assure even distribution of incident light on the target leaf at a distance of 9 mm from the diode itself. The amount of transmitted radiation was captured by a Raspberry Pi Camera V2.1 with a Sony IMX219 8 Mpix sensor (Fig. 1.5) (Table 2) in the form of a colour image. The sensor quantum efficiency curves for RGB bands are given in Fig. 2b. A rubber ring with an 11 mm diameter secured the surroundings of the sensor from natural light intrusion (Fig. 1.4).

Additionally, the RPi thermal control was in question. Since thermal noise can significantly affect the spectral information of a colour image, a passive aluminium heatsink was placed on a processor chip to avoid overheating. Furthermore, as described above, RPi and Pi Camera were stored separately in the two 3D prints. Eventually, both 3D printed components were combined to create a singular piece of hardware,
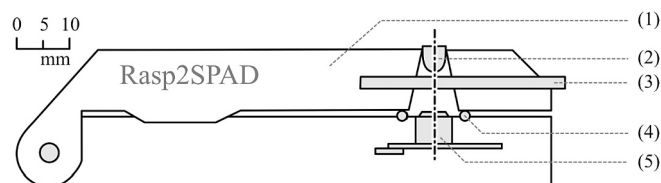
Fig. 1. Cut view of the forceps-shaped 3D print (1) ensuring uniform light conditions by providing the fixed position of the light source (2), the diffuser layer (3), the rubber sealing ring (4), and the Pi Camera (5). This component was placed atop the 3D printed case containing the single-board computer Raspberry 3B+ to create the Rasp2SPAD prototype.
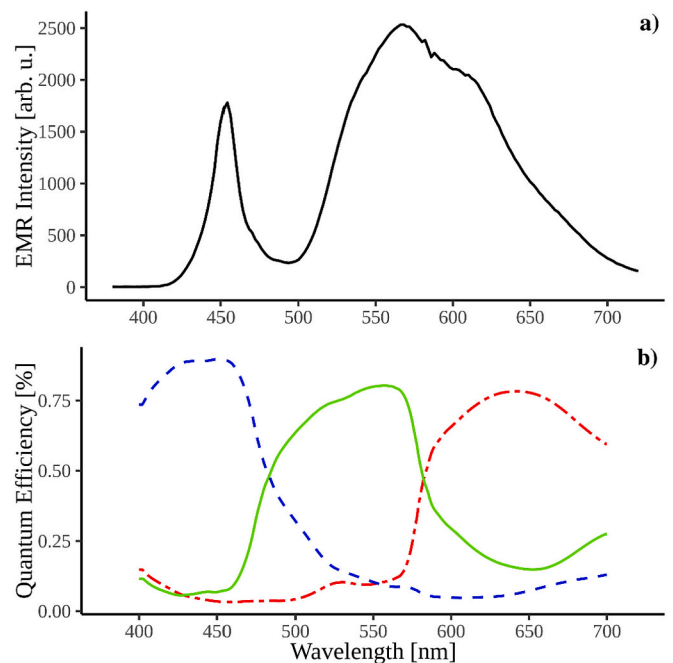
Fig. 2. Response curves representing a) spectrum of wavelengths emitted by the LED Yoldal YZ-WS5N40N as the active light source of the proposed prototype and b) the quantum efficiency of Raspberry Pi Camera Module V2.1 with a CMOS Sony IMX219 8 Mpix sensor.

Table 2

Technical specifications of the Raspberry Pi Camera Module V2.1 with the Sony IMX219 sensor chip that was used in the Rasp2SPAD prototype to capture a colour image as the source of RGB values for further calculations.

Camera	
Lens focal length	3.04 mm
f-number	2.0
Instantaneous field of view	0.368 mrad
Field of view	62.2 deg. (H) × 48.8 deg. (V)
Sensor	
Image sensor type	Back-lit CMOS
Resolution	8 Mpix, 3280 (H) × 2464 (V) pix
Pixel size	1.12 μm (H) × 1.12 μm (V)
Bit depth	10-bit
Operating temperature	−20 to +60 °C

which should be easily manageable with one hand by pressing a single button. Finally, to achieve the most portable solution, Xiaomi Mi Power Bank 2S power bank with a capacity of 10 Ah supplied Rasp2SPAD with electrical power.

2.2. Rasp2SPAD source code and measurement procedure

By prototyping, solely open-source means were used (operating system, programming language, libraries). The RPi itself ran on the Raspbian GNU/Linux 9 that was stored and loaded directly from a memory card. The crucial feature of the Rasp2SPAD is that the algorithm is responsible for running the whole process from acquiring the image, processing it, and finally storing the results (Fig. 3). The code is written in Python 3.7 using available libraries *PiCamera*, *RPi. GPIO* and *numpy*.

The algorithm is designed to run in an infinite loop initiating automatically approximately 30 s after the operating system starts until the SBC shutdown by disconnecting it from the power. This simple processing approach ensures operability by one button, while the procedure stage is indicated by LED flashing.
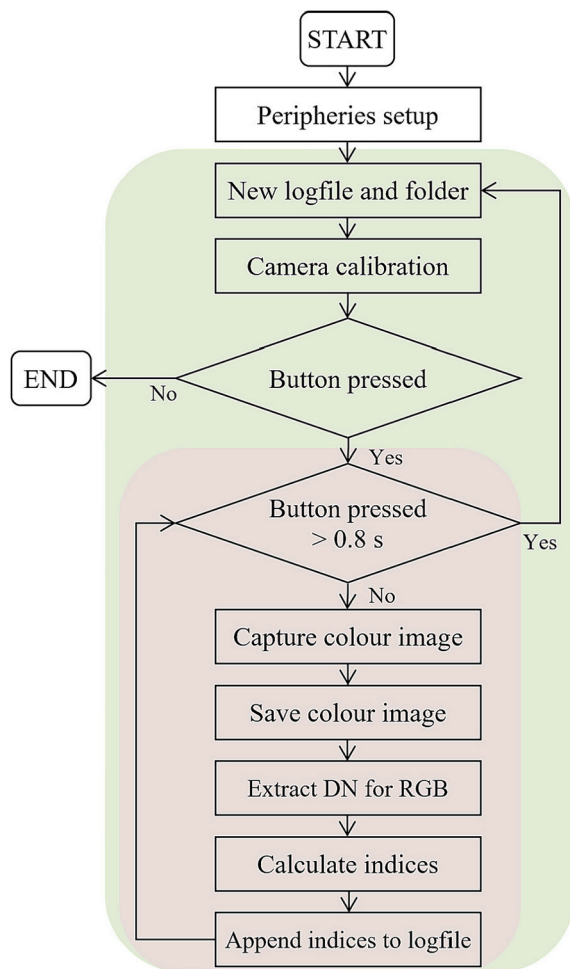
Fig. 3. Flow diagram of the algorithm responsible for the image acquisition and its processing aiming to generate the set of selected colour indices. The pink area represents the loop of spot measurements on a single leaf, while the green area depicts the initialization of the new leaf measurement. (For interpretation of the references to colour in this figure legend, the reader is referred to the web version of this article.)

After initialization of the peripheries (namely, light emitter and button pins), a new folder is created to store the results for one leaf measurement. In addition to the captured colour images, there is a logfile containing the results of image analysis. Calibration of the sensor follows the analysis and takes approx. 2 s. By clasping the empty forceps component (Fig. 1.1), the camera's shutter speed, white balance, and gains are fixed to ensure consistent sensing conditions. The measurement itself involves inserting the intact leaf into the forceps component (facing the light source). By pressing the button shorter than 0.8 s, the image is taken and saved in *.jpg format with 1280×720 resolution, which takes approximately 3 s. The following steps extract a mean digital number (DN) at 8 bit depth for each band (R, G, B), calculate 19 other colour indices, and record the results to the logfile. This procedure is repeated in several spot measurements (standard 10 per leaf) until the button is pressed for longer than 0.8 s, which initiates a new leaf measurement comprising of the set of spot measurements. Finally, the data from logfiles are combined into one *.csv file, and a local Wi-Fi net is extracted using the SFTP protocol of the WinSCP application.

The selection of 22 derived parameters (3 DN for RGB and 19 colour indices) was based on the results of other scientific studies published on the topic of colour imaging in agricultural applications (Table 3).

Table 3

Set 22 parameters derived from colour images acquired by the proposed prototype. DN for three channels of the visible region (RGB) followed by 19 colour indices that were selected based on their utilization in similar studies concerning low-cost chlorophyll content estimates. Note: $c = \max (R, G, B) - \min (R, G, B)$; $cmax = \max (R, G, B)$.

Index	Description	Equation	Reference
R	Actual pixel value in red band	–	–
G	Actual pixel value in green band	–	–
B	Actual pixel value in blue band	–	–
NRI	Normalized redness intensity (r)	$R/(R + G + B)$	(Tavakoli and Gebbers, 2019)
NGI	Normalized greenness intensity (g)	$G/(R + G + B)$	(Tavakoli and Gebbers, 2019)
NBI	Normalized blueness intensity (b)	$B/(R + G + B)$	(Tavakoli and Gebbers, 2019)
H	Hue	$cmax = G \rightarrow hue = 60 \times (2 + ((B - R)/c))$	(Vesali et al., 2015)
S	Saturation	$c/cmax$	(Vesali et al., 2015)
Br	Brightness	$cmax/255$	(Vesali et al., 2015)
Y	Luma component	$0.257R + 0.504G + 0.098B + 16$	(Vesali et al., 2015)
Cb	Blue chrominance component	$-0.148R - 0.291G + 0.439B + 128$	(Vesali et al., 2015)
Cr	Red chrominance component	$0.439R - 0.368G - 0.071B + 128$	(Vesali et al., 2015)
GMR	–	$G - R$	(Wang et al., 2013)
GDR	–	G/R	(Adamsen et al., 1999; Tavakoli and Gebbers, 2019)
GDB	–	G/B	(Tavakoli and Gebbers, 2019)
RDB	–	R/B	(Tavakoli and Gebbers, 2019)
NDI	Normalized difference index	$(G - R)/(G + R)$	(Pérez et al., 2000)
(R-B)/ (R + B)	–	$(R - B)/(R + B)$	(Kawashima and Nakatani, 1998)
DGCI	–	$[(Hue/60-1) + (1 - S) + (1 - Br)]/3$	(Vesali et al., 2015)
ExG	Excess Green Index	$2 g - r - b$	(Woebbecke et al., 1995)
ExR	Excess Red Index	$1.4 (r - b)$	(Meyer and Neto, 2008)
ExG-ExR	–	$ExG - ExR$	(Meyer and Neto, 2008)

2.3. Experimental design

The proposed prototype was tested on experimental plant material that was prepared specifically for this research in cooperation with the Crop Research Institute in Prague. Winter rapeseed (*Brassica napus* L.) was chosen as a test crop since the leaf size was suitable for contact imaging, and concurrently, the experimental material could be planted in the laboratory much easier than maize, which was also used in similar studies. A set of 50 individual plants was planted under controlled temperature conditions (18 °C) with a 12-hour photoperiod in 450 ml plastic pots. The intensity of leaf colouration is mainly determined by the chlorophyll content and has been shown to correlate strongly with the nitrogen content in the leaves (Evans, 1983). This fact was used to optimize the nitrogen dose for crops and was the staple prerequisite of the experimental design. A specific fertilization scheme was therefore applied to provide wide nutrient diversity of plant material. To achieve a low nutrient substrate, garden soil was mixed with sand in a 1:1 ratio. After seed germination and seedling selection, rapeseed was planted in pure substrate for three weeks to provide equal initial nutrient uptake within all 50 pots. This ensured the ideal conditions for the following

fertilization management that was held for one more month. Complete nutrient solution with graded nitrogen content was applied. Nitrogen was supplied every second day in a volume of 100 ml of solution with specific N doses (treatment 1 = 350 μM, treatment 2 = 750 μM, treatment 3 = 1500 μM, treatment 4 = 2500 μM, treatment 5 = 4000 μM) until the plants had at least two true leaves. Eventually, five distinct variants with ten rapeseed plants for each were prepared for Rasp2SPAD testing.

2.4. Evaluation procedure

After the experimental plant material was prepared, Rasp2SPAD was tested. The evaluation process itself involved the selection of the first and second fully developed rapeseed leaves (Fig. 4.), followed by measurements by both SPAD-502Plus and Rasp2SPAD. A detailed comparison of these two devices is provided in Fig. 5. In total 100 rapeseed leaves were examined. In practice, SPAD-502Plus standardly requires 10 spot measurements to calculate the final SPAD value for one sample. Rasp2SPAD was programmed to work similarly, i.e., 10 measurements (and images) per leaf, to obtain the final average value for all derived parameters. SPAD values were stored in the device's internal memory and were later downloaded as a *.csv file into a computer for subsequent data processing. Rasp2SPAD data were gathered as described in Chapter 2.2 in the form of a *.csv file.

2.5. Statistical analysis

As the first descriptive statistics of acquired parameters, a correlation plot was constructed for a general overview of the linear relationship of all 22 parameters (see Table 3) generated by Rasp2SPAD and the SPAD

Fig. 4. The proposed Rasp2SPAD prototype in the evaluation procedure on the winter rapeseed.

value gained by SPAD-502Plus (Fig. 6). Furthermore, modelling of the SPAD value was performed by a) a simple linear model (LM), b) a generalized linear model with a gamma distribution (GLM), and c) an artificial neural network (ANN). The dataset contained 89 valid records (outliers were removed according to the empirical rule), while one record represented the mean value of the total 10 spot measurements on one leaf. For the purpose of SPAD value modelling, the dataset was divided into a "training dataset" containing 60 randomly selected records and a "testing dataset" that contained the remaining 29 records. All three models were then fitted using the "training dataset" and further validated using the "testing dataset".

The fitting of a simple linear model included the full model containing all (22) parameters and its stepwise optimization based on Akaike information criterion (AIC) change (Akaike, 1974). The remaining nonsignificant parameters were manually removed from the model. Due to high correlations among the remaining parameters, predictors were also stepwise removed based on the variance inflation factor (VIF). Predictors with VIF > 4 were removed from the model in each step. Eventually, the final model was manually edited to achieve statistical significance of all predictors (insignificant and marginally significant parameters were also removed stepwise). This exact approach was later used during the fitting of the GLM (using the gamma distribution and inverse value as a link function) to assess if even more significant results could be found. The normality of residuals was also tested, and the residuals were nonzero (model bias).

As the third approach for SPAD value modelling based on the Rasp2SPAD indices, an artificial neural network was implemented. The same predictors as in the previously described LM and GLM were utilized. All predictors were scaled prior to analysis. The ANN was constructed empirically, with the first layer containing two input nodes (one per each of the two parameters that were found to be the most suitable by LM and GLM) and the last layer containing only one node (predicted SPAD value). As the fit of the ANN does not give the same output for each run (because of a random number generator used for numerical optimization of the model), 100 successful runs were performed, and the model residuals obtained in each run were analysed for a more reliable evaluation of the model performance.

Finally, as the main measure for the convenience of model fit, the mean absolute difference of the predicted value from the measured value was used. This enabled the use of one model measure for all three approaches. The evaluation was performed on "test dataset" records for all three modelling approaches.

All computations were performed in R 4.0.2 (R Core Team, 2020) using a selected alpha level of 0.05, together with the packages *readxl* (Wickham and Bryan, 2019), *tidyverse* (Wickham et al., 2019), and *reshape2* (Wickham, 2007). Plots were constructed using *corrplot* (Wei and Simko, 2017) and *ggplot2* (Wickham, 2016). The artificial neural net was fitted using the *Keras* package in Python 3.8.

3. Results and discussion

Rasp2SPAD was developed with the intention of introducing a portable and affordable device for basic in-field data gathering. The utilization of low-cost components together with 3D printing seems promising since the financial load was approximately 5% of the SPAD-502Plus commercial price. Moreover, the configuration based on the RPi controlled by the Python code made the prototype easily programmable, which might also be convenient for any further development.

In terms of the data quality, Rasp2SPAD demonstrated to be able to provide a complex dataset by capturing and processing the simple colour image as a result of the evaluation procedure on the winter rapeseed. In addition to the extraction of DN for RGB channels, 19 other indices were calculated. These parameters were all tested on their relationship to the SPAD value gained by the SPAD-502Plus handheld sensor. The correlogram (Fig. 6) provided an initial hint of more or less correlated indices with the six best performing NRI ($r = -0.869$), hue ($r = 0.865$), ExG-ExR
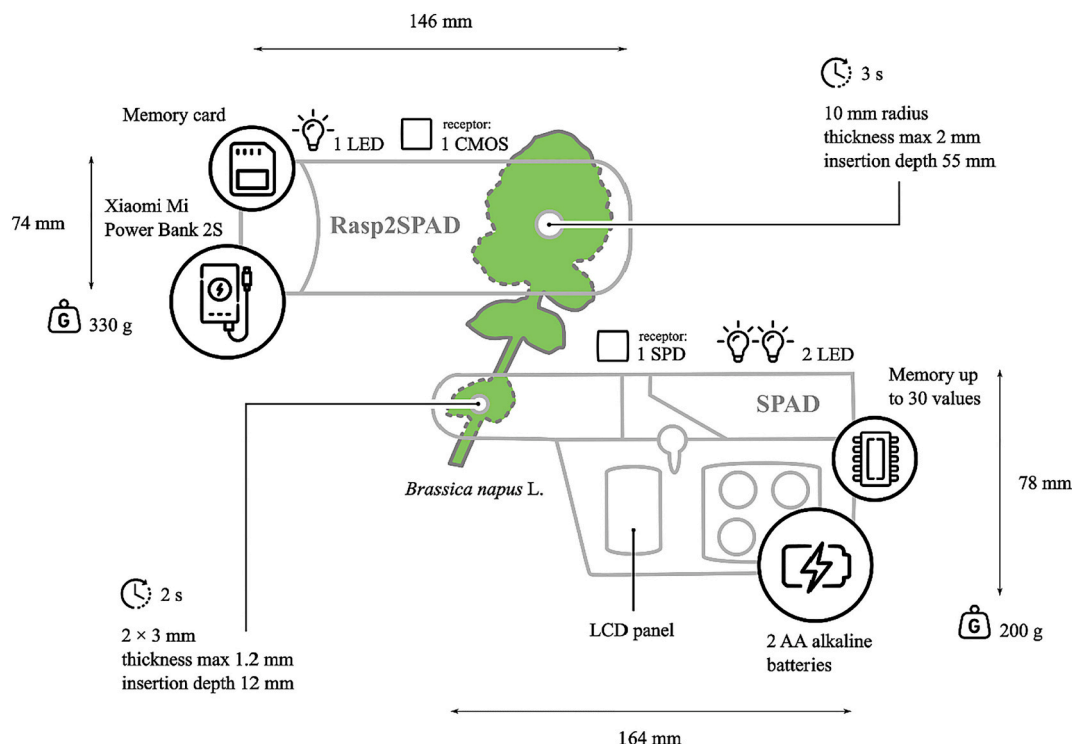
Fig. 5. Technical specifications of the proposed sensor Rasp2SPAD as the low-cost alternative to the standard commercial handheld sensor SPAD-502Plus (Konica Minolta).
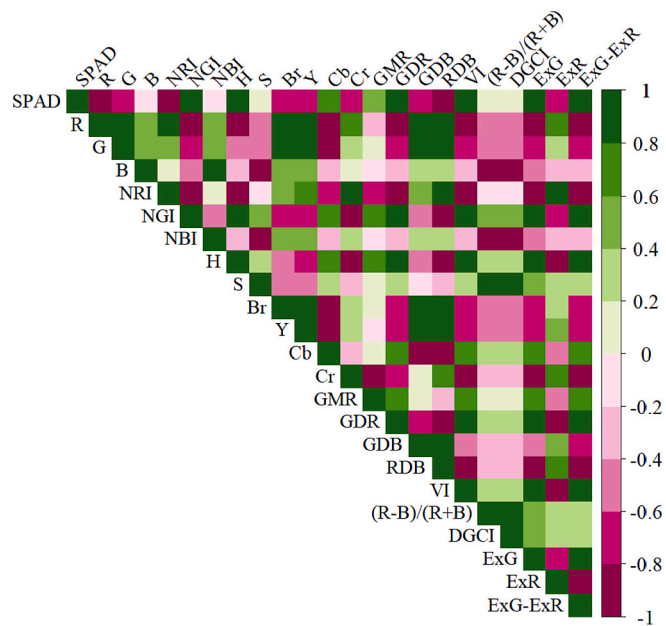

Fig. 6. Correlation matrix of the actual SPAD value obtained by the commercial sensor SPAD-502Plus and the set of the 22 parameters derived by Rasp2SPAD based on 89 rapeseed leaf samples.

($r = 0.86$), NDI ($r = 0.858$), GDR ($r = 0.854$), and RDB ($r = -0.846$).

In the first stage, LM for modelling the SPAD value based on selected parameters showed relatively high accuracy: R-squared = 0.81 on training data; mean absolute deviance of testing data =1.85, max. Absolute deviance = 2.42 (one-sided t-test, alpha = 0.05). Detailed results are given in Table 4. The calibration equation was thus defined as:

$$SPAD = 89.538 + 0.475Cb - 0.761Cr \tag{1}$$

Table 4
The best fitting simple linear model (LM) for SPAD value prediction was based on parameters obtained by the Rasp2SPAD prototype.

Response: SPAD value			
Coefficients			
	Estimate	t value	p value
Intercept	89.53762	7.56	< 0.001
Cb	0.47547	10.18	< 0.001
Cr	−0.76144	−8.51	< 0.001
R-squared (training data): 0.81			
Mean absolute difference (test data): 1.85			

Furthermore, the GLM approach applied on the dataset also achieved significant results (Table 5), although only slightly better than LM. Artificial R-squared = 0.81 on training data reached the same level as by LM; nevertheless, lower mean absolute deviance of testing data = 1.79

Table 5
The best fitting generalized linear model (using the Gamma distribution and inverse value as a link function) for SPAD value prediction was based on parameters obtained by the Rasp2SPAD prototype.

Response: SPAD Value			
Generalized linear model (Gamma distribution)			
Link function: Inverse value			
Coefficients			
	Estimate	t value	p value
Intercept	−0.0113	−1.462	0.149
Cb	−0.00003	−9.738	< 0.001
Cr	0.0005	8.523	< 0.001
Null deviance: 0.807			
Residual deviance: 0.155			
Artificial R-squared: 0.81			
Mean absolute difference (test data): 1.79			

and max. Absolute deviance = 2.30 (one-side *t*-test, alpha = 0.05) were achieved. Here, the SPAD value estimate can be described by Eq. 2. SPAD value estimates based on both mentioned models are given in Fig. 7.

$$SPAD = \frac{1}{(-0.011 - 0.00003Cb + 0.0005Cr)} \qquad (2)$$

To achieve the utmost accuracy, a test was completed by engaging the artificial ANN. Only *Cb* and *Cr* were used as the input variables since they were considered the most sensitive variables during the two preceding testing stages. Thus, the simple ANN was fitted with two inputs and one output, as the addition of any hidden layers returned less accuracy of the prediction on the test data due to overfitting. The results were considered comparable in terms of accuracy as the previous methods. The mean deviance of the model response from SPAD value measurements was 1.904 (95% CI: 1.89–1.92), while the best "run" showed a mean deviation of 1.70 (max. 2.22, 95% CI, one-sided t-test).

All three modelling approaches could be incorporated in the source code at this stage to provide the SPAD value estimate for the following rapeseed measurements. However, LM was concluded to be the simplest method with a high level of accuracy. A complex overview of the plant material, representative colour image, and actual and estimated SPAD value across five distinctive N treatments is given in Fig. 8.

Studies dealing with low-cost nondestructive chlorophyll estimates often based their approach on common types of digital cameras followed by postprocessing using specific software, mostly MATLAB. Misra et al. (2018) used a digital camera to compare selected existing approaches on water-stressed plants. Since the whole plant was sensed, the postprocessing procedure necessarily included region of interest segmentation, extraction of DN of RGB colour components, and desired model application. A similar approach was used in the study of Tavakoli and Gebbers (2019). The in-field canopy was sensed by a digital camera and processed later in MATLAB. Kawashima and Nakatani (1998) processed their in-field digital camera imagery even in Photoshop. None of these studies, however, appeared to address natural light conditions, although this kind of illumination might generate certain noise in the acquired image (Pérez-Patricio et al., 2018), and an artificial light source with known parameters of the light spectrum should be used. Pérez-Patricio et al. (2018) developed its own in-house device that sensed the crop leaf inserted in a dark chamber with an LED lamp and a mirror. Nevertheless, the obtained imagery had to be transferred to the computer for image processing using MATLAB to obtain the final values. For the particular reason of reducing the effect of lighting conditions, Ali et al. (2012)

developed an interesting alternative by using a portable scanner (Pico Life) rather than a camera to obtain the image. Again, data post-processing using MATLAB had to be involved. Hence, natural light illumination of the image, the necessity of data postprocessing, or their combination appear to be the most common drawbacks that need to be eliminated by developing Rasp2SPAD. Incorporating the LED as the active light source together with the convenient design of forceps 3D printing ensured uniform illumination conditions. To address the data postprocessing issue, utilization of programmable RPi SBC was a clear choice, since well-prepared source code performed all the necessary steps from image capture to producing a dataset with final SPAD value estimates.

Regarding the generated indices, recent studies on this topic achieved certain results while dealing solely with the most common RGB model for colour representation (Nelis et al., 2020). This study, however, presents the potential of other colour spaces, since indices derived by Rasp2SPAD covered HSB (*hue, saturation, brightness*) and YUV (*Y, Cb, Cr*) colour space in addition to the RGB model. The conversion of initial DN representing the RGB channels according to the equations listed in Table 3 brought a new dimension of knowledge in terms of simple colour image utilization for plant status assessment, as the blue- *Cb* and red chroma component *Cr* were the most important parameters during SPAD value modelling. The YUV colour model, whose domain has digital record compression via chroma subsampling (Choudhury, 2014), has also been in the field of agriculture and has used for segmentation of pixels representing vegetation from the image background (Hernández-Hernández et al., 2016) or to detect crop disease in combination with RGB colour indices (Kerkech et al., 2018). Although its three components are derived from RGB, the information they provide is different. Since the luma component (*Y*) represents the image brightness, the other two chroma components (*Cb, Cr*) represent solely the colour. Therefore, chroma components might be more sensitive to colour variations that indicate the plant status in terms of its nutrition saturation. More colour models were also used in the study of Vesali et al. (2015), which focused on developing an Android app for chlorophyll estimation using a smartphone. They covered parameters from RGB, the same as from HSV and YUV. However, according to their results of maize measurements, the *hue* component was the most significant parameter for SPAD value modelling. By fitting the SPAD value by a linear model, they achieved $R^2 = 0.74$ and $R^2 = 0.82$ by a neural network. This complex approach of the contact imaging of a leaf and supplying the SPAD value estimate directly on a display might be very convenient. However, the issue of natural light noise is still questionable. Additionally, differences in leaf
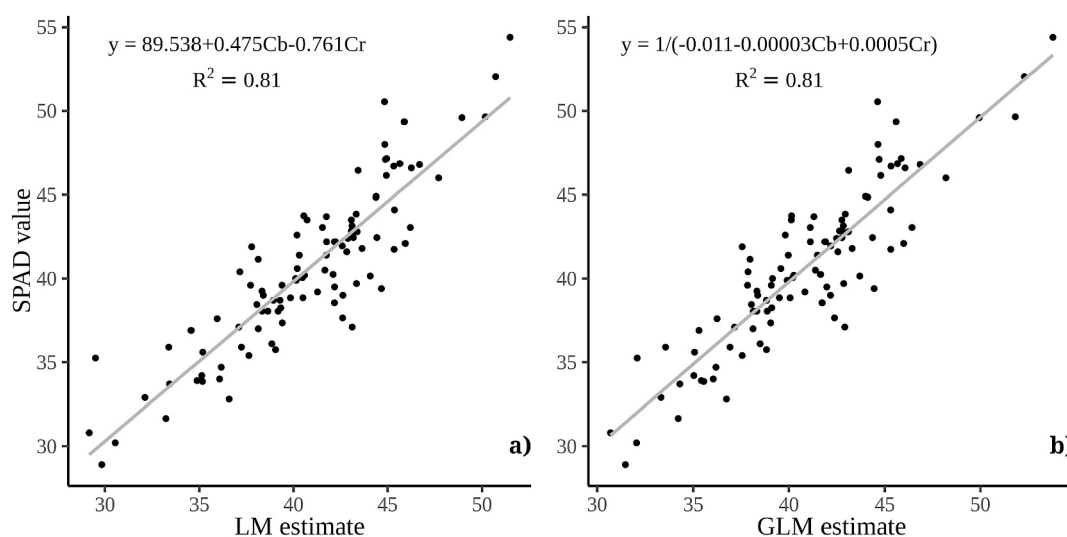

Fig. 7. Model diagnostics of the actual SPAD value estimates by a) a simple linear model and b) a generalized linear model based on the *Cb* and *Cr* chrominance components of the YUV colour model.
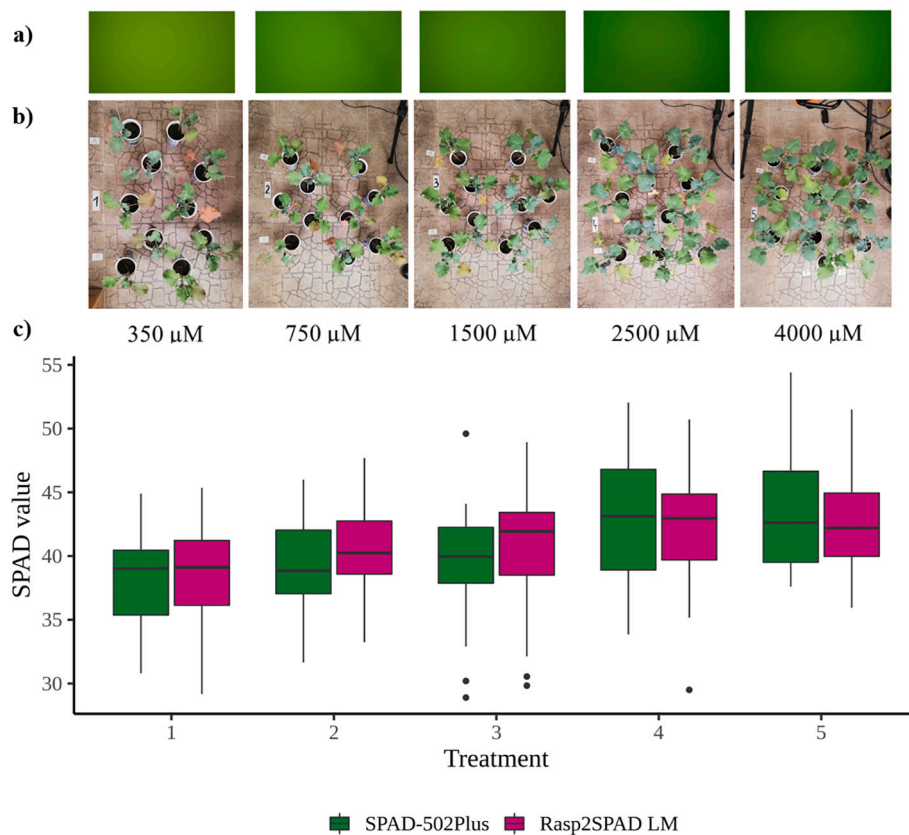
Fig. 8. Overview of the experimental design and results, depicting a) the representative Rasp2SPAD colour images, b) the experimental plant material (winter rapeseed), and c) actual- (SPAD-502Plus) and estimated SPAD value (Rasp2SPAD simple linear model) data variability across five distinctive N treatments.

structure among crops may cause dissimilar results (Ali et al., 2012; Pérez-Patricio et al., 2018; Richardson et al., 2002). Most of the abovementioned studies were conducted mainly to demonstrate the feasibility of the described technique on crops. Therefore, in the case of Rasp2SPAD, crop-specific equations for chlorophyll estimates must also be developed. Since the whole technology is now shown to be running, it is only a matter of applying this method to other crops. By generating the most utilized colour indices, finding the best fit, and incorporating it into the source code, Rasp2SPAD has the potential to meet the needs of farmers, as it is easily constructed and the code is provided under an open-source licence.

4. Conclusion

In-field sampling is a significant source of information involving crop status. Such data are highly desirable for creating well-adjusted agricultural management to follow the principles of sustainable crop production. To bring the opportunity to benefit from a nondestructive sampling method closer to the end-users, a low-cost device based on a Raspberry Pi single-board computer named Rasp2SPAD was developed. The prototype was designed to capture and process a colour image while further producing chlorophyll-related indices based on which the SPAD value was to be modelled. The evaluation procedure conducted on winter rapeseed provided satisfactory results in terms of the cost-performance ratio. The calibration equation was derived using the values of the blue- and red chroma components from the YUV colour representation model that came out as the most sensitive colour indices from the analysis. Rasp2SPAD predicted the SPAD value with $R^2 = 0{,}81$. By achieving this level of accuracy, initial objectives were fulfilled. It has been shown that a) a functional hand-held crop sensor can be constructed while keeping the financial costs low compared to the commercial SPAD-502Plus (5% of the commercial price), b) a simple colour

image is able to provide valuable information about crop status, and c) the prototype is easily programmable, which might be useful for testing it on other crops. By reflecting the above-described drawbacks of already existing similar methods, Rasp2SPAD represents a solution that eliminates the majority of them. First, the colour image properties are prevented from natural light noise. Second, image postprocessing is performed internally, which ensures prompt and consistent results. After this pilot study, the outlook for Rasp2SPAD might include a) testing on other crops followed by species-specific equation determination and incorporation in the source code and b) technological improvements, such as using an NIR diode to quantify leaf chlorophyll content by illumination with near-infrared wavelengths. The Rasp2SPAD prototype, as it is configured now, incorporates a multidisciplinary approach embracing knowledge of computer science, optical methods, spectral behaviour of vegetation, and plant physiology to fill the gap between research and practice by introducing affordable crop sensor that might help to gather in-field data on the way towards sustainable agriculture.

Declaration of Competing Interest

None.

advice and kind help with the experimental preparation, data processing or final writing of the manuscript.

References

Adamsen, F.J., Pinter, P.J., Barnes, E.M., LaMorte, R.L., Wall, G.W., Leavitt, S.W., Kimball, B.A., 1999. Measuring wheat senescence with a digital camera. Crop Sci. 39, 719–724. https://doi.org/10.2135/cropsci1999.0011183X003900030019x.

Akaike, H., 1974. A New Look at the Statistical Model Identification. Springer, New York, NY, pp. 215–222. https://doi.org/10.1007/978-1-4612-1694-0_16.

Ali, M.M., Al-Ani, A., Eamus, D., Tan, D.K.Y., 2012. A new image processing based technique to determine chlorophyll in plants. Am. J. Agric. Environ. Sci. 12, 1323–1328. https://doi.org/10.5829/idosi.aejaes.2012.12.10.1917.

Choudhury, A.K.R., 2014. Using instruments to quantify colour. In: Principles of Colour and Appearance Measurement. Elsevier, pp. 270–317. https://doi.org/10.1533/9780857099242.270.

Cortazar, B., Koydemir, H.C., Tseng, D., Feng, S., Ozcan, A., 2015. Quantification of plant chlorophyll content using Google glass. Lab Chip 15, 1708–1716. https://doi.org/10.1039/C4LC01279H.

Domínguez, J.A., Kumhálová, J., Novák, P., 2016. Winter oilseed rape and winter wheat growth prediction using remote sensing methods. Plant Soil Environ. 61, 410–416. https://doi.org/10.17221/412/2015-PSE.

Evans, J.R., 1983. Nitrogen and photosynthesis in the flag leaf of wheat (Triticum aestivum L.). Plant Physiol. 72, 297–302. https://doi.org/10.1104/pp.72.2.297.

Filella, I., Serrano, L., Serra, J., Peñuelas, J., 1995. Evaluating wheat nitrogen status with canopy reflectance indices and discriminant analysis. Crop Sci. 35, 1400–1405. https://doi.org/10.2135/cropsci1995.0011183X003500050023x.

Hernández-Hernández, J.L., García-Mateos, G., González-Esquiva, J.M., Escarabajal-Henarejos, D., Ruiz-Canales, A., Molina-Martínez, J.M., 2016. Optimal color space selection method for plant/soil segmentation in agriculture. Comput. Electron. Agric. 122, 124–132. https://doi.org/10.1016/j.compag.2016.01.020.

Johnston, S., Cox, S., 2017. The raspberry pi: a technology disrupter, and the enabler of dreams. Electronics 6, 51. https://doi.org/10.3390/electronics6030051.

Kanani, P., Padole, M., 2020. Improving pattern matching performance in genome sequences using run length encoding in distributed raspberry pi clustering environment. Proc. Comput. Sci. 171, 1670–1679. https://doi.org/10.1016/j.procs.2020.04.179.

Kawashima, S., Nakatani, M., 1998. An algorithm for estimating chlorophyll content in leaves using a video camera. Ann. Bot. 81, 49–54.

Kerkech, M., Hafiane, A., Canals, R., 2018. Deep leaning approach with colorimetric spaces and vegetation indices for vine diseases detection in UAV images. Comput. Electron. Agric. 155, 237–243. https://doi.org/10.1016/j.compag.2018.10.006.

Kumhálová, J., Matějková, Š., 2017. Yield variability prediction by remote sensing sensors with different spatial resolution. Int. Agrophys. 31, 195–202. https://doi.org/10.1515/intag-2016-0046.

Meyer, G.E., Neto, J.C., 2008. Verification of color vegetation indices for automated crop imaging applications. Comput. Electron. Agric. 63, 282–293. https://doi.org/10.1016/j.compag.2008.03.009.

Misra, T., Priyadarshini, S., Arora, A., Marwaha, S., Roy, H.S., Ray, M., 2018. A comparative study of chlorophyll content estimation techniques through image analysis. J. Crop Weed. 14 (3), 165–168.

Mohr, H., Schopfer, P., 2012. Plant Physiology. Springer Science & Business Media.

Nasir, M., Muhammad, K., Lloret, J., Sangaiah, A.K., Sajjad, M., 2019. Fog computing enabled cost-effective distributed summarization of surveillance videos for smart cities. J. Parallel Distrib. Comput. 126, 161–170. https://doi.org/10.1016/j.jpdc.2018.11.004.

Nelis, J.L.D., Tsagkaris, A.S., Dillon, M.J., Hajslova, J., Elliott, C.T., 2020. Smartphone-based optical assays in the food safety field. Trends Anal. Chem. 129, 115934 https://doi.org/10.1016/j.trac.2020.115934.

Osroosh, Y., Khot, L.R., Peters, R.T., 2018. Economical thermal-RGB imaging system for monitoring agricultural crops. Comput. Electron. Agric. 147, 34–43. https://doi.org/10.1016/j.compag.2018.02.018.

Pagnutti, M., Ryan, R.E., Cazenavette, G., Gold, M., Harlan, R., Leggett, E., Pagnutti, J., 2017. Laying the foundation to use raspberry pi 3 V2 camera module imagery for scientific and engineering purposes. J. Electron. Imaging 26, 013014. https://doi.org/10.1117/1.JEI.26.1.013014.

Pérez, A.J., Ló Pez, F., Benlloch, J.V., Christensen, S., 2000. Colour and shape analysis techniques for weed detection in cereal fields. Comput. Electron. Agric. 25, 197–212.

Pérez-Bueno, M.L., Pineda, M., Barón, M., 2019. Phenotyping plant responses to biotic stress by chlorophyll fluorescence imaging. Front. Plant Sci. 10, 1135. https://doi.org/10.3389/fpls.2019.01135.

Pérez-Patricio, M., Camas-Anzueto, J., Sanchez-Alegría, A., Aguilar-González, A., Gutiérrez-Miceli, F., Escobar-Gómez, E., Voisin, Y., Rios-Rojas, C., Grajales-Coutiño, R., 2018. Optical method for estimating the chlorophyll contents in plant leaves. Sensors 18, 650. https://doi.org/10.3390/s18020650.

Porra, R.J., Thompson, W.A., Kriedemann, P.E., 1989. Determination of accurate extinction coefficients and simultaneous equations for assaying chlorophylls a and b extracted with four different solvents: verification of the concentration of chlorophyll standards by atomic absorption spectroscopy. Biochim. Biophys. Acta Bioenerg. 975, 384–394. https://doi.org/10.1016/S0005-2728(89)80347-0.

Prasad, S., Mahalakshmi, P., Sunder, A.J.C., Swathi, R., 2017. Smart surveillance monitoring system using raspberry pi and PIR sensor. J. Comput. Sci. Inf. Technol. 5, 7107–7109.

Richardson, A.D., Duigan, S.P., Berlyn, G.P., 2002. An evaluation of noninvasive methods to estimate foliar chlorophyll content. New Phytol. 153, 185–194. https://doi.org/10.1046/j.0028-646X.2001.00289.x.

Tavakoli, H., Gebbers, R., 2019. Assessing nitrogen and water status of winter wheat using a digital camera. Comput. Electron. Agric. 157, 558–567. https://doi.org/10.1016/j.compag.2019.01.030.

Uddling, J., Gelang-Alfredsson, J., Piikki, K., Pleijel, H., 2007. Evaluating the relationship between leaf chlorophyll concentration and SPAD-502 chlorophyll meter readings. Photosynth. Res. 91, 37–46. https://doi.org/10.1007/s11120-006-9077-5.

Vasishth, P.D., Bavarva, A., 2016. Image processing method for embedded optical Peanut sorting. Int. J. Image Graph. Signal Process. 8, 20–27. https://doi.org/10.5815/ijigsp.2016.02.03.

Vesali, F., Omid, M., Kaleita, A., Mobli, H., 2015. Development of an android app to estimate chlorophyll content of corn leaves based on contact imaging. Comput. Electron. Agric. 116, 211–220. https://doi.org/10.1016/j.compag.2015.06.012.

Wang, J., Li, X., Lu, L., Fang, F., 2013. Estimating near future regional corn yields by integrating multi-source observations into a crop growth model. Eur. J. Agron. 49, 126–140. https://doi.org/10.1016/j.eja.2013.03.005.

Wei, T., Simko, V., 2017. R Package "Corrplot": Visualization of a Correlation Matrix [WWW Document]. R Packag. version 0.84. URL. https://github.com/taiyun/corrplot%0A.

Wickham, H., 2007. Reshaping data with the reshape package. J. Stat. Softw. 21, 1–20.

Wickham, H., 2016. ggplot2: Elegant Graphics for Data Analysis. Springer-Verlag, New York.

Wickham, H., Bryan, J., 2019. readxl: Read Excel Files [WWW Document]. R Packag. version 1.3.1. URL. https://cran.r-project.org/package=readxl.

Wickham, H., Averick, M., Bryan, J., Chang, W., McGowan, L., François, R., Grolemund, G., Hayes, A., Henry, L., Hester, J., Kuhn, M., Pedersen, T., Miller, E., Bache, S., Müller, K., Ooms, J., Robinson, D., Seidel, D., Spinu, V., Takahashi, K., Vaughan, D., Wilke, C., Woo, K., Yutani, H., 2019. Welcome to the Tidyverse. J. Open Source Softw. 4, 1686. https://doi.org/10.21105/joss.01686.

Woebbecke, D.M., Meyer, G.E., Von Bargen, K., Mortensen, D.A., 1995. Color indices for weed identification under various soil, residue, and lighting conditions. Trans. Am. Soc. Agric. Eng. 38, 259–269.

Yildiz, M.Z., Boyraz, Ö.F., 2019. Development of a low-cost microcomputer based vein imaging system. Infrared Phys. Technol. 98, 27–35. https://doi.org/10.1016/j.infrared.2019.02.010.

Zhai, Z., Martínez, J.F., Beltran, V., Martínez, N.L., 2020. Decision support systems for agriculture 4.0: survey and challenges. Comput. Electron. Agric. 170, 105256 https://doi.org/10.1016/j.compag.2020.105256.